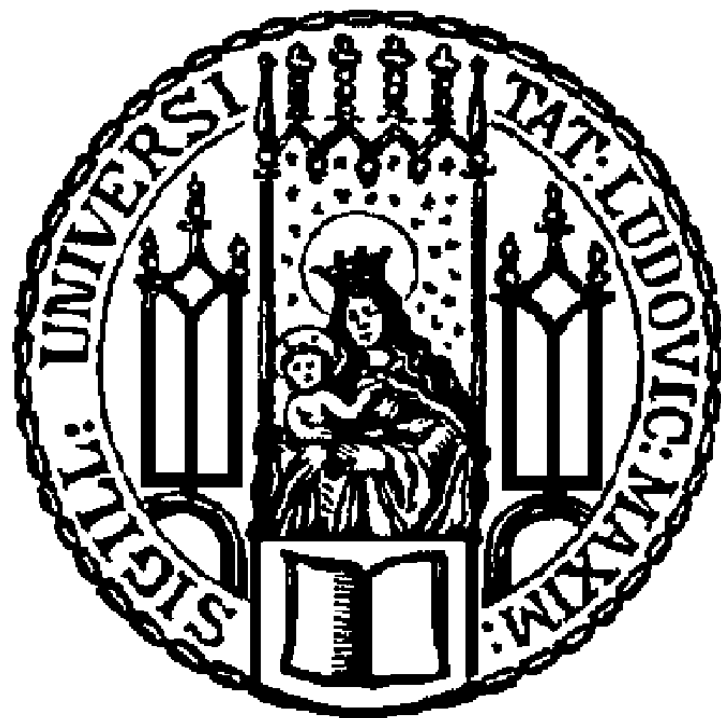


Functional characterisation and Mutational analysis of a bacterial dynamin-like protein, DynA

by Prachi Sawant



Dissertation

Zur Erlangung des Doktorgrades der Naturwissenschaften

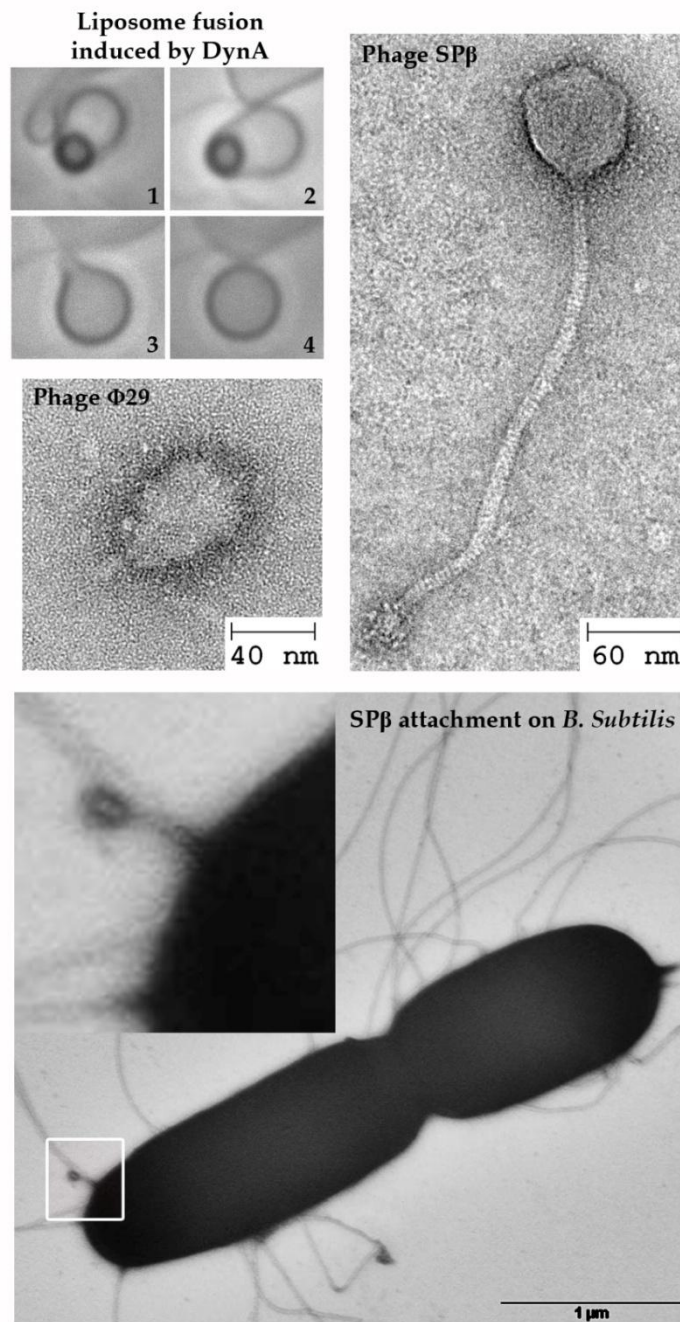
(Dr. rer. nat.)

an der Fakultät für Biologie der

Ludwig-Maximilians Universität München

May, 2015

Functional characterisation and Mutational analysis of a bacterial dynamin-like protein, DynA



PhD thesis by Prachi Dilip Sawant

Supervised by Professor Dr. Marc Bramkamp

Ludwig-Maximilians Universität

Biology, Department I

Eidesstattliche Erklärung

Hiermit versichere ich an Eides statt, dass ich die vorliegende Arbeit selbstständig verfasst habe, keine als die angegebenen Quellen und Hilfsmittel benutzt wurden und alle Zitate kenntlich gemacht sind. Des Weiteren versichere ich, nicht anderweitig ohne Erfolg versucht zu haben, eine Dissertation einzureichen oder mich einer Doktorprüfung zu unterziehen. Die vorliegende Dissertation liegt außerdem keiner anderen Prüfungskommission vor.

I hereby confirm that I have written the accompanying thesis by myself, without contributions from any sources other than those cited in the text. This also applies to all graphics, drawings and images included in this thesis. Moreover, I declare that I have not submitted or defended a dissertation previously without success. This thesis has not been presented to any other examining board.

Ort, Datum

Martinsried,

Gutachter:

1. Prof. Dr. Marc Bramkamp

2. Prof. Dr. Thorsten Mascher

Datum der Abgabe: 27.05.2015

Datum der Prüfung: 03.07.2015

Index	1
Abstract	5
Zusammenfassung	7
Abbreviations	9
Introduction	12
1 Environmental stress in bacteria	13
1.1 Antibiotic induced cell-envelope stress	13
1.2 Phage stress	17
2 Bacterial responses to environmental stress	18
2.1 Phage Shock Protein (PSP) response against envelope stress	19
2.2 Membrane remodelling as bacterial defence strategy	21
3 Dynamin and dynamin-like proteins: Membrane remodelling proteins	23
4 DLPs have diverse functions	25
4.1 Dynamin mediates vesicle scission	25
4.2 Dynamins regulate organelle dynamics	25
4.3 DLPs provide defence against viruses	28
5 Bacterial dynamin-like proteins (BDLPs)	29
5.1 BDLP1 from <i>Nostoc punctiforme</i>	30
5.2 IniA, B and C from <i>Mycobacterium tuberculosis</i>	30
5.3 DynA from <i>Bacillus subtilis</i>	31
6 Aims	35
Material and Methods	38
1 Materials	38
1.1 Chemicals, enzymes and expendables	38
1.2 Media and Buffers	38
1.3 Antibiotics	39
1.4 Oligonucleotides	39
1.5 Plasmids	42
1.6 <i>E. coli</i> strains	45
1.7 <i>B. subtilis</i> strains	45
2 Cultivation of bacteria	49
2.1 Storage and growth conditions	49
2.2 Transformation of <i>E. coli</i>	50
2.3 Transformation of <i>B. subtilis</i>	50
2.4 Generation of deletion mutants	51
2.4.1 Deletion of <i>dynA</i> , in strain DSM 25152	51
2.4.2 Deletion of potential interacting partners (<i>yflN</i> , <i>yukF</i> and <i>mfd</i>) identified in synthetic lethal screen	51
2.5 Bacterial two hybrid assay	51
2.5.1 Plasmid isolation	51

2.5.2	Co-transformation	52
2.6	Spot assay	53
2.7	Quantitative plaque assay (QPA)	53
2.8	Protein expression in <i>E. coli</i>	53
3	Biomolecular DNA techniques	54
3.1	Site directed mutagenesis (SDM)	54
3.2	Polymerase Chain Reaction (PCR)	54
3.3	Agarose gel electrophoresis	55
3.4	DNA digestion with restriction endonucleases	55
3.5	DNA ligation	55
3.6	Sequencing	55
3.7	Plasmid isolation from <i>E. coli</i>	55
3.8	DNA isolation from <i>B. subtilis</i>	55
4	Biomolecular protein techniques	56
4.1	Protein purification	56
4.2	Protein quantification	57
4.3	Protein concentration	57
4.4	SDS Polyacrylamide gel electrophoresis (SDS-PAGE)	57
4.5	Immunoblotting	57
4.6	GTPase assay	58
4.7	Liposome sedimentation assay	58
4.7.1	Liposome preparation	58
4.7.2	Lipid-binding assay	59
4.7.3	Liposome staining	59
4.8	Phage-protein crosslinking <i>in vitro</i>	59
4.9	Phage-protein labeling <i>in vitro</i>	59
5	Microscopy	60
5.1	Light microscopy	60
5.2	Fluorescence Loss In Photobleaching (FLIP)	60
Results		61
1	Functional characterisation of DynA	61
1.1	DynA confers resistance against membrane stress-causing antibiotics	61
1.2	DynA becomes static under nisin-induced membrane stress	65
1.3	DynA is not involved in maintaining <i>B. subtilis</i> membrane potential	67
1.4	Over-expression of DynA facilitates <i>B. subtilis</i> membrane remodelling	70
1.5	<i>B. subtilis</i> lacking DynA is sensitive to phage stress	73
1.6	DynA binds to phage particles <i>in vitro</i>	76
2	Mutational analysis of DynA	79
2.1	DynA preferentially binds to anionic phospholipids (PLs)	79
2.2	DynA mediates liposome tethering, tubulation and fusion	80
2.3	Single point mutation, R512A, alters membrane localisation of DynA	82

2.4	Amino acid region 591-620 of DynA is required for dimerisation	87
3	Characterisation of potential DynA-interacting partners identified in a bacterial two-hybrid screen	91
3.1	Potential DynA-interacting partners localise to bacterial membrane	91
3.2	Interaction matrix of potential DynA-interacting proteins	93
4	Characterisation of potential DynA-interacting partners identified in a synthetic lethal screen	94
4.1	Identified partners fail to produce synthetic lethal/sick phenotype with DynA	95
4.2	DynA-GFP localisation is not affected in strains lacking the identified potential partner/s	96
5	Localisation studies of DynA	98
5.1	Lack of flotillins does not disturb membrane localisation of DynA	98
5.2	DynA-GFP localises into distinct foci and fails to spread across the cell membrane in the absence of YpbQ and YpbS	98
Discussion		100
1	Functional characterisation of DynA	101
1.1	DynA is a bacterial membrane remodelling system	101
1.2	DynA phenocopies Mx proteins by providing defence against bacteriophages	106
2	Mutational analysis of DynA	109
2.1	Membrane-foci formation is oligomerisation-dependent and GTP hydrolysis is required for disassembly of oligomers	109
2.2	Region 591-620 is required for dimerisation	111
3	Potential interaction partners YneK, YmdA and YwpG have different patterns of interaction with DynA	114
4	Outlook	117
References		119
Appendix		135
Figure 1	FRAP analysis of wild-type and D591-620 DynA-GFP	135
Figure 2	Membrane deformations are observed in <i>dynA</i> upon nisin-exposure	136
Figure 3	Spot assay with phages, Φ 29 and SP β	136
Figure 4	Confirmation of deletion of <i>dynA</i> in strain 25152	137
Figure 5	Calibration curve for standard protein samples on Superose 6 10/300 GL column	138
Figure 6	Δ 591-620 lipid binding <i>in vitro</i>	139
Figure 7	Deletion of <i>yukF</i> , <i>mfd</i> and <i>yflN</i>	139
Table 1	Values for calibration curve for standard protein samples on Superose 6 10/300 GL column	137
Table 2	Estimation of molecular weight (MW) of eluted protein	138
Figures and tables		
Figure 1	Cell-envelope targeting antibiotics and their mechanism of action	15
Figure 2	Structural models of BDLPs, BDLP1 and DynA	34
Figure 3	A Δ <i>dynA</i> strain takes longer to recover from nisin-stress, than wild-type	62
Figure 4	A Δ <i>dynA</i> strain is more sensitive to antibiotic induced membrane stress	64
Figure 5	DynA-GFP responds to nisin induced membrane stress	66
Figure 6	DynA is not involved in maintaining bacterial membrane potential but requires	69

	the membrane potential for correct localisation	
Figure 7	Over-expression of DynA facilitates <i>B. subtilis</i> membrane remodelling	72
Figure 8	A $\Delta dynA$ strain is more sensitive to phage infection than wild-type	74
Figure 9	<i>dynA</i> deletion by <i>tet</i> insertion does not cause pleiotropic effects	75
Figure 10	DynA binds to phage particles <i>in vitro</i>	77
Figure 11	DynA binds to labelled-phage particles <i>in vitro</i>	79
Figure 12	DynA binds to negatively charged membranes	80
Figure 13	DynA is a membrane remodelling protein	82
Figure 14	Proposed lipid-binding or paddle loops in D1	83
Figure 15	Localisation of wild-type and mutant DynA-GFP in a $\Delta dynA$ background	85
Figure 16	R512A DynA-His binds to membrane <i>in vitro</i>	86
Figure 17	R512A mutation influences lipid-binding behaviour of DynA	87
Figure 18	Characterisation of DynA stalk domain, 591-620	89
Figure 19	<i>In vivo</i> membrane-binding analysis of wild-type and mutant DynA	90
Figure 20	YneK-GFP, YwpG-GFP and YmdA-GFP localise to as foci to the bacterial membrane	92
Figure 21	Interaction matrix of YwpG, RNaseY, and YneK with D1 and D2 subunits of DynA and their GTPase mutants (D1M and D2M)	94
Figure 22	Deletion of putative partners, identified in SLS, fail to produce synthetic lethal/sick phenotype with $\Delta dynA$	95
Figure 23	DynA-GFP localisation is not affected in strains lacking the identified potential partner/s	97
Figure 24	Membrane localisation pattern of DynA-GFP is altered in strain lacking <i>ypbQ</i> and <i>ypbRS</i> operon	99
Figure 25	Proposed model for membrane protection by DynA	109
Figure 26	Model for $\Delta 591-620$ DynA oligomerisation and localisation <i>in vivo</i>	114
Table 1	Media and buffers used in this work	38
Table 2	Antibiotics and the end concentrations used in this work	39
Table 3	Oligonucleotides used in this work	39
Table 4	Plasmids constructed in this study	42
Table 5	<i>E. coli</i> strains used in this study	45
Table 6	<i>B. subtilis</i> strains used and constructed in this thesis	45
Table 7	Bacterial two-hybrid co-transformations.	52
Table 8	PCR components	54
Table 9	List of proteins detected in mass peptide fingerprinting.	77
Table 10	Statistical analysis of the localisation of YneK, YmdA and YwpG into foci associated with the cell membrane in a wild-type and $\Delta dynA$ background.	93
	Acknowledgements	140
	Curriculum Vitae	141

Abstract

Membrane remodeling is a dynamic process that occurs in bacterial cells to facilitate substrate transport and to provide protection to bacteria during environmental stress. In eukaryotic cells, membrane remodeling is carried out by dynamin-like proteins (DLPs). These proteins are involved in diverse membrane-associated functions such as cargo transport via vesicles, cytokinesis, division of cell organelles and resistance to pathogens. DLPs are also conserved in bacterial species; however, their function is still not clearly understood. The genome of *B. subtilis* contains a gene *dynA* (*ypbR*), which encodes a large DLP (136 KDa), DynA, that can tether membranes and induce membrane fusion *in vitro*. Deletion of *dynA* in *B. subtilis* strain 168 fails to produce any observable growth phenotype under standard laboratory conditions. *B. subtilis* is a soil bacterium and prey to several environmental stress factors to which laboratory strains are normally not exposed. Hence, it was conceivable that DynA might be required when bacteria are exposed to stress. To address this hypothesis, the behavior of DynA was examined under conditions causing membrane-stress, such as exposure to antibiotics and phage infection. A strain lacking *dynA* showed impaired growth in the presence of sublethal amounts of antibiotics that target the cell membrane and was more sensitive to phage infection compared to wild-type strains. Time-lapse microscopy and fluorescence loss in photobleaching (FLIP) experiments showed that $\Delta dynA$ cells have compromised membrane remodeling compared to wild-type strain. In conclusion, all results propose DynA to play a role in protecting the cell membrane under stress conditions. Also, for the first time, it is shown that a bacterial DLP contributes to innate immunity of bacteria.

DynA not only has a unique membrane protection function but also distinctive structural features. A single DynA polypeptide contains two dynamin-like subunits, each consisting of a GTPase domain and a dynamin-like stalk region. Both subunits, D1 and D2, share strong intra-molecular cooperativity to facilitate GTPase activity. Here, a combination of mutational analysis and subsequent *in vivo* and *in vitro* investigation was applied to further characterise structural assembly and biochemical properties of DynA. Size-exclusion chromatography

elucidated that DynA dimerisation requires C-terminal amino acids 591-620. In addition, *in vivo* localisation, *in vitro* lipid-binding and GTPase analysis revealed arginine at position 512 of DynA to be a key regulator of GTP hydrolysis as well as lipid-binding. Furthermore, *in vivo* localisation and bacterial two-hybrid experiments were employed to confirm interaction of DynA with putative interaction partners (YneK, YwpG and YmdA). YneK was found to interact with D1 and YwpG with D1 and D2 individually, whereas YmdA required a full-length DynA (D1+D2) for interaction. Taken together, the results presented here greatly expand on current knowledge regarding functional, biochemical and structural properties of a bacterial dynamin-like protein (BDLP). This thesis not only demonstrates the preserved membrane-remodeling function of DLPs in bacteria but also explain their conservation from bacteria to higher-organisms.

Zusammenfassung

Membranremodellierung ist ein dynamischer Prozess, der bakteriellen Zellen den Im- und Export von Substraten über die Membran ermöglicht und für den Erhalt der Zellintegrität unter Umweltstressbedingungen sorgt. Die Membranremodellierungseigenschaften Dynamin-ähnlicher Proteine (dynamamin-like proteins [DLPs]) wurden bereits intensiv in eukaryotischen Zellen untersucht. Proteine aus dieser Familie sind dort in diverse membranassoziierte Prozesse involviert, wie z.B. dem vesikulärem Cargotransport, der Zytokinese, der Teilung von Zellorganellen und bei der Resistenz gegenüber Pathogenen. Obwohl DLPs in vielen Bakterien konserviert vorliegen, ist noch nicht geklärt, welche Funktion sie in diesen Organismen ausüben. Das im Genom von *Bacillus subtilis* kodierte DynA ist ein bakterielles DLP mit einem Molekulargewicht von 136 kDa. *In vitro* Studien haben gezeigt, dass DynA Membranen zusammenführen und fusionieren kann. Die Deletion von *dynA* im *B. subtilis* Stamm 168 führte allerdings nicht zu einem Wachstumsdefekt unter standardisierten Kultivierungsbedingungen. In seiner natürlichen Umgebung im Erdboden ist das Bakterium jedoch einer Reihe von Stressfaktoren ausgesetzt, die unter Laborbedingungen keine Rolle spielen. Es wurde daher die Möglichkeit in Betracht gezogen, dass DynA hauptsächlich unter besonderen Stressbedingungen von der Zelle benötigt wird. Um diese Hypothese zu untersuchen, wurde das Verhalten von DynA unter erhöhtem Membranstress untersucht. Stämme ohne DynA zeigten im Vergleich zum Wildtypen ein beeinträchtigtes Wachstum in Anwesenheit von Antibiotika und eine höhere Sensitivität gegenüber Infektion durch Phagen. Zusätzlich konnte durch Zeitraffer-Mikroskopie und *Fluorescence Loss in Photobleaching* (FLIP) eine verminderte Membranremodellierungsaktivität von $\Delta dynA$ im Vergleich zum Wildtypen festgestellt werden. Diese Ergebnisse deuten darauf hin, dass DynA eine Funktion zum Schutz der Zellmembran von *B. subtilis* unter Stressbedingungen ausübt. Zusätzlich konnte damit zum ersten Mal gezeigt werden, dass ein bakterielles DLP zu der angeborenen Immunantwort von Bakterienzellen gegen Phagen beitragen kann.

Neben seiner außergewöhnlichen Funktion zum Schutz der Zellmembran besitzt DynA auch spezielle strukturelle Eigenschaften: ein einziges DynA Polypeptid beinhaltet zwei Dynamin-ähnliche Untereinheiten, die jeweils wiederum aus einer GTPase und einer „dynamin-like stalk-region“ Region zusammengesetzt sind. Die beiden D1 und D2 genannten Untereinheiten zeigen beide jeweils eine starke intramolekulare Kooperativität zur Stimulierung ihrer GTPase Aktivität. Durch das Einführen von gezielten genetischen Veränderungen in *dynA* und der anschließenden funktionellen *in vivo* und *in vitro* Charakterisierung wurden in dieser Arbeit der Einfluss einer veränderten Aminosäuresequenz auf die biochemischen Eigenschaften sowie die strukturelle Assemblierung des Proteins untersucht. Studien mittels Größenausschlusschromatographie zeigten, dass die C-terminalen Aminosäuren 591-620 essentiell für die Fähigkeit zu Dimerisierung von DynA sind. Zusätzliche *in vivo* Lokalisationsstudien, *in vitro* Lipidbindestudien und GTPase Aktivitätsuntersuchungen zeigten, dass Arginin an Stelle 512 des Proteins eine Schlüsselrolle bei der Regulation der GTP Hydrolyse und der Lipidbindung zukommt. Weiterhin wurden *in vivo* Lokalisationsstudien und *bakterielle Zwei-Hybrid-Experimente* durchgeführt um die Interaktion von DynA mit seinen potentiellen Interaktionspartnern YneK, YwpG und YmdA zu bestätigen und weiter zu untersuchen. Während YneK nur mit der D1 Untereinheit und YwpG individuell mit beiden Untereinheiten interagiert, benötigt YmdA das komplette DynA Protein mit D1 und D2 Untereinheit zur Interaktion. Zusammenfassend betrachtet konnten durch diese Ergebnisse der derzeitige Wissensstand über die funktionellen, biochemischen und strukturellen Eigenschaften bakterieller DLPs deutlich erweitert werden. Diese Arbeit zeigt nicht nur, dass DLPs ebenfalls in Bakterien eine Membranremodellierungsfunktion ausüben können, sondern liefert damit auch abschließend eine Erklärung für die Konservierung der DLPs von Bakterien bis hin zu höheren Organismen.

Abbreviations

3CS	3 component system
aaRS	aminoacyl-tRNA synthetase
ABC	ATP binding cassette
Abp1	Actin-binding protein 1
ATP	Adenosine triphosphate
AtpA	ATP synthase subunit alpha
BDLP	Bacterial dynamin-like protein
BTH	Bacterial two-hybrid
Caf4	CCR4-associated factor 4
CCCP	carbonyl cyanide <i>m</i> -chlorophenylhydrazone
CH	Casein hydrolysate
CL	Cardiolipin
CLMP1	Clumped chloroplasts 1
CRL	Chromophore lyase
DAPI	4',6-diamidino-2-phenylindole
DisC ₃ (5)	3,3'-Dipropylthiadicarbocyanine iodide
DLP	Dynamin-like protein
DMF	Dimethylformamide
DNA	Deoxyribonucleic acid
Dnm1	Dynamin 1
Drp1	Dynamin-related protein 1
ER	Endoplasmic reticulum
FA	Formaldehyde
Fis1	Fission 1 protein
FLIP	Fluorescence loss in photobleaching
FM4-64	<i>N</i> -(3-Triethylammoniumpropyl)-4-(6-(4-(Diethylamino) Phenyl) Hexatrienyl) Pyridinium Dibromide
FRAP	Fluorescence recovery after photobleaching
FTSZ	Filamenting Temperature-Sensitive Mutant Z
Fzo1	Fuzzy onions homolog 1
GBP1	Guanylate-binding protein 1
GDP	Guanosine diphosphate
GED	GTPase effector domain
GFP	Green fluorescent protein

GMP-PNP	5'-Guanylyl imidodiphosphate
GTP	Guanosine triphosphate
His	Histidine
HR	Heptad repeat
LPS	Lipopolysaccharide
LTA	Lipoteichoic acid
mDNA	Mitochondrial Deoxyribonucleic acid
MDR	Multi-drug resistant
Mdv1	Mitochondrial division protein 1
Mfn1/2	Mitofusin 1/2
Mgm1	Mitochondrial genome maintenance protein 1
MPF	Mass-peptide fingerprinting
mRNA	Messenger Ribonucleic acid
MW	Molecular weight
NAG	N-acetylglucosamine
NAM	N-acetylmuramic acid
NP	Nucleoprotein
OM	Outer membrane
OPA1	Optic atrophy protein 1
PBP	Penicillin-binding protein
PC	Phosphatidylcholine
PDV1/2	Plastid division protein 1/2
PE	Phosphatidylethanolamine
Pex10	Peroxisome biogenesis factor 10
PG	Phosphatidylglycerol
PH	Pleckstrin homology
PL	Phospholipid
PMF	Proton motive force
PML	Promyelocytic leukemic protein
PRD	Proline-rich domain
PSP	Phage shock protein
QPA	Quantitative plaque assay
RNA	Ribonucleic acid
ROS	Reactive oxygen species
RR	Response regulator
SDM	Site-directed mutagenesis

SDS-PAGE	Sodium dodecyl sulfate- Polyacrylamide gel electrophoresis
SLS	Synthetic lethal screen
SNARE	<u>SNAP</u> (Soluble NSF Attachment Protein) <u>RE</u> ceptor
SNX9	Sorting nexin-9
SUMO	Small ubiquitin-related modifier
TA	Teichoic acid
TCS	Two-component system
TM	Transmembrane
TP	Terminal protein
UDP	Uridine diphosphate
Vps1	Vacuolar protein sorting-associated protein 1

Introduction

The endosymbiotic theory, articulated by Konstantin Mereschkowsky in 1910, claims eukaryotic cells to have originated from symbiotic associations between single-celled organisms. Best examples of such associations are chloroplasts that are known to have a cyanobacterial origin and mitochondria, which seem to have developed from heterotrophic proteobacteria (Kutschera and Niklas 2005). Eukaryotic cells are larger than bacteria and complicated in terms of structure and function. Hence, it is conceivable that some non-essential genes from bacteria that were passed on to eukaryotes might have evolved an essential function during evolution. A classic example of such an evolutionary conservation is the dynamin group of proteins (conserved in chloroplasts as well as mitochondria), preserved across prokaryotic and eukaryotic species. While known to be essential in eukaryotic cells, prokaryotic dynamins remain poorly characterized. Eukaryotic dynamins and dynamin-like proteins (DLPs) are lipophilic GTPases with conserved membrane-remodelling features. Membrane remodelling is required by bacteria to counteract changes in the external environment (i.e., temperature, pH, osmolality, ions, solute, etc.) for survival. Several bacteria encode DLPs, including the Gram-positive *Bacillus subtilis* which is well known for its diverse survival strategies under external stress. This bacterium lives in soil habitats and are frequently exposed to environmental stress and starvation. *B. subtilis* can easily adapt to changes in the external environment by activating several stress-response pathways, the most common being stress-resistant endospore formation and starvation-induced biofilm generation. *B. subtilis* encodes a DLP called DynA, which shows membrane remodelling characteristics *in vitro* but was found to be non-essential for bacterial growth. However, DLPs such as Mx proteins and IniA have demonstrated their essentiality under stress conditions that were induced by viruses and antibiotics, respectively (discussed below). This PhD project has therefore focused on unravelling the importance of DynA in *B. subtilis*, upon exposure to environmental stress.

1. Environmental stress in bacteria

Environmental stress is a condition, which refers to the adverse effects caused by an external factor on the physical well-being of a bacterial cell. These factors include extremes of pH, temperature, osmolality, nutrient supply and presence of antimicrobial compounds. Two of the most common environmental factors that induce stress in bacterial cells are antibiotics (Kohanski et al 2010) and bacteriophages (Samson and Moineau 2013), their portal of entry being the host cell membrane.

1.1 Antibiotic induced cell-envelope stress

Exposure to antibiotics can adversely affect several cellular processes that ultimately lead to bacteriostaticity or bacterial lysis, whereas exposure to sub-lethal concentrations can induce cross-protection leading to development of antibiotic resistant bacteria. The cell envelope is the first accessible target as well as the first line of defense against antimicrobial compounds. It comprises the cell membrane, periplasmic space and the cell wall. Peptidoglycan is the major component of the cell wall and therefore, a major target of antibiotics. Peptidoglycan synthesis (Figure 1) involves crosslinking of disaccharide (NAM and NAG) pentapeptide precursor molecules (Typas et al 2012, van Heijenoort 2001). Uridine diphosphate-N-acetyl muramic acid (UDP-NAM) and Uridine diphosphate-N-acetyl glucosamine (UDP-NAG) form the starting material for peptidoglycan synthesis. Formation of UDP-NAM is achieved from UDP-NAG, which is followed by the addition of five amino acids that give rise to UDP-NAM-pentapeptide. Formation of UDP-NAM-pentapeptide is an enzyme-catalyzed process that occurs within the cytoplasm. Further, NAM-pentapeptide is transferred to the membrane-associated bactoprenol pyrophosphate and NAG is added to bactoprenol pyrophosphate-NAM from UDP-NAG to form the final disaccharide pentapeptide precursor called lipid II (comprising of disaccharide-pentapeptide-pyrophosphate-bactoprenol chain). Lipid II is flipped across the cell membrane, transfers the disaccharide-pentapeptide to the expanding peptidoglycan chain, and then is moved back to the cytoplasmic side to continue transfer of precursor molecules. Finally, transpeptidation step occurs to link the peptide side chains,

giving rise to a tough peptidoglycan layer (Bugg and Walsh 1992, van Heijenoort 1998, Ward 1984). Bacteria can maintain their cell integrity by developing resistance mechanisms to several cell envelope-targeting antibiotics. Of these, the β -lactams are well studied. They inhibit bacterial cell wall synthesis by binding to penicillin-binding proteins (PBPs) and preventing the last step of peptidoglycan synthesis (Georgopapadakou 1993). Similarly, glycopeptides (vancomycin and teicoplanin) can target the C-terminal of D-Ala-D-Ala dipeptide on the outer surface of the cytoplasmic membrane to inhibit cell wall synthesis (Barna and Williams 1984). Some glycopeptides, such as telavancin, bind to lipid II on the cytoplasmic side of the membrane, leading to membrane depolarization and cell death (Lunde et al 2009). Bacitracin is another classic antibiotic known to induce envelope stress (including cell wall and cell membrane stress) in bacteria by binding to peptidoglycan synthesis precursor, undecaprenyl pyrophosphate (Storm and Strominger 1973). Another target of bacterial cell wall machinery is the endopyruvyl transferase enzyme, MurA, which catalyzes the first step in peptidoglycan biosynthesis. Antibiotics belonging to the phosphonic acid group (fosfomicin) bind MurA to disrupt bacterial cell envelope (Kahan et al 1974).

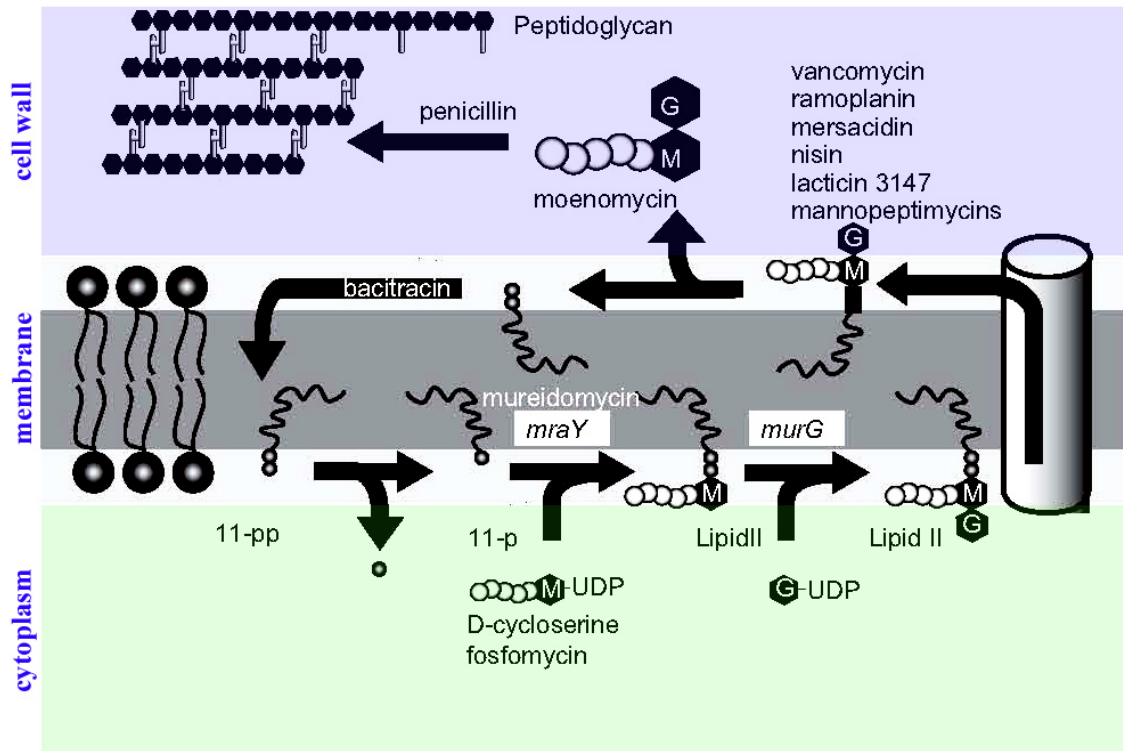


Figure 1. Cell envelope targeting antibiotics and their mechanism of action. Many antimicrobial peptides target different steps of peptidoglycan synthesis in bacteria. Penicillin and moenomycin are examples of antibiotics that target transpeptidase and transglycosylase activity of penicillin-binding proteins (PBPs), respectively. Antibiotics such as vancomycin, ramoplanin, mersacidin, nisin, lacticin 3147 and mannopeptimycins specifically target Lipid II, whereas bacitracin binds undecaprenyl phosphate to inhibit recycling of the polyisoprenoid anchor. Peptides like D-cycloserine and fosfomycin block the synthesis of UDP-MurNAc-pentapeptide whereas mureidomycin specifically inhibits MraY activity. Figure is adapted from (de Kruijff et al 2008).

The development of bacterial resistance against antibiotics targeting the cell wall/peptidoglycan synthesis machinery is well known. Therefore, several membrane targeting antimicrobial compounds are under study for therapeutic purposes. One promising group of compounds are antimicrobial cationic peptides, well known for their lipid affinity and membrane disruption properties. Cationic antibiotics can follow one of the following modes of action for disrupting bacterial membranes: 1) pore or ion channel formation by α -helical peptides due to membrane-peptide or peptide-peptide interactions, 2) membrane depolarisation and decomposition due to ionic interactions between cationic peptides and

negatively charged membrane components on the surface, or 3) membrane curvature induction due to bending of membrane leaflets upon peptide binding (Herzog and Fridman 2014). Most of the cationic peptides have low molecular masses and hence, incapable of forming large oligomers that are necessary for pore formation. Such peptides usually follow the second mode of action to damage bacterial membranes. A widely studied cationic antibiotic is pore-forming nisin, a lanthionine peptide produced by *Lactococcus lactis* and active against a wide range of Gram-positive bacteria including *B. subtilis*. Nisin has been shown to target cell wall biosynthesis proteins, lipid II (Hyde et al 2006) and undecaprenyl pyrophosphate (Aravind and Koonin 1998). Nisin results in permeabilization of the cell membrane followed by interference in cell wall biosynthesis. Other examples of peptides that directly interact with Gram-positive bacterial membranes include gramicidin and daptomycin. Depending upon the environmental conditions, gramicidin peptides may adopt one of the two folding conformations; a channel forming single stranded helical dimer or a non-channel forming double stranded intertwined helix (Kelkar and Chattopadhyay 2007). Linear gramicidin can form well defined transmembrane ion channels for transport of monovalent cations and alkali metals (Burkhart et al 1999, Dubos 1939). Daptomycin is an anionic lipopeptide that requires the presence of Ca^{2+} ions and negatively charged membranes (especially PG head groups) for its bactericidal action. It acts by forming aggregates in solution, which then form micelles in the presence of Ca^{2+} . Binding to calcium ions initiates a conformational change in daptomycin oligomers which dissociate from the micellar structure prior to inserting in the membrane (Straus and Hancock 2006). Other membrane targeting antimicrobial compounds include cyclopeptides (polymyxins) and ionophores (salinomycin and monensin). Polymyxins have been shown to bind to lipid A (Morrison and Jacobs 1976) from lipopolysaccharide (LPS) in Gram-negative bacteria and damage both inner and outer membranes, since their hydrophobic tail has high affinity for phospholipid molecules. Ionophores can form ion channels across the cell membrane, which leads to disruption of membrane potential, ultimately resulting in cell death.

1.2 Phage stress

A major threat to any living cell in its natural environment is viral attack. Bacteria, including *B. subtilis* fall prey to several viruses. Large phages, such as PBS1 and SP15, to the smallest known double-stranded DNA phages such as ϕ 29 and ϕ 15 have been recovered from *Bacillus* species (Hemphill and Whiteley 1975). The *B. subtilis* 168 genome is also a host to about 10 prophage-like elements (Kunst et al 1997). The most widely studied *Bacillus* phages include infectious ϕ 29 and the lysogenic prophage, SP β .

ϕ 29 is one of the smallest known double-stranded DNA phage that infects *B. subtilis* (Hemphill and Whiteley 1975). ϕ 29 virion has a molecular mass of about 18×10^6 daltons (Rubio et al 1974). Its structure consists of a hexagonal head with a flattened base connected to the tail through two collars. The lower collar harbours 12 spindle-shaped appendages whereas the head radiates several projections (Anderson et al 1966). Based on several polypeptide studies, it is reported that the phage is composed of 7 proteins – 3 comprising the head, 3 forming the neck and 1 present in the tail (Mendez et al 1971, Ramirez et al 1972, Salas et al 1972). Head surface, head fibres and neck appendages of ϕ 29 have been shown to promote antigenicity (Tosi and Anderson 1973). Previous DNA preparations have shown ϕ 29 DNA to have a molecular weight of about 11×10^6 (Anderson and Mosharrafa 1968). This phage, upon infecting *B. subtilis* produces small plaques. ϕ 29 DNA replication has been quite extensively studied. Upon attachment to the host, ϕ 29 injects about 65% of its DNA into the host cytoplasm by using energy that is built up in its capsid during DNA packaging. This is followed by initiation of transcription of early genes that are required along with unknown host proteins, to pull the remaining viral DNA into the cytoplasm (Gonzalez-Huici et al 2004). Positioning of ϕ 29 DNA replication machinery on the bacterial membrane requires an interaction between viral membrane protein, p16.7 and bacterial cytoskeleton protein, MreB (Munoz-Espin et al 2009). ϕ 29 DNA replication is initiated upon binding of viral terminal protein (TP) to DNA. TP forms a heterodimeric complex with ϕ 29 DNA polymerase and provides a free hydroxyl group to start initiation of DNA replication. Further, viral protein p6

is required for unwinding DNA ends and protein p5 is required for stabilizing the elongated single DNA strands (Meijer et al 2001).

The inducible prophage, SP β is large with a complex structure, and a double-stranded DNA genome of about 62×10^6 daltons. The virus head measures about 82 nm in diameter and its tail is 358 nm long along with six radial spikes (Warner et al 1977). *B. subtilis* 168 strain is lysogenic for SP β (Warner et al 1977). However, the factor that prevents this phage from undergoing a lytic cycle in 168 still remains undetermined. The prophage attachment site, gene *spsM* (spore polysaccharide synthesis protein M), lies between *ilvA* and *kauA* regions of 168 genome (Zahler et al 1977). The *spsM* gene is split into two gene fragments, *yodU* (5' end of *spsM*) and *ypqP* (3' end of *spsM*) upon SP β integration (Eichenberger et al 2004). SP β is an active prophage, capable of undergoing a lytic cycle during SOS response (Lazarevic et al 1999). Prophage excision from the host genome requires a putative site-specific recombinase, SprA (or *yokA*) encoded by SP β . During sporulation, excision of SP β from the mother cell DNA is initiated for the expression of *spsM*, which is required for spore coat formation. *spsM* expression is regulated by the mother cell-specific sigma factor, σ^K . σ^K expression requires excision of another cryptic prophage, skin element that is integrated into the *sigK* gene. Thus, the excision of SP β prophage is a developmentally regulated event. SP β prophage is maintained in the spore DNA since, the 135 kb viral genome contains genes that are required for production and providing resistance to the antibiotic sublancin (Mendez et al 2012)

2. Bacterial responses to environmental stress

Environmental stress can cause adaptive and survival changes in bacteria leading to alterations in gene expressions that are mediated by RNA polymerase-binding sigma factors (Raivio and Silhavy 2001). Sigma factors play an important role in the survival of bacteria in different environmental conditions. Apart from primary sigma factors that are responsible for the transcription of basic genes under normal growth conditions, many bacteria contain alternating sigma factors that regulate transcription of stress response genes. *B. subtilis*

contains seven such alternating sigma factors (σ^M , σ^V , σ^W , σ^X , σ^Y , σ^{YlaC} , σ^Z) that can be induced by diverse stimuli, (Souza et al 2014). σ^W , encoded by the *sigW* gene, is induced upon sensing cell envelope damage (Butcher and Helmann 2006, Cao et al 2002) and known to regulate transcription of several genes that respond to envelope stress, including the *pspA* or *ydjF* (phage shock protein A) and *floT* or *yuaG* (flotillin T) operons. Under normal growth conditions σ^W is bound to its cognate anti-sigma factor, RsiW and held inactive. Upon induction, RsiW is subjected to proteolytic cleavage by proteases such as PrsW, RasP and ClpXP/ClpCP, thus alleviating σ^W inhibition (Ho and Ellermeier 2012).

Apart from sigma factor activation, bacterial stress responses also include regulation of two component systems (TCS). TCS is comprised of a membrane-bound histidine kinase (HK) sensor and a cognate response regulator (RR). The HK senses an external stimulus and passes the signal to the RR, which then activates the expression of stress response genes (Bijisma and Groisman 2003, Hoch 2000, Mascher et al 2003, Stock et al 2000). In Gram-positive bacteria, ABC transporters that are often associated with TCS can also provide resistance against cell envelope targeting antibiotics. ATP-binding cassette (ABC) transporters are large multi-domain membrane spanning proteins that utilise their ATP-binding and hydrolysis energy for translocation of various substrates across the cell membrane. Some ABC transporters are known to combat stress induced by antimicrobial peptides, for example by removing these peptides from the cell surface or by altering their target (Gebhard 2012).

2.1 Phage Shock Protein (PSP) response against envelope stress

Bacteria have evolved extracytoplasmic stress response systems to counteract cell envelope stresses, of which the RpoE (Erickson and Gross 1989) and Cpx (Danese et al 1995) systems in *E. coli* are well characterised. Another classic example of such stress response in bacteria is the phage shock protein (PSP) system. The PSP system was first identified in *E. coli* upon filamentous phage infection that resulted in the upregulation of a protein, hence termed PspA (phage shock protein A) (Brissette et al 1990). *E. coli* PspA protects the damaged cell membrane from proton leakage (Kobayashi et al 2007). It is thought to form MreB (actin

homolog in bacteria) dependent large dynamic scaffolds that can maintain membrane integrity during stress (Engl et al 2009, Standar et al 2008). The PSP system is encoded by the *psp* operon, consisting of *pspABCDEF*, and by *pspG*. PSP mutants show defects in growth and survival at stationary phase at an alkaline pH, as well as in maintenance of the proton motive force (pmf) and in protein export via the *tat* and *sec* pathways (Darwin 2005, Joly et al 2010, Model et al 1997). PspA is considered to be the PSP response regulator. Under uninduced condition, PspA is bound to and held inactive by PspF, a transcriptional regulator of the PSP operon. PspB and PspC are membrane-binding proteins that sense extracytoplasmic membrane stress and communicate with PspA, to enable PSP response in bacteria (Darwin 2005). The PSP response can be induced when the cell envelope senses stress such as filamentous phage infection, temperature variation, osmotic pressure, envelope-protein mislocalisation (eg. secretin), dissipation of proton-motive force (PMF) and presence of protonophores (eg. Carbonyl cyanide m-chlorophenylhydrazone) (Model et al 1997). The PSP protein family is highly conserved in firmicutes, cyanobacteria, proteobacteria, archae and plant chloroplasts. In Gram-positive bacterial species like *Mycobacterium* and *Bacillus*, PSP homologues are involved in maintenance of cell envelope stability upon extracytoplasmic stress, for example by contributing resistance against antibiotics which target cell wall and membrane integrity (Joly et al 2010, Jordan et al 2008, Mascher et al 2004, Wiegert et al 2001).

B. subtilis has two PspA homologues, LiaH and PspA, with about 25% amino acid sequence homology. LiaH is encoded within the *liaIH* operon which is regulated by the three component system (3CS) LiaFRS. Extracytoplasmic stress, such as antibiotic induced interference with the lipid II cycle (bacitracin, vancomycin or nisin), is sensed by LiaFRS leading to strong induction of the promoter of *liaIH*, P_{liaI} (Wolf et al., 2010). Furthermore, the *lia* operon, consisting of *liaIHGFRS*, can be weakly induced by detergents, ethanol, alkaline shock and secretion stress (Wiegert et al., 2001; Wolf et al., 2010). The Lia system is proposed to scan the cytoplasmic membrane for perturbations, which then induces LiaR activation by

LiaS and subsequent induction of the *liaIH* operon (LiaS-LiaR-LiaIH). LiaIH is thought to provide resistance against envelope stress, alkaline shock, secretion stress, organic solvents and oxidative stress. Under non-inducing conditions, LiaI localises as dynamic foci to the bacterial membrane, whereas LiaH is dispersed in the cytoplasm. Upon sensing envelope stress, LiaI recruits LiaH to the membrane and their localisation becomes highly static (Dominguez-Escobar et al 2014, Wolf et al 2010).

The second PspA homolog in *B. subtilis*, also termed as PspA is encoded by the gene *ydjF*. This PSP operon consists of *ydjFGHI*. Induction of this operon can give rise to two transcripts: the monocistronic *pspA* (*ydjF*) and the polycistronic *ydjFGHI* transcript (Wiegert *et al.*, 2001; Serizawa *et al.*, 2004). Expression of the this operon is induced by the extracytoplasmic sigma factor σ^W in response to envelope stress induced by phage infection, alkaline shock and certain antibiotics that affect cell wall biosynthesis (Wiegert *et al.*, 2001; Hachmann *et al.*, 2009; Wenzel *et al.*, 2012). The *ydjFGHI* operon is repressed by the AbrB regulon during the logarithmic growth phase (Qian *et al.*, 2002). Apart from minor stress related phenotypes observed for PSP mutants (Wolf et al 2010), the actual function of the PspA homologs in *B. subtilis* is not known. A recent study on *B. subtilis* proteome analysis, upon exposure to a small cationic peptide, MP196, revealed an upregulation of several stress-response proteins, including PspA, liaH, floT and DynA (Wenzel et al 2014).

2.2 Membrane remodelling as bacterial defence strategy

The bacterial membrane functions not only to encapsulate, but also to protect the cargo of the cytoplasmic environment. Membrane remodelling is required by bacteria to survive the changes in the external environment. One survival strategy is to regulate the membrane fluidity and permeability by altering the pre-existing fattyacids in the membrane. This is achieved either by decreasing fatty-acid saturation levels or incorporating cyclopropane within their hydrocarbon chains (Zhang and Rock 2008). Thereby, bacteria can adjust the electrostatic properties of their pre-existing membrane components when under stress. The outer membrane (OM) of Gram-negative bacteria, comprising of a bilayer of

lipopolysaccharide (LPS) and phospholipids (PLs), adds an extra layer of defence against extracytoplasmic stress. The inner leaflet is comprised mostly of 80% phosphatidylethanolamine (PE), 15% phosphatidylglycerol (PG) and 5% cardiolipin (CL) (Kadner 1996). Lipid moieties in the LPS contain six saturated fatty acid chains rather than two saturated/unsaturated chains that are common for Gram-positives, thus making these membranes more hydrophobic than Gram-positive membranes (Nikaido 1996). Apart from LPS and PLs, a large number of proteins reside in the OM that provide membrane flexibility during trafficking of goods in and out of the cell (such as diffusion porins), and also proteins that maintain the cellular structure (such as OmpA and Lpp). Additionally, the OM comprises of specialised channels, receptors and enzymes that are required for different cellular processes. The OM can provide resistance to several cationic antibiotics by carrying out LPS modifications, such as palmitoylation of lipid A, to increase inter-LPS molecule interactions or by adding amino arabinose and PE moieties to the LPS to lower its overall negative charge, which might be required for cationic peptide binding (Delcour 2009, Nikaido 2003, Prost et al 2007). Another way in which bacteria alter membrane permeability is through outer membrane transport proteins, porins. Porins are mostly present in Gram-negative membranes (Nakae 1976, Nikaido 1996), some mycolic acid containing Gram-positive bacteria (such as actinomycetes) (Trias et al 1992), mitochondria (Linden et al 1984) and chloroplasts (Fischer et al 1994). Diffusion porins usually form β -barrelled central hydrophilic pores that allow passage of ions and serve as sites of interaction for specific phages and colicins (Delcour 2009). Apart from bacterial defences, the nature of the external environment has a great influence on resistance to antimicrobial agents. The external environmental pH and the internal membrane potential together can influence the uptake of certain antibiotics (such as aminoglycosides). Changes in the external pH can alter the net charge on antibiotic peptides, whereas alterations in membrane potential can reduce the driving force required for the uptake of antibiotics, thus providing resistance to bacteria. External osmolality too can reduce internal membrane potential, thus increasing resistance

to aminoglycoside antibiotics (Damper and Epstein 1981). Gram-positive bacteria lack an OM, but possess a thick outer peptidoglycan layer along with an inner cell membrane that sandwich in teichoic acid (TA) and lipoteichoic acid (LTA) polymers and together provide resistance to harsh environmental conditions. Surrounding the cell surface and in the membrane, lie several proteins that provide envelope integrity to bacteria. Gram-positive bacteria can modify their TA and LTA with D-alanine to decrease the overall negative charge of the bacterial cell envelope to reduce cationic antimicrobial peptide binding (Peschel et al 2000). Another membrane remodelling strategy adopted by Gram-positive as well as Gram-negative bacteria is aminoacylation of phosphatidylglycerol (PG), catalyzed by aminoacyl-tRNA synthetase (aaRS) to develop resistance against several antimicrobial compounds (Friedman et al 2006, Weidenmaier et al 2005). Addition of lysine or alanine neutralizes the negative head groups of PG phospholipid, thus preventing binding of cationic peptides.

3. Dynamin and dynamin-like proteins: Membrane remodelling proteins

GTPases are GTP-binding and hydrolysing proteins involved in different cellular functions such as translation, signal transduction, cell motility, intracellular transport, protein localisation, chromosome partitioning and membrane transport (Leipe et al 2002). One such family of GTPase proteins called the dynamin superfamily is involved in processes such as vesicle budding and scission, organelle-division, microbial resistance and membrane dynamics (Praefcke and McMahon 2004). The importance of dynamin proteins was first revealed in 1991 in *Drosophila melanogaster*, since absence of this protein was seen to block the diffusion of neurotic vesicles containing neurotransmitters, which disturbed signal transduction between neurons leading to temperature-sensitive paralytic phenotype, *shibire*. The *shibire* gene encodes for a mechano-chemical dynamin GTPase protein that is involved in endocytosis and membrane recycling (van der Blik and Meyerowitz 1991). Here after, dynamin proteins were shown to participate in trafficking of molecules across the membrane, vesicle formation and in actin cytoskeleton dynamics (Gu et al 2010). Dynamin GTPases are

conserved in eukaryotes as well as prokaryotes. Mutations in dynamin encoding genes are linked to peripheral nervous system disorders in human such as Charcot-marie-Tooth neuropathy and centronuclear myopathies (Gonzalez-Jamett et al 2013). Down-regulation of DLPs has been shown to affect mitochondrial division and endocytosis in *Trypanosoma brucei*, cytokinesis in *Dictostelium discoideum*, phagocytosis in *Paramecium*, endocytosis in *Giardia lamblia*, generation of secretory vesicles in *Toxoplasma gondii* and macronuclear development in *Tetrahymena thermophila* (Bhattacharya et al 2010).

The first full-length structure of a dynamin, human guanylate-binding protein 1 (GBP1) (Prakash et al 2000), revealed the N-terminal GTPase domain to be a modified form of Ras GTPase (Pai et al 1990) and its sequence to be conserved between dynamin family members (Manstein et al 2005). Like Ras, dynamin GTPase domains have four well-conserved nucleotide binding motifs. The P-loop (G1) motif binds to nucleotide tri-phosphates, G2 Thr and G3 Gly form the switch I and switch II regions that move upon GTP hydrolysis, thus imparting conformational changes, whereas the G4 motif renders guanine specificity (Vetter and Wittinghofer 2001). Dynamins differ from other regulatory GTPases like ras, in that they have large GTPase domains, oligomerisation or self-assembling activity (Hinshaw and Schmid 1995), low affinities for nucleotides, high intrinsic rates of GTP hydrolysis and they show interaction with lipid bilayers (Sever 2002, Tuma and Collins 1994).

Structurally, dynamins are classified as proteins with a GTPase, middle and GTPase effector domain (GED). Some molecules possess extra domains such as pleckstrin homology (PH) domain, proline/arginine rich domain (PRD), heptad repeat (HR), transmembrane (TM) domain, and/or matrix targeting signal, which are responsible for species and functional specificity (Bramkamp 2012a, Praefcke and McMahon 2004). The dynamin superfamily can be further subdivided into two classes, classical dynamins and dynamin-like proteins (DLPs). Classical dynamins are involved in vesicle-budding events whereas DLPs are involved in functions such as mitochondrial membrane reorganization, peroxisomal division, plastid division, antiviral resistance and vacuolar trafficking from the endoplasmic reticulum and

Golgi. Although conserved in prokaryotes and eukaryotes, the function of dynamin and DLPs have only been extensively studied in eukaryotic model systems, thus far.

4. DLPs have diverse functions

4.1 Dynamin mediates vesicle scission

Classical mammalian dynamin1 exists in three different tissue specific isoforms. Initially considered as a GTPase associated with microtubule, dynamin1 later gained importance in endocytic processes in *Drosophila melanogaster* (van der Bliet and Meyerowitz 1991). Endocytosis is a process initiated by invagination of the plasma membrane followed by formation of a tubular bud-like ingression that is concentrated by various proteins (Liu et al 2009). Human dynamin1 localises to the neck of these invaginations to mediate vesicle scission upon GTP hydrolysis (Praefcke and McMahon 2004). Several models for dynamin-dependent clathrin-coated vesicle scission have been proposed. It is suggested that GDP-bound dynamin molecules are directed to the target membrane pits, where they self-assemble to form a collar around the neck of the pit upon GTP/GDP exchange. Self-assembly potentially stimulates GTPase activity (Warnock et al 1996). Upon GTP hydrolysis, dynamin molecules in the assembly undergo a conformational change, which constricts, stretches or twists membranes to mediate destabilization and fission (Ramachandran 2011). On the other hand, dynamin can co-assemble with membrane curvature-generating protein members (e.g. SNX9, syndapin) that function cooperatively to drive membrane fission and vesicle release (Ramachandran 2011). Hence, dynamin may act either as a mechanochemical enzyme that uses GTP hydrolysis energy for membrane scission or may behave as regulatory GTPase co-ordinating endocytic events.

4.2 DLPs regulate organelle dynamics

DLPs regulate membrane dynamics of eukaryotic organelles: mitochondria, chloroplasts, peroxisomes and vacuoles. ATP synthesizing mitochondria have to undergo dynamic fusion and fission events in order to maintain their shape, size and population within a cell. DLPs are

known to regulate both, mitochondrial fusion and fission events (Hoppins et al 2007). In yeast, the mitochondrial fusion machinery includes DLP members such as the outer membrane Fzo1 protein (Hermann et al 1998) and an inner membrane protein Mgm1 (Meeusen et al 2006). A third protein, Ugo1, acts as a bridge between Fzo1 and Mgm1, thereby linking the two GTPases during mitochondrial fusion (Sesaki and Jensen 2004). For fusion to occur, protein complexes from two mitochondrial membranes have to tether, which is usually achieved upon Fzo1 homo dimerisation. First, outer membrane lipids undergo rearrangement to form a highly unstable intermediary stalk model and finally Mgm1-mediated inner membrane fusion occurs. The energy required for these transition steps is provided by GTP hydrolysis of DLPs (Jahn 2008, Pfanner et al 2004). In mammals, DLPs such as outer membrane mitofusins, Mfn1 and Mfn2 (homologs of Fzo1) and inner membrane OPA1 (homolog of Mgm1) carry out mitochondrial fusion (Chan et al 2009). Loss of Mgm1 and Fzo1 in yeast leads to loss of mDNA consequently resulting in respiratory incompetence (Hermann et al 1998, Jones and Fangman 1992, Rapaport et al 1998), whereas in flies loss of Fzo leads to male sterility (Hales and Fuller 1997). In mice, loss of Mfn1 or Mfn2 or OPA1 causes embryonic lethality (Chen et al 2003), whereas loss of OPA1 in mammals leads to apoptosis (Olichon et al 2003). The mitochondrial fission machinery in yeast involves four proteins; Fis1 that localises to the outer mitochondrial membrane and three cytosolic proteins (Dnm1, Mdv1 and Caf4) that localise to division site on the mitochondrial membrane. Fis1 has an N-terminal tetratricopeptide repeat motif that provides interaction sites for the recruitment of fission proteins from the cytosol (Zhang and Chan 2007). Mdv1 and Caf4 are soluble proteins that interact with Dnm1, and link it with Fis1 (Griffin et al 2005, Zhang and Chan 2007). Dnm1 forms a spiral assembly around the mitochondrial tubule to drive fission of two lipid bilayers, upon GTP hydrolysis (Ingelman et al 2005). Mammalian homolog of Dnm1 is called Drp1. Loss of Drp1 causes embryonic lethality in worms (Labrousse et al 1999) and mice (Ishihara et al 2009, Wakabayashi et al 2009). Altered Drp1 function has also been linked to a variety of diseases, including

Parkinson's disease (Wang et al 2011), Alzheimer's disease (Wang et al 2008), and Huntington's disease (Costa et al 2010).

Like bacteria, the endosymbiotically-originated chloroplasts possess FtsZ-like division machinery that requires a DLP, ARC5/DRP5, for final constriction of chloroplast membranes. Chloroplast division in plants such as *Arabidopsis thaliana* is a highly regulated process that involves tethering of the inner and outer chloroplast membranes and finally constricting them to give rise to two daughter plastids. Tethering of the two membranes is achieved by formation of polymeric rings. The inner dividing ring is an assembly of FtsZ homologs, FtsZ1 and FtsZ2, at the mid-plastid region positioned by plant min system that comprises of MinD1, MinC-like ARC3, MinE1 and MCD1. This assembly is stabilized by the interaction of FtsZ2 to ARC6, an integral inner membrane protein and its paralog, PARC6. ARC6/PARC6 further interacts with integral outer membrane proteins, PDV1 and PDV2. The outer-dividing ring comprises of an assembly of ARC5/DRP5 that is stabilized via interaction with PDV1/PDV2. Thus, PDV1/PDV2 and ARC6/PARC6 act as connectors between the inner and outer-dividing rings of chloroplasts. DRP5 provides a motive force for membrane constriction, thus enabling chloroplast division. Finally, other cytoplasmic proteins, CLMP1 and CRL, induce plastid separation by mediating chloroplast attachment to the actin cytoskeleton (Osteryoung and Pyke 2014).

DLPs are also known to regulate peroxisome fission in yeast, plant and mammals (Thoms and Erdmann 2005). Yeast cells lacking the vacuolar protein sorting 1 (Vps1) DLP were shown to contain fewer and larger peroxisomes as compared to wild-type cells, indicating that Vps1 is involved in peroxisomal division (Hoepfner et al 2001) upon recruitment by a peroxisomal protein, Pex19 (Vizeacoumar et al 2006). Vps1 is also involved in vacuolar maintenance in yeast. Rothman and Stevens could show that Vps1 lacking yeast fails to deliver carboxypeptidase Y, which travels from the Golgi to late endosomes and then to the vacuole (Rothman and Stevens 1986). In addition, absence of Vps1 led to mis-sorting of Golgi membrane proteins, example kex2 (Nothwehr et al 1995). Hereafter, Vps1 was found to be a

major candidate in regulating intracellular endocytic events between ER and Golgi. The actual mechanism of Vps1 mediated vacuolar fusion is still not clear but it is believed to depend on self-assembly of Vps1, which triggers interaction with SNARE complexes. However, the actual mechanism that targets Vps1 to vacuolar membrane remains to be explored.

4.3 DLPs provide defence against viruses

Mx proteins are well known for their defence against viruses in eukaryotic cells (Haller et al 2015, Verhelst et al 2013). Mx proteins have a conserved GTPase domain, middle domain and highly variable C-terminal domain. The C-terminal domain, also called GTPase effector domain (GED), contains two leucine zippers whose back-folding onto the middle domain promotes Mx oligomerisation, which in turn increases the GTP hydrolysis rate (Haller et al 2007b). The two leucine zippers have the ability to form amphipathic helices that might promote lipid membrane-binding (Schumacher and Staeheli 1998). Mx proteins have high molecular weight and show properties such as self-assembly, low affinity for GTP and high hydrolysis rate (Haller et al 2007b). Discovered and eponymous by the resistance to myxovirus, these proteins turned out to offer resistance not only to RNA viruses but also to a wide range of DNA viruses (Haller et al 2007a) upon interferon stimulation. Mouse Mx1 protein, upon α/β interferon activation, accumulates in the nucleus, the site of orthomyxovirus replication. In the nucleus, it is shown to directly interact with the polymerase PB2 subunit of the influenza virus and block its transcription (Pavlovic et al 1993). Unresolved association of Mx1 with promyelocytic leukemic protein (PML) bodies and components of the SUMO-1 protein modification system have also been observed (Haller et al 2007b). Moreover, Mx1 interacts with interferon-induced ubiquitin-like protein modifier, ISG15 (Zhao et al 2005). Mouse Mx2 occurs mostly in the cytoplasm, which is the site of replication for viral members of *Bunyaviridae* family. However, upon translocation to the nucleus, Mx2 acquires activity against influenza, whereas Mx1 loses anti-viral activity upon translocation to the cytoplasm (Haller et al 2007b). Human MxA protein accumulates in the cytoplasm and is also found in association with the ER. Upon complete induction by

interferon, MxA may constitute up to 1% of total cytosolic proteins (Horisberger 1992). It acts at the post-transcriptional level and exhibits a broader spectrum of anti-viral activity. MxA binds to the nucleocapsid NP protein of Thogoto virus and prevents viral entry into the cell nucleus (Kochs and Haller 1999). It acts against measles virus either by blocking synthesis of viral glycoproteins or RNA production (Schneiderschaulies et al 1994). Human MxB has been recently shown to inhibit HIV-1 by reducing chromosomal integration of viral DNA (Liu et al 2013). Although several antiviral Mx proteins have been identified, no definite mechanism for their function has been elucidated so far. However, Haller and colleagues have proposed a model for antiviral activity of MxA. According to this model, MxA is induced by interferon upon viral attack and oligomerises on intracellular membranes. Formation of large oligomers induces protein stability and enables GTPase activity, as well as viral recognition. Upon interaction with viral nucleocapsid proteins, MxA is thought to form complexes that immobilise viral components (Haller et al 2007b). Thus, Mx class of DLPs, conserved in all vertebrate species, is a proof of existence of defence against viruses.

5. Bacterial dynamin-like proteins (BDLPs)

More than 900 bacterial species have been identified that encode for DLPs. Bacterial dynamin like proteins (BDLPs) are a widely conserved group of proteins whose cellular function still remains ethereal. DLPs are usually present in two copies organised in a single operon on the bacterial genome. A detailed comparison of the structural and functional properties of eukaryotic and bacterial DLPs has been well summarized in a review recently (Bramkamp 2012b). Alignment analysis using the GTPase domain sequences of dynamin members reveals that BDLPs fall into the mitofusin or atlastin class and are only distantly related to classical dynamins (Bramkamp 2012a). From the available data, it can be hypothesized that BDLPs, like their eukaryotic counterparts, participate in membrane remodelling events.

5.1 BDLP1 from *Nostoc punctiforme*

BDLP1 from cyanobacteria, *N. punctiforme* was shown to interact with lipid bilayers and to induce membrane deformations, *in vitro*. BDLP1 is a dynamin-like GTPase with a Michaelis constant (K_m) of 68.6 mM and a catalytic rate constant (k_{cat}) of 0.53 min^{-1} (Low and Löwe 2006). Mutation of the well-conserved P-loop lysine (K82A) reduced the GTPase activity of BDLP1 by 15-fold. Cryo-electron microscopy uncovered the nucleotide-free, GDP-bound and lipid-bound crystal structures of this BDLP1 and proposed the protein to be closely related to mitochondrial mitofusins. The GDP-bound BDLP1 structure represents a GTPase head, a four-helix neck and trunk region (GED and middle domain) and a tip region. The region between the middle and GED represents a paddle domain that interacts with lipid bilayers (Figure 2). In the presence of a non-hydrolysable GMP-PNP and liposomes, BDLP1 dimers acquire a T-shaped symmetry around the bilayer to form helical tubes of about 50 nm in diameter. On the basis of results obtained, a BDLP1 polymersation/depolymerisation model for fusion and fission was speculated. According to this model, BDLP1 dimers can undergo conformational changes upon GTP-binding. These changes allow binding of BDLP1 to lipid bilayers via the paddle domain. GTP-binding also accelerates self-oligomerisation of BDLP1 onto lipid bilayers resulting in highly curved membranes and tubes. Nucleotide hydrolysis causes helical disassembly leaving the curved membranes in an unfavourable state. Lipid rearrangement in-between two close membranes could occur at this stage leading to either fusion or fission (Low et al 2009). However, the exact mechanism of membrane fusion and fission by BDLP1 remains elusive.

5.2 IniA, B and C from *Mycobacterium tuberculosis*

The *iniBAC* operon of *Mycobacterium tuberculosis* encodes a dynamin related protein (IniA), which, upon overexpression, was shown to confer resistance to the cell wall acting antibiotics, isoniazid and ethambutol (Colangeli et al 2005). Deletion of *iniA* resulted in increased susceptibility to ethambutol, isoniazid and ethidium bromide. Several multi-drug resistant (MDR) pumps are known to efflux ethidium bromide in *M. tuberculosis*. Therefore,

iniA was thought to be a part of an efflux pump that confers drug tolerance to both isoniazid and ethambutol. IniA is predicted to form hollow multimeric structures at the cell membrane but its role in conferring antibiotic resistance still remains ethereal. Further investigation of biochemical and structural properties of this protein might shed light on its actual mechanism of action.

5.3 DynA from *Bacillus subtilis*

B. subtilis is one of the finest prokaryotic model organisms in cell biology. Its excellent genetic amenability and relatively large cell size (1.0-1.2 μM in length) has provided an insight into the dynamic structure of a single cell organism. It models for studying several gene-protein molecules as well as cell cycle events in bacteria that provide mechanistic implications in the eukaryotic world. Recent discovery in this bacterium is protein DynA, which is speculated to be a bacterial candidate representing other DLPs. Sequence and structural similarity to other dynamin-like proteins led to the investigation of dynamin-specific properties of DynA such as GTPase activity, oligomerisation and membrane-binding.

DynA is a 136 KDa GTPase protein. It is a two-headed DLP with two separate GTPase and dynamin-like subunits (Figure 2), which suggest DynA to be a product of gene duplication and fusion events. Both fragments, D1 and D2 share 27% similarity and are united in a single-polypeptide. When modelled with I-Tasser, the D1 and D2 subunits showed high structural similarity with BDLP1, except for the lack of paddle region in D2 (Figure 2). A thorough biochemical analysis of DynA was performed previously (Bürmann et al 2011b). Size exclusion analysis of 6X His-tagged variants of DynA, D1/D2 subunits and the respective P-loop mutants suggested that the protein is able to form dimers and high-molecular weight polymers, demonstrating its oligomerisation capability, like other DLPs. DynA is unique, since it encodes two separate GTPase domains on a single polypeptide. Each GTPase molecule has 4 well-conserved GTP binding-motifs – G1, G2, G3 and G4. G1 binds to the γ -phosphate of NTPs, a conserved threonine of G2 regulates the co-ordination of Mg^{2+} cofactor, glycine from G3 binds to the γ -phosphate and a conserved motif (NKxD) in G4 is responsible for GTP

specificity. Mutations in these well-conserved regions affect GTPase activity (Leipe et al 2002, Vetter and Wittinghofer 2001). GTP hydrolysis of wild-type DynA increases with increasing substrate concentrations, as well as in the presence of lipids. DynA has a $K_{0.5}$ of 0.12 μM (± 0.02), a v_{max} of 3.9 min^{-1} (± 0.14) and a Hill-constant of 2.3 (± 0.6) (s.e. $n=3$). Its specific activity was found to increase with its increasing concentration. Also, the GTPase activity of DynA with P-loop mutations in both or individual subunits was abolished, indicating a strong intra and inter-molecular interaction between GTPase domains. Interestingly, both mutants with a single mutation in the P-loop were able to bind GTP specifically, whereas the double P-loop mutant does not clearly bind GTP specifically. Thus far, the kinetic data findings illustrate that one intact GTPase domain of DynA is capable of binding GTP, whereas both GTPase domains are required for cooperative GTP hydrolysis. Hence, both subunits are predicted to have an intimate functional relationship (Bürmann et al 2011b). Apart from the kinetic study, localisation study was performed *in vivo* where full-length DynA and the D1 subunit were found to be membrane associated, whereas D2 subunit displayed cytoplasmic localization. DynA appeared as foci on the bacterial membrane as well as at the site of septation. When expressed in yeast cells, DynA could form extensive membrane tethering zones between cellular compartments. Additionally, DynA and D1 proteins demonstrated lipid-membrane binding and tethering *in vitro*. DynA acted as a fusogen when incubated with synthetic liposomes, *in vitro*. This phenomenon is reminiscent of mitochondrial DLPs. However, this fusion process was nucleotide-independent but magnesium dependent (Bürmann et al 2011b). Deletion of *dynA* in *B. subtilis* strain 168 fails to produce any growth or morphological phenotype under standard laboratory conditions. However, the ΔdynA strain was found to be sensitive to salt stress and defective in septa formation upon salt stress, which was analysed by electron microscopy. The ΔdynA strain showed decreased sensitivity to tetracycline, chloramphenicol and kanamycin compared to the wild-type strain (PhD thesis of Suey van Baarle, 2009). These antibiotics are active within the cytosol and block protein elongation. However, no difference in sensitivity between wild-type and ΔdynA

could be observed with spectinomycin, which also targets 30S ribosome to block protein elongation. The decreased sensitivity of $\Delta dynA$ to antibiotics might be caused due to differences in transport and/or diffusion pathway of these compounds and not due to abrogated protein synthesis. The above observations hint towards a role of DynA in bacterial cell membrane remodelling under stress conditions.

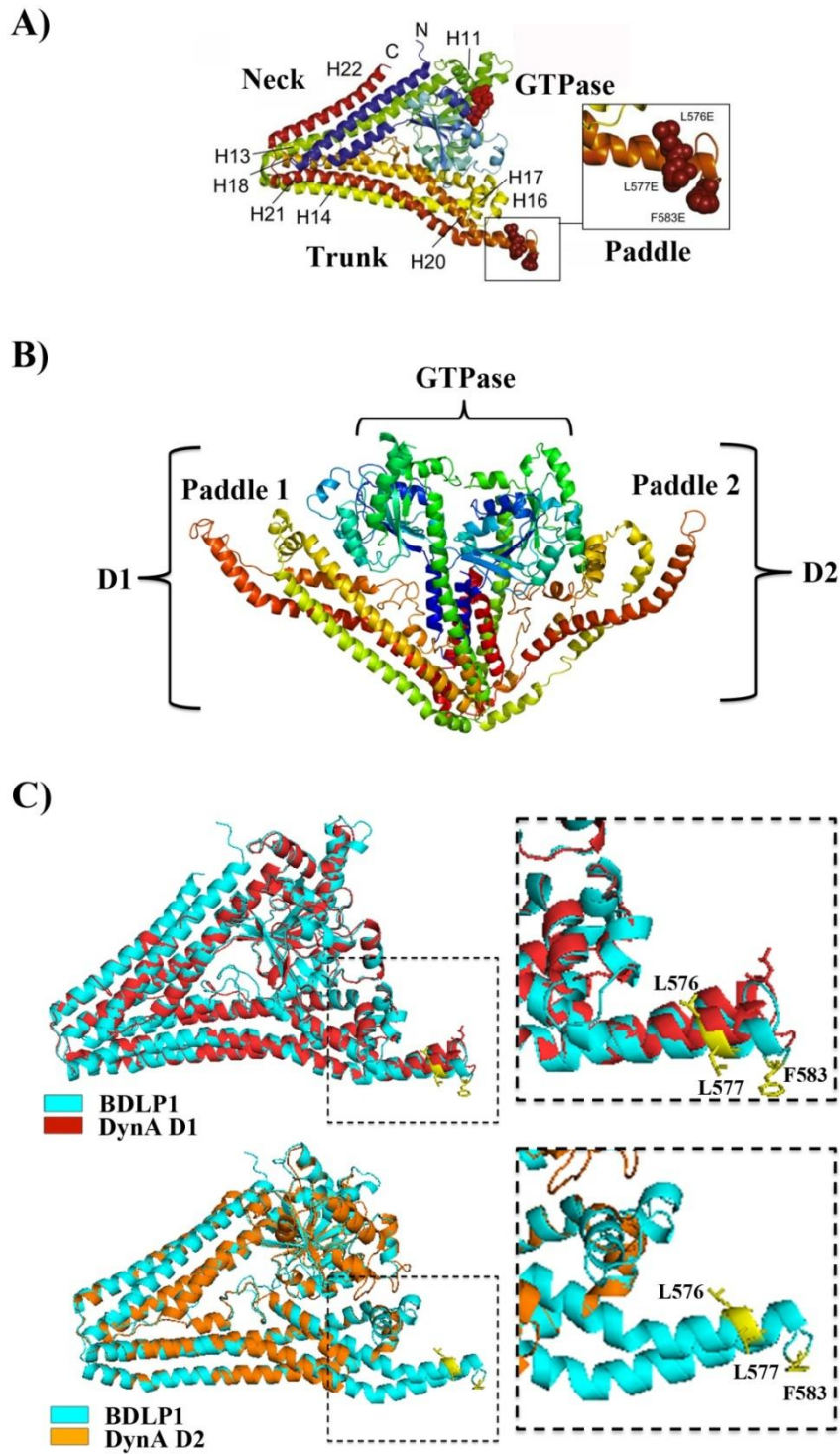


Figure 2. Structural models of BDLPs, BDLP1 and DynA. (A) Annotated BDLP-GDP crystal structure, PDB 2J68, showing paddle surface mutants required for lipid-binding (Low et al 2009). (B) Proposed structural model of DynA using BDLP1 structure as template. (C and D) Structural models of the DynA D1 (C) and D2 (D) domain were build using the I-Tasser platform (Roy et al 2010). The structure of the *N. punctiforme* BDLP (2J68) is used as template. Shown are aligned structures of DynA-D1 (red) and DynA-D2 (orange) with BDLP1 (cyan). Amino acid residues in BDLP1 required for membrane-binding (L576, L577 and F583) are highlighted in yellow.

6. Aims

The first line of defence for bacteria during stress is the cell membrane. Many bacteria have evolved mechanisms that regulate membrane-remodelling events in order to maintain the optimal cell integrity and also to avoid the host immune defences during infection (in the case of pathogens). Some of the most common environmental threat to bacteria (viruses and antibiotics) that have direct influence on the cell membrane and a novel bacterial membrane-defence strategy (DynA) have been discussed in this thesis.

The main aim of this project was to unravel the function of DynA in *B. subtilis*. Deletion of *dynA* in *B. subtilis* strain 168, however, fails to produce any observable growth phenotype under standard laboratory conditions. *B. subtilis* is a soil bacterium with ubiquitous existence and prey to several environmental stress factors to which the lab strain (168) is not exposed. A plausible hypothesis is that the conservation of a DLP might be important to the bacterium under environmental stress conditions, such as bacteriophage infection and antibiotic-induced membrane stress. Taking into account all similarities between DynA and antiviral Mx proteins, it was ideal to analyse if DynA exhibited antiviral activity. Another aim was to address whether DynA, like the homologous BDLP IniA, influences antibiotic-susceptibility in *B. subtilis*. DynA localises at the sites of septation and this localisation was disturbed in the absence of MinJ protein, a component of the Min system in *B. subtilis* that regulates positioning of the site of septation (Bramkamp et al 2008a, Patrick and Kearns 2008). DynA showed a dispersed localisation along the entire cell membrane in a $\Delta minJ$ strain (Bürmann et al 2011a). This altered localisation in a $\Delta minJ$ background would imply its role in bacterial cell division. However, no drastic phenotype was observed in $\Delta dynA$ *B. subtilis*, which might point out the fact of the existence of redundant systems compensating for the loss of DynA. Bacterial multiplication is achieved by cell elongation followed by division at the site of septation, which is the mid-cell region. Membrane fusion is the ultimate step in bacterial cell division. At this stage, several fusogens may play an inductive role by mediating fusion of two

biological membranes. DynA is suspected to be one such potential fusogenic candidate. However, its role in cell division is not known.

Apart from functional characterisation, mutational analysis on DynA was performed to have a better understanding of the coordination between two bacterial DLPs that exist as a single copy, a phenomenon that is anti-parallel to eukaryotic DLPs. Both subunits of DynA, D1 and D2, are suspected to modulate self-interaction, which is a representative characteristic of eukaryotic DLPs. This interaction is hampered when either of the subunit is mutated suggesting their strong communication. This work aims to analyse the GTPase activity of DynA with various mutants to enable a better understanding of oligomerisation, nucleotide binding, as well as inter/ intra-molecular cooperativity between two subunits. Also, it was important to analyze the membrane-binding behaviour of DynA, *in vivo* and *in vitro*, along with protein dynamics across the bacterial membrane. Full-length DynA and the D1 subunit localises to *B. subtilis* membrane as distinct foci and at the site of septation. In yeast, it localises homogenously throughout the membrane. Sequence analysis suggested that DynA lacks any transmembrane region, which is necessary for membrane integration. DLPs are shown to bind lipid molecules via its PH or paddle domain. Therefore, one could speculate that DynA binds membranes via mediator proteins and then interact with lipids via aminoacid residues in its paddle domain to disrupt membrane structure and mediate fusion. Dynamins molecules such as human dynamin1 and BDLP1 from *Nostoc punctiforme* oligomerise to form a helical assembly around lipid tubes. Upon GTP addition, helical assembly undergoes change depending on the structure of lipid membrane resulting in constriction of the assembly if the lipid template is flexible or compaction of the dynamin helix if the lipid template is rigid (Faelber et al 2011). Therefore, lipid-binding affinity of DynA under varying conditions is worth testing. This will help us identify DynA's target on biological membranes.

Further, the thesis also aimed at characterising potential DynA-interacting partners to unravel a prospective DynA-interactome. A bacterial two-hybrid screening was performed

previously and identified YneK, YmdA and YwpG as potential candidates, all of which are membrane-associated proteins. YmdA is an essential RNase protein involved in processing of glycolytic mRNA (Commichau et al 2009) whereas YneK and YwpG are uncharacterised proteins. This project aims to carry out localisation studies of DynA and its physical interactors in the presence and absence of each other to enlighten protein-protein interactions and explain the upstream and downstream pathway members, of which DynA is a part.

Finally, studies directed towards DLPs using simple and extensively studied bacterial models such as *E. coli* and *B. subtilis* will not only provide mechanistic implications of dynamin members in different cellular pathways but also simplify the evolutionary relationship between eukaryotic and prokaryotic dynamins.

Material and Methods

1. Materials

1.1 Chemicals, enzymes and expendables

All materials were obtained from Avanti Polar Lipids, Carl Roth, GE Healthcare, Macherey-Nagel, Merck, Operon, Sigma-Aldrich, Thermo scientific or Roche. Enzymes were obtained from Invitrogen, Fermentas or New England Biolabs.

1.2 Media and Buffers

Table 1. Media and buffers used in this work

Medium	Contents	pH
LB	10 g/L tryptone, 5 g/L yeast extract, 10 g/L NaCl	7
LB agar	10 g/L tryptone, 5 g/L yeast extract, 10 g/L NaCl, 15 g/L Agar	7
10 X Phosphate citrate (PC) buffer	107 g K ₂ HPO ₄ (dibasic anhydrous), 60 g KH ₂ PO ₄ (monobasic anhydrous), 10 g Sodium citrate 2H ₂ O, dH ₂ O to 1L	7
MD	10 X PC 1 mL, 40% glucose 500 µL, 0.2% L-tryptophan 250 µL, 2.2 mg/mL ferric ammonium citrate 50 µL, 50 mg/mL L-aspartate 500 µL, 1M MgSO ₄ 30 µL, dH ₂ O to 10 mL. Adjust pH with KOH	7
NA	13 g/L Nutrient Broth (Oxoid) powder, 15 g/L Agar	7
0.6% Overlay agar	5 g/L tryptone, 2.5 g/L yeast extract, 5 g/L NaCl, 6 g/L Agar	7
Solution G	25.0 g casein hydrolysate, 9.2 g L-glutamic acid, 3.125 g L-alanine, 3.48 g L-asparagine, 3.4 g KH ₂ PO ₄ , 1.34 g NH ₄ Cl, 0.27 g Na ₂ SO ₄ , 0.24 g NH ₄ NO ₃ , 2.45 mg FeCl ₃ ·6H ₂ O, dH ₂ O 2.35 L	7
CH	50 ml solution G, 0.05 ml 0.1 M CaCl ₂ , 0.02 ml 1 M MgSO ₄ ·7H ₂ O, 0.1 ml 0.0475 M MnSO ₄ , 0.5 ml 2 mg/mL tryptophan	7
Phage buffer	7 g Na ₂ HPO ₄ anhydrous, 3 g KH ₂ PO ₄ anhydrous, 5 g NaCl, 10 ml 0.1 M MgSO ₄ , 10 ml 0.1 M CaCl ₂ , dH ₂ O to 1 L	7

T2	50 mM Tris, 200 mM NaCl, 10 % glycerol	8
T5	50 mM Tris, 500 mM NaCl, 10 % glycerol	8

1.3 Antibiotics

Table 2. Antibiotics and the end concentrations used in this work

Antibiotic	<i>E. coli</i>	<i>B. subtilis</i>
Carbenicillin	50 µg/ml	-
Chloramphenicol	-	5 µg/ml
Kanamycin	50 µg/ml	5 µg/ml
Erythromycin	-	1 µg/ml
Spectinomycin	-	50 µg/ml
Tetracycline	-	10 µg/ml

1.4 Oligonucleotides

Table 3. Oligonucleotides used in this work

Number	Name	Sequence
FBE 33	ypbR 200 bps UP	GAATTCGATCCGGGGTTTTTTCTCAAGTCTGAACCCCTTTGTGC
FBE 36	ypbR 200 bps DO	AAGGCTCATCGTTTCTGCATTTAGC
PSP 8	Tet R	GAGAAAAAACCCCGGATCGAATTCTATTGTTGTATAAGTGATGA
PSP 9	Tet F	TCAGTTAGCTAGCTGAGCTCGAGTTAGAAATCCCTTTGAGAAT
PSP 10	YneK xhoI F	CATCTCGAGATGCTGGAAGGATGGTTTTTATG
PSP 11	YneK hinIII R	CATAAGCTTTTTGAGAAGGGTCTGATAAGG

PSP 13	YmdA EcoRI R	CATGAATTCTTTTGCATACTCTACGGCTC
PSP 14	YwpG xhoI F	CATCTCGAGATGAATCAATTTTCGTTTAAAAG
PSP 15	YmdA (SalI)F	CATGTCGACATGACCCCAATTATGATGG
PSP 17	YwpG hindIII R	CATAAGCTTGCCTCTGTTTTTATC
PSP 37	Δ496-500 ypbr F	GCCGCGGCCCTTCAAGAACAGGCACG
PSP 38	Δ496-500 ypbr R	GGCCGCGGCTGATTCTTGGACGAGCC
PSP 43	K497E F	CTCGTCCAAGAATCAGAAGAACTTGTCTTTCTTCAAG
PSP 44	K497E R	CTTGAAGAAAGACAAGTTCTTCTGATTCTTGGACGAG
PSP 45	L498Q F	GTCCAAGAATCAGAAAAACAGGTCTTTCTTCAAGAACAGG
PSP 46	L498Q R	CCTGTTCTTGAAGAAAGACCTGTTTTTCTGATTCTTGGAC
PSP 47	V499Q F	GTCCAAGAATCAGAAAACTTCAGTTTCTTCAAGAACAGGCACG
PSP 48	V499Q R	CGTGCCTGTTCTTGAAGAACTGAAGTTTTTCTGATTCTTGGAC
PSP 51	L501Q F	CAGAAAACTTGTCTTTCAGCAAGAACAGGCACGTTTAG 3'
PSP 52	L501Q R	CTAAACGTGCCTGTTCTTGCTGAAAGACAAGTTTTTCTG 3'
PSP 53	R506A F	CTTTCTTCAAGAACAGGCAGCTTTAGAGAATAATGCCCC
PSP 54	R506A R	CGGGCATTATTCTCTAAAGCTGCCTGTTCTTGAAGAAAG
PSP 55	R512A F	GTTTAGAGAATAATGCCGCAGAGAAAACCGATCGC
PSP 56	R512A R	GCGATCGGTTTTCTCTGCGGCATTATTCTCTAAAC
PSP 61	K514A F	GAATAATGCCCGAGAGGCGACCGATCGCCTGTGG 3'
PSP 62	K514A R	CCACAGGCGATCGGTGCCTCTCGGGCATTATTC 3'
PSP 63	R517A F	CGAGAGAAAACCGATGCGCTGTGGGCCATTTGG
PSP 64	R517A R	CCAAATGGCCCACAGCGCATCGGTTTTCTCTCG
PSP 65	W519A F	GAAAACCGATCGCCTGGCGGCCATTTGGGAAGAAG
PSP 66	W519A R	CTTCTTCCCAAATGGCCGCCAGGCGATCGGTTTTTC

PSP 67	W522A F	CCTGTGGGCCATTGCGGAAGAAGAGTC
PSP 68	W522A R	GACTCTTCTTCCGCAATGGCCCACAGG
PSP 69	W536A F	CCAATGCATATAGACACAGAAGCCTTTAAATCGAAGAAAAACAAG
PSP 70	W536A R	CTTGTTTTCTTCGATTTAAAGGCTTCTGTGTCTATATGCATTGG
PSP 73	Pxyl F	TTCATGAAAACTAAAAAAATATTG
PSP 74	Pxyl R	TATGTCATATTGTAAGTAAGTTGCAC
PSP 89	78 bps Up ypbR (SalI)	CGTGTGACGTGTAAAATGAAAAG
PSP 101	K56A F	CCGGGCATTATTCAGCGGGGGCATCGTCACTGCTG
PSP 102	K56A R	CAGCAGTGACGATGCCCCGTAATAATGCCCCG
PSP 106	YflN UP F (AatII)	GCCGA GACGTCTAACCGTACTGTTTGTTCATT
PSP 107	YflN UP R (Sacl)	CGA GAGCTCAATGACACCTCCGGAATGTT
PSP 108	YflN DO F (EcoRV)	GCCGA GATATC TGACACCCGCACCACGCGGG
PSP 109	YflN DO R (NotI)	CGA GCGGCCGCCAGCCGAGCTCTTCGCAGGC
PSP 110	YukF UP F (AatII)	GCCGA GACGTC AATACTTCTTGGCTTTCAAC
PSP 111	YukF UP R (Sacl)	CGA GAGCTC CTCATCCCCTTCTTTTATT
PSP 112	YukF DO F (EcoRV)	GCCGA GATATCTAATCAAACAAAGAATTTTC
PSP 113	YukF DO R (NotI)	CGA GCGGCCGCACAACGCCTCCTCCGATAAT
PSP 118	Mfd UP F (AatII)	GCCGA GACGTC AGGGCACAATGGCATCAAAT
PSP 119	Mfd UP R (Sacl)	CGA GAGCTC ATGGCCCCTCCTCTCTGTTT
PSP 120	Mfd DO F (EcoRV)	GCCGA GATATC TAAATTTTGTACTCTCTGG
PSP 121	Mfd DO R (NotI)	CGA GCGGCCGC ATCTTTTGAAAAGATCACCA
PSP 124	Δ518-522 F	GAGGAG GAA GAA GAG TCC GCA TGC CCA
PSP 125	Δ518-522 R	CTCCTC GCGATCGGTTTTCTCTCGGGCATT
PSP 126	Δ591-620 F	C ATT TTA GGC GAA TTT AGC TCG GGG AAA TCA TCA

PSP 127	Δ591-620 R	CCCCGAGCTAAATTCGCCTAAAATGTCAGAC
PSP 128	Δ594-596 F	GAA TGC AGC ATG CAA ACT TCA GCG TTT CG
PSP 129	Δ594-596 R	CTGAAGTTTGCATGCTGCATTTCGCCTAAAATG
PSP 130	Δ601-608 F	CT TCA GCG GAG GAA CGG AAA TTT ACA C
PSP 131	Δ601-608 R	CCGTTCCCTCCGCTGAAGTTTGCTTTAAC
PSP 132	Δ611-613 F	CTT GAG GAA ACA CTC GCT CTT TTT GGA G
PSP 133	Δ611-613 R	GAGCGAGTGTTTCCTCAAGCCTTTTC
PSP 134	Δ579-581 F	GAC CAA ATC TAC ACT TTG TCT GACATT TTA GG
PSP 135	Δ579-581 R	CAAAGTGTAGATTTGGTCTTGAAGCGG
PSP 144	Ypb UP (AatII) F	GCCGA GACGTCGAAAAAATCAAATATACATAG
PSP 145	Ypb UP (SacI) R	CGA GAGCTCGAGTCAGGCCCTTTTCC
PSP 146	ypb DO (SalI) F	GCGCGTCTGACTAAGCTGGATGATCCTG
PSP 147	ypb DO (NotI) R	CGA GCGGCCGCTGCGGAATCAGCTC
PSP 152	FBE133 correction F	CAA AAC AGA AAA GAG CTT TTG C
PSP 153	FBE133 correction R	CTCTTTTCTGTTTTGATCTGTCAT
PSP 177	200 bps up yukF	AGTCTTGCCTCCGATGACTTTC
PSP 178	200 bps do yukF	AGAGTTGTATATTCCGCCAAAAGC

1.5 Plasmids

Table 4. Plasmids used in this study

Number	Plasmid	Description/Source
FBE152	<i>WT dynA-GFP</i>	Diploma thesis of Frank Bürmann
PSC 2	<i>pUT18 zip</i>	Euromedex
PSC 3	<i>pKT zip</i>	Euromedex

PSC 4	<i>pUT18c WT dynA</i>	Diploma thesis of Frank Bürmann
PSC 5	<i>pKT25c WT dynA</i>	Diploma thesis of Frank Bürmann
PSC 6	<i>pUT18c minJ</i>	Diploma thesis of Frank Bürmann
PSC 7	<i>pKT25c ezrA</i>	Diploma thesis of Frank Bürmann
PSC 8	<i>pKT25 yneK</i>	Diploma thesis of Frank Bürmann
PSC 9	<i>YneK-gfp</i>	Xylose inducible C-terminal GFP fusion in pSG1154 (this work)
PSC 10	<i>YmdA-gfp</i>	Xylose inducible C-terminal GFP fusion in pSG1154 (this work)
PSC 11	<i>YwpG-gfp</i>	Xylose inducible C-terminal GFP fusion in pSG1154 (this work)
PSC 12	<i>YwpG-gfp</i>	Xylose inducible N-terminal GFP fusion in pSG1154 (this work)
PSC 13 (FBE036)	<i>Wt dynA-his</i>	Diploma thesis of Frank Bürmann
PSC 14	<i>Δ496-500 dynA-his</i>	Site-directed mutagenesis on plasmid FBE036 (this work)
PSC 15	<i>Δ511-522 dynA-his</i>	Site-directed mutagenesis on plasmid FBE036 (this work)
PSC 16	<i>R506A dynA-his</i>	Site-directed mutagenesis on plasmid FBE036 (this work)
PSC 17	<i>R512A dynA-his</i>	Site-directed mutagenesis on plasmid FBE036 (this work)
PSC 18	<i>R517A dynA-his</i>	Site-directed mutagenesis on plasmid FBE036 (this work)
PSC 19	<i>WT dynA-GFP</i> (FBE152)	Diploma thesis of Frank Bürmann
PSC 20	<i>Δ496-500 dynA-GFP</i>	Site-directed mutagenesis on plasmid FBE152 (this work)
PSC 21	<i>Δ511-522 dynA-GFP</i>	Site-directed mutagenesis on plasmid FBE152 (this work)
PSC 22	<i>K497E dynA-GFP</i>	Site-directed mutagenesis on plasmid FBE152 (this work)
PSC 23	<i>L498Q dynA-GFP</i>	Site-directed mutagenesis on plasmid FBE152 (this work)
PSC 24	<i>V499Q dynA-GFP</i>	Site-directed mutagenesis on plasmid FBE152 (this work)
PSC 25	<i>R506A dynA-GFP</i>	Site-directed mutagenesis on plasmid FBE152 (this work)
PSC 26	<i>R512A dynA-GFP</i>	Site-directed mutagenesis on plasmid FBE152 (this work)
PSC 27	<i>K514A dynA-GFP</i>	Site-directed mutagenesis on plasmid FBE152 (this work)
PSC 28	<i>W522A dynA-GFP</i>	Site-directed mutagenesis on plasmid FBE152 (this work)
PSC 29	<i>W536A dynA-GFP</i>	Site-directed mutagenesis on plasmid FBE152 (this work)
PSC 30	<i>ΩymdA</i>	pGP774 (Commichau et al 2009)

PSC 32	<i>RBS-dynA-pJPR1</i>	For DynA complementation at <i>amyE</i> (this work)
PSC 34	<i>Δ496-500 RBS-dynA-pJPR1</i>	Site-directed mutagenesis on plasmid PSC32 (this work)
PSC 35	<i>R512A RBS-dynA-pJPR1</i>	Site-directed mutagenesis on plasmid PSC32 (this work)
PSC 36	<i>Δ511-522 RBS-dynA-pJPR1</i>	Site-directed mutagenesis on plasmid PSC32 (this work)
PSC 37	<i>ΔyflN</i>	(this work)
PSC 38	<i>ΔyukF</i>	(this work)
PSC 39	<i>Δmfd</i>	(this work)
PSC 40	<i>K56A RBS-dynA-pJPR1</i>	Site-directed mutagenesis on plasmid PSC32 (this work)
PSC 42	<i>ΔypbQRS</i>	(this work)
PSC 44	<i>Δ579-581 dynA-GFP</i>	Site-directed mutagenesis on plasmid FBE152 (this work)
PSC 45	<i>Δ591-620 dynA-GFP</i>	Site-directed mutagenesis on plasmid FBE152 (this work)
PSC 46	<i>Δ594-596 dynA-GFP</i>	Site-directed mutagenesis on plasmid FBE152 (this work)
PSC 47	<i>Δ601-608 dynA-GFP</i>	Site-directed mutagenesis on plasmid FBE152 (this work)
PSC 48	<i>Δ611-613 dynA-GFP</i>	Site-directed mutagenesis on plasmid FBE152 (this work)
PSC 49	<i>Δ579-581 dynA-his</i>	Site-directed mutagenesis on plasmid FBE036 (this work)
PSC 50	<i>Δ591-620 dynA-his</i>	Site-directed mutagenesis on plasmid FBE036 (this work)
PSC 51	<i>Δ594-596 dynA-his</i>	Site-directed mutagenesis on plasmid FBE036 (this work)
PSC 52	<i>Δ601-608 dynA-his</i>	Site-directed mutagenesis on plasmid FBE036 (this work)
PSC 53	<i>Δ611-613 dynA-his</i>	Site-directed mutagenesis on plasmid FBE036 (this work)
PSC 54	<i>D1-yfp (pSG1193)</i>	FBE133 corrected for R6S mutation (this work)
PSC 55	<i>Δ518-522 dynA-GFP</i>	Site-directed mutagenesis on plasmid FBE152 (this work)
PSC 56	<i>511-522 D1-yfp (pSG1193)</i>	Site-directed mutagenesis on plasmid PSC054 (this work)
PSC 57	<i>518-522 D1-yfp (pSG1193)</i>	Site-directed mutagenesis on plasmid PSC054 (this work)
PSC 58	<i>537-43 D1-yfp (pSG1193)</i>	Site-directed mutagenesis on plasmid PSC054 (this work)
PSC 60	<i>ΔypbQ</i>	(this work)

1.6 *E. coli* strains

Table 5. *E. coli* strains used in this study

Name	Genotype	Source
DH5 α	F ⁻ ϕ 80 <i>lacZ</i> .M15 .(<i>lacZYA-argF</i>)U169 <i>recA1 endA1 hsdR17</i> (rk-, mk+) <i>phoA supE44 thi-1 gyrA96 relA1</i> λ -	Invitrogen
XL1-Blue	<i>recA1 endA1 gyrA96 thi-1 hsdR17 supE44 relA1 lac</i> [F <i>proAB lacI</i> q. ZAM15 Tn10 (Tet r.)]	Stratagene
BTH101	F ⁻ <i>cya-99 araD139 galE15 galK16 rpsL1</i> (Strr) <i>hsdR2 mcrA1 mcrB1</i>	Euromedex
BL21(DE3)	F ⁻ <i>ompT gal dcm lon hsdSB</i> (r-B m-B)_(DE3 [<i>lacI lacUV5-T7</i> gene 1 <i>ind1 sam7 nin5</i>])	(Studier and Moffatt 1986)

1.7 *B. subtilis* strains

Table 6. *B. subtilis* strains used in this thesis

Strain number	Genotype	Description/Source
***	<i>trpC2</i> (168)	Laboratory stock
NEB006	<i>trpC2, dynA-prom::tet, amyE::pSG1154_dynA-prom-gfp</i>	Master thesis of Nina Ebert
FBB018	<i>trpC2, dynA::tet, amyE::pSG1154_dynA-gfp</i>	Diploma thesis of Frank Bürmann
PSB001	<i>trpC2, amyE::yneK-GFP</i>	Strain WT 168 transformed with plasmid PSC 9
PSB002	<i>trpC2, amyE::ywpGc-GFP</i>	Strain WT 168 transformed with plasmid PSC 11
PSB003	<i>trpC2, amyE::ymdA-GFP</i>	Strain WT 168 transformed with plasmid PSC 10
PSB004	<i>trpC2, dynA::tet, amyE::yneK:GFP</i>	Strain PSB001 transformed with gDNA from FBB002
PSB005	<i>trpC2, dynA::tet, amyE::ywpG:GFP</i>	Strain PSB002 transformed with gDNA from FBB002
PSB006	<i>trpC2, dynA::tet, amyE::ymdA-GFP</i>	Strain PSB003 transformed with gDNA from FBB002

PSB007	<i>trpC2, minJ::tet, amyE::yneK::GFP</i>	Strain PSB001 transformed with gDNA from $\Delta minJ$
PSB008	<i>trpC2, minJ::tet, amyE::ywpG::GFP</i>	Strain PSB002 transformed with gDNA from $\Delta minJ$
PSB009	<i>trpC2, minJ::tet, amyE::ymdA::GFP</i>	Strain PSB003 transformed with gDNA from $\Delta minJ$
PSB010	<i>trpC2, ezrA::cam, dynA::tet, amyE::dynA-GFP-spec</i>	Strain FBB018 transformed with gDNA from $\Delta ezrA$
PSB011	<i>trpC2, ezrA::cam, dynA::tet</i>	Strain FBB002 transformed with gDNA from $\Delta ezrA$
PSB016	<i>trpC2, dynA::tet, amyE::dynA ($\Delta 496-500$)-GFP-spec</i>	Strain FBB002 transformed with plasmid PSC 20
PSB017	<i>trpC2, dynA::tet, amyE::dynA (K497E)-GFP-spec</i>	Strain FBB002 transformed with plasmid PSC 22
PSB018	<i>trpC2, dynA::tet, amyE::dynA (L498Q)-GFP-spec</i>	Strain FBB002 transformed with plasmid PSC 23
PSB019	<i>trpC2, dynA::tet, amyE::dynA (V499Q)-GFP-spec</i>	Strain FBB002 transformed with plasmid PSC 24
PSB020	<i>trpC2, dynA::tet, amyE::dynA (R506A)-GFP-spec</i>	Strain FBB002 transformed with plasmid PSC 25
PSB021	<i>trpC2, dynA::tet, amyE::dynA (R512A)-GFP-spec</i>	Strain FBB002 transformed with plasmid PSC 26
PSB022	<i>trpC2, dynA::tet, amyE::dynA (W536A)-GFP-spec</i>	Strain FBB002 transformed with plasmid PSC 29
PSB023	<i>trpC2, dynA::tet, amyE::dynA ($\Delta 511-522$)-GFP-spec</i>	Strain FBB002 transformed with plasmid PSC 21
PSB025	25152 (WT)	DSMZ
PSB026	25152, <i>dynA::tet</i>	Strain PSB025 transformed with gDNA from FBB002
PSB027	<i>trpC2, dynA::tet, amyE::dynA (K514A)-GFP-spec</i>	Strain FBB002 transformed with plasmid PSC 27
PSB028	<i>trpC2, pspA::cam, liaH::kan</i>	(Wolf et al 2010)
PSB029	<i>trpC2, pspA::cam, liaH::kan, dynA::tet</i>	Strain PSB028 transformed with gDNA from FBB002
PSB030	<i>trpC2, dynA::tet, amyE::dynA (W522A)-GFP-spec</i>	Strain FBB002 transformed with plasmid PSC 28
PSB032	<i>trpC2, dynA::tet, amyE::RBS-dynA-cam</i>	Strain FBB002 transformed with plasmid PSC 32
PSB033	25152, <i>dynA::tet, amyE::RBS-dynA-cam</i>	Strain PSB026 transformed with plasmid PSC 28
PSB034	25152, <i>dynA::tet, amyE::RBS-dynA ($\Delta 496-500$)-cam</i>	Strain PSB026 transformed with plasmid PSC 34

PSB035	<i>trpC2, dynA::tet, amyE::RBS-dynA (R512A)-cam</i>	Strain FBB002 transformed with plasmid PSC 35
PSB038	<i>trpC2, dynA::tet, amyE::RBS-dynA (Δ496-500)-cam</i>	Strain FBB002 transformed with plasmid PSC 34
PSB039	<i>trpC2, dynA::tet, amyE::RBS-dynA (Δ511-522)-cam</i>	Strain FBB002 transformed with plasmid PSC 36
PSB040	<i>trpC2, dynA::tet, amyE::RBS-dynA (K56A)-cam</i>	Strain FBB002 transformed with plasmid PSC 40
PSB041	<i>trpC2, dynA::tet, amyE::RBS-dynA-cam, yukF::kan</i>	Strain PSB032 transformed with plasmid 38
PSB042	<i>trpC2, dynA::tet, amyE::RBS-dynA-cam, yf1N::kan</i>	Strain PSB032 transformed with plasmid 37
PSB043	<i>25152, dynA::tet, amyE::RBS-dynA (Δ496-500)-cam</i>	Strain PSB026 transformed with plasmid PSC 34
PSB044	<i>25152, dynA::tet, amyE::RBS-dynA (Δ511-522)-cam</i>	Strain PSB026 transformed with plasmid PSC 36
PSB045	<i>25152, dynA::tet, amyE::RBS-dynA(R512A)-cam</i>	Strain PSB026 transformed with plasmid PSC 35
PSB046	<i>25152, dynA::tet, amyE::RBS-dynA (K56A)-cam</i>	Strain PSB026 transformed with plasmid PSC 40
PSB047	<i>trpC2, yf1N::kan</i>	Strain 168 WT transformed with gDNA from PSB042
PSB048	<i>trpC2, dynA::tet, yf1N::kan</i>	Strain FBB002 transformed with gDNA from PSB042
PSB049	<i>trpC2, dynA::tet, amyE::RBS-dynA-cam, yf1N::kan</i>	Strain PSB032 transformed with gDNA from PSB042
PSB050	<i>trpC2, yukF::kan</i>	Strain 168 WT transformed with gDNA from PSB041
PSB051	<i>trpC2, dynA::tet, yukF::kan</i>	Strain FBB002 transformed with gDNA from PSB041
PSB052	<i>trpC2, dynA::tet, amyE::RBS-dynA-cam, yukF::kan</i>	Strain PSB032 transformed with gDNA from PSB041
PSB053	<i>trpC2, dynA::tet, yf1N::kan, amyE::Prom-dynA-GFP-spec</i>	Strain PSB048 transformed with gDNA from NEB006
PSB054	<i>trpC2, dynA::tet, yukF::kan, amyE::Prom-dynA-GFP-spec</i>	Strain PSB051 transformed with gDNA from NEB006 (Prom = promoter)
PSB055	<i>trpC2, dynA::tet, amyE::dynA (Δ518-522) - GFP-spec</i>	Strain FBB002 transformed with plasmid PSC 55
PSB057	<i>trpC2, dynA::tet, mfd::kan, amyE::Prom-dynA-GFP-spec</i>	Strain NEB006 transformed with gDNA from PSB056
PSB058	<i>trpC2, mfd::kan</i>	Strain 168 WT transformed with gDNA from PSB056
PSB059	<i>trpC2, dynA::tet, mfd::kan</i>	Strain FBB002 transformed with gDNA from PSB056

PSB060	<i>trpC2, dynA::tet, amyE::RBS-dynA-cam, mfd::kan</i>	Strain PSB032 transformed with gDNA from plasmid PSC 39
PSB061	<i>trpC2, dynA::tet, amyE::dynA (Δ591-620)-GFP-spec</i>	Strain FBB002 transformed with plasmid PSC 45
PSB062	<i>trpC2, dynA::tet, amyE::dynA (Δ601-608)-GFP-spec</i>	Strain FBB002 transformed with plasmid PSC 47
PSB063	<i>trpC2, dynA::tet, amyE::dynA (Δ611-613)-GFP-spec</i>	Strain FBB002 transformed with plasmid PSC 48
PSB064	<i>trpC2, dynA::tet, amyE::dynA (Δ594-596)-GFP-spec</i>	Strain FBB002 transformed with plasmid PSC 46
PSB065	<i>trpC2, dynA::tet, amyE::dynA (Δ579-581)-GFP-spec</i>	Strain FBB002 transformed with plasmid PSC 44
PSB066	<i>trpC2, ezrA::cam</i>	(Haeusser et al 2004)
PSB067	<i>25152, mfd::kan</i>	Strain PSB025 transformed with gDNA from PSB058
PSB068	<i>25152, dynA::tet, mfd::kan</i>	Strain PSB026 transformed with gDNA from PSB058
PSB069	<i>25152, dynA::tet, amyE::RBS-dynA-cam, mfd::kan</i>	Strain PSB033 transformed with gDNA from PSB058
PSB070	<i>25152, dynA::tet, amyE::RBS-K56A dynA-cam</i>	Strain PSB026 transformed with plasmid PSC 40
PSB071	<i>25152, ypbQRS::cam</i>	Strain PSB025 transformed with plasmid PSC 42
PSB072	<i>trpC2, ypbQRS::cam</i>	Strain WT 168 transformed with plasmid PSC 42
PSB073	<i>25152, ypbQRS::cam, amyE::dynA-GFP-spec</i>	Strain PSB071 transformed with plasmid FBE152
PSB075	<i>25152, dynA::tet, amyE::dynA-GFP-spec</i>	Strain PSB026 transformed with plasmid FBE152
PSB079	<i>trpC2, dynA::tet, amyE::dynA (Δ537-453)-GFP-spec</i>	Strain FBB002 transformed with plasmid PSC 61
PSB080	<i>trpC2, dynA::tet, amyE::dynA D1-YFP-spec</i>	Strain FBB002 transformed with plasmid PSC 54
PSB081	<i>trpC2, dynA::tet, amyE::dynA (Δ511-522) D1-YFP-spec</i>	Strain FBB002 transformed with plasmid PSC 56
PSB082	<i>trpC2, dynA::tet, amyE::dynA (Δ518-522) D1-YFP-spec</i>	Strain FBB002 transformed with plasmid PSC 57
PSB083	<i>trpC2, dynA::tet, amyE::dynA (Δ537-543) D1-YFP-spec</i>	Strain FBB002 transformed with plasmid PSC 58
PSB084	<i>trpC2, dynA::tet, amyE::dynA-GFP-spec, mfd::kan</i>	Strain FBB018 transformed with gDNA from PSB058
PSB085	<i>trpC2, ypbQRS::cam, amyE::dynA-GFP-spec</i>	Strain PSB072 transformed with plasmid FBE152

PSB086	<i>trpC2, pspA::cam, liaH::kan, dynA::tet, amyE::dynA-GFP-spec</i>	Strain PSB029 transformed with plasmid FBE152
PSB087	<i>B. subtilis, CU1065</i>	Personal communication with Thorsten Mascher
PSB088	<i>CU1065, pspA::cam</i>	Strain CU1065 transformed with gDNA from PSB028
PSB089	<i>CU1065, liaH::kan</i>	Strain CU1065 transformed with gDNA from PSB028
PSB090	<i>trpC2, liaH::liaH-mRFP ruby</i>	Personal communication with Thorsten Mascher
PSB091	<i>trpC2, pspA::pspA-GFP</i>	Personal communication with Thorsten Mascher
PSB092	<i>trpC2, P_{lial}-lux</i>	Personal communication with Thorsten Mascher
PSB093	<i>trpC2, P_{pspA}-lux</i>	Personal communication with Thorsten Mascher
PSB094	<i>trpC2, amyE::Pxyl-accDA-spec</i>	(Mercier et al 2013)
PSB095	<i>trpC2, pspA::cam</i>	Strain WT 168 transformed with gDNA from strain PSB028
PSB096	<i>trpC2, pspA::cam, dynA::tet</i>	Strain PSB095 transformed with gDNA from strain FBB002
PSB097	<i>trpC2, liaH::kan</i>	Strain WT 168 transformed with gDNA from strain PSB028
PSB098	<i>trpC2, pspA::pspA-GFP, dynA::tet</i>	Strain PSB091 transformed with gDNA from strain FBB002
PSB099	<i>trpC2, amyE::Pxyl-accDA-spec, dynA::tet</i>	Strain PSB094 transformed with gDNA from strain FBB002
PSB100	<i>trpC2, amyE::ywpGn-GFP</i>	Strain WT 168 transformed with plasmid PSC 12

2. Cultivation of bacteria

2.1 Storage and growth conditions

For short-term storage, *E. coli* was kept at 4° C and *B. subtilis* at room temperature. For long term storage, 2 ml aliquots containing 20 % glycerol were flash frozen and kept at -80° C. Cultures of *E. coli* and *B. subtilis* were grown at 37° C on LB or NA. *E. coli* was cultivated LB + antibiotic, in glass test-tubes for plasmid isolation. Nutrient broth supplemented with tryptophan was used for growth of *B. subtilis* in baffled flasks.

For growth experiments, *B. subtilis* was cultured from a freshly plated colony in LB supplemented with tryptophan (final concentration of 20 µg/mL) and xylose (final concentration of 0.4%) to an OD₆₀₀ 1.0. Cells were further diluted in fresh medium to an OD₆₀₀ of 0.1 and grown up to OD₆₀₀ 1.0. Antibiotic was then added, at appropriate concentrations, to the growing culture and optical density was measured at appropriate time intervals, all throughout the growth experiments at 600 nm. (nisin 30 µg/mL , bacitracin 200 µg/mL or 250 µg/mL , vancomycin 0.5 µg/mL , gramicidin D 10 µg/mL , daptomycin 15 µg/mL or 20 µg/mL).

2.2 Transformation of *E. coli*

E. coli cells were made competent by divalent cation treatment. Cells were grown overnight until A₆₀₀~0.6 or more in SOB medium at room temperature (RT), harvested by centrifugation at 2500 rpm for 20 minutes and resuspended in chilled TB (10 mM PIPES, 15 mM CaCl₂, 250 mM KCl, 55 mM MnCl₂, pH 6.7/25° C) for 10-15 minutes. Fraction of pelleted cells were resuspended in chilled TB buffer and subjected to 1.4 mL DMSO drop by drop. This cell mixture was incubated on ice for 10 minutes and 200 µl cell aliquots were frozen in liquid nitrogen and stored at -80°C. For every transformation, an aliquot was thawed on ice, incubated with the insert DNA for 30 minutes, heat shocked for 1 minute at 42° C and cooled on ice for 2 minutes. Cells were grown in 800 µl LB and plated onto LB-carbenicillin plates.

2.3 Transformation of *B. subtilis*

B. subtilis can be made competent only in certain media (Dubnau 1991). The minimal synthetic medium of Davies (MD) was used for transformation of *B. subtilis*. The medium contained K₂HPO₄, KH₂PO₄, sodium citrate pentahydrate, ferric ammonium citrate, MgSO₄, L-aspartate, L-tryptophan and glucose. Cells were grown in 10 mL MD + 50 µL 20 % casamino acids and upto E₆₀₀ = 1.5 at 37° C. 10 mL pre-warmed MD was then added to the culture and grown for an additional hour. 800 mL culture in a pre-warmed reaction tube was used for transformation. DNA was added to a final concentration of 1 mg/mL for circular plasmid DNA or genomic DNA and at least 2 mg/mL for linearised plasmid DNA. The culture was incubated

for 20 min at 37° C after which 25 µL 20% casamino acids were added and the cells were grown for 1 hour before plating on selective media. Plates were incubated overnight at 37° C.

2.4 Generation of deletion mutants

2.4.1 Deletion of *dynA*, in strain DSM 25152

For genomic deletion of *dynA* from strain wild-type, 25152, DNA harbouring the deletion was isolated (as per instructions given in 3.8) from a previously established strain FBB002, *dynA::tet trpC2* (Bürmann et al 2011b) and transformed into competent WT, 25152. Cells were plated on NA plate containing 10 µg/mL tetracycline and transformants were further verified by PCR.

2.4.2 Deletion of potential interacting partners (*yflN*, *yukF* and *mfd*) identified in synthetic lethal screen

Plasmid backbone of pMG9 (Gimpel and Brantl 2012) was modified by replacing *amyE1* and *amyE2* fragments with 900 bps upstream and 600 bps downstream regions of *yflN*, *yukF* and *mfd* genes, respectively to generate plasmids PSC 37, PSC 38 and PSC 39. Primers with appropriate restriction enzyme sites were designed to enable cloning of the plasmids. Plasmids were linearised with *BsaI* before transforming into *B. subtilis*. Positive colonies, where the respective gene was deleted, were verified by PCR.

2.5 Bacterial two hybrid assay

Two-hybrid screen was adopted to test the interaction pattern of potential DynA-interaction partners (YneK, YmdA and YwpG) with individual subunits of DynA, D1 and D2. BACTH (Bacterial Adenylate Cyclase-based Two-Hybrid) system (from EUROMEDEX) was adopted for studying these interactions.

2.5.1 Plasmid isolation

Previously established plasmids pKNT25 D1, pKNT25 D1M, pKNT25 D2 and pKNT25 D2M were isolated from *E. coli* cells respectively. Here, D1/D2 and D1M/D2M represent wild-type and GTPase mutant subunits (K56A D1 and K625A D2) of DynA. Also, pUT18C YneK, pUT18C

YwpG and pUT18C YmdA plasmids were isolated from DH5 α *E. coli* cells. Plasmid purification was performed with mini-spin columns from Macherey-Nagel as per manufacturer's protocol.

2.5.2 Co-transformation

For the assay, competent BTH101 cells were co-transformed with plasmid combination as follows (table 7)

Table 7. Bacterial two-hybrid co-transformations. pKNT25 and pUT18 are bait and prey plasmids respectively. D1/D2 and D1M/D2M represent wild-type and mutant subunits of DynA.

DynA subunit	DynA interacting partners		
	pUT18 YmdA	pUT18 YwpG	pUT18 YneK
pKNT25 D1	pKNT25 D1/ pUT18 YmdA	pKNT25 D1/ pUT18 YwpG	pKNT25 D1/ pUT18 YneK
pKNT25 D1M	pKNT25 D1M / pUT18 YmdA	pKNT25 D1M / pUT18 YwpG	pKNT25 D1M / pUT18 YneK
pKNT25 D2	pKNT25 D2/ pUT18 YmdA	pKNT25 D2/ pUT18 YwpG	pKNT25 D2/ pUT18 YneK
pKNT25 D2M	pKNT25 D2M / pUT18 YmdA	pKNT25 D2M / pUT18 YwpG	pKNT25 D2M / pUT18 YneK

For every transformation, a 100 μ L-aliquot of cells was thawed on ice, incubated with the insert DNA for 30 minutes, heat shocked for 1 minute at 42°C and cooled on ice for 10 minutes. Cells were regenerated in 600 μ L of warm LB for 15 minutes at 37°C, washed four times with M63 medium in order to remove all traces of the rich medium used in the transformation procedure and spotted onto M63 as well as LB agar plates containing carbenicillin (50/100 μ g/mL), kanamycin (25/50 μ g/mL kanamycin), a chromogenic substrate X-Gal (5-bromo-4-chloro-3-indolyl- β -D-galactopyranoside, 40 μ g/mL) and IPTG (0.5 mM). Plates were incubated at 30°C till growth was observed. pKNT25-zip and pUT18C-zip plasmids were co-transformed to serve as positive control whereas empty plasmids were used for negative control.

2.6 Spot assay

A freshly plated colony of the respective strain was grown overnight in LB supplemented with tryptophan to an OD₆₀₀ 1.0. Cells were further diluted in fresh medium to an OD₆₀₀ of 0.1 and grown up to to an OD₆₀₀ 1.0. This pre-culture was then used to inoculate fresh medium and cells grown to a higher OD₆₀₀ (> 1.5) to perform plaque assay. Φ29 and SPβ phage stocks were purchased from DSMZ. 10-fold serial dilutions (10⁻¹ to 10⁻⁸) of phage stock were prepared in phage buffer. The dilution that could be used to perform respective plaque assay was determined by spotting 5 ul of each dilution on plates over-layered with wild-type 168 culture in 0.6% overlay agar. 1 mL cells were swirled in the overlay agar and poured on LB plates. Appropriate dilutions that produced distinct countable plaques were used for performing quantitative plaque assays (QPA).

2.7 Quantitative plaque assay (QPA)

QPAs required mixing of 100 µl of appropriate phage dilution with 1 ml culture in 0.6 % overlay agar and pouring on LB agar plates. Φ29 plaques could be detected after 5 hours of incubation whereas SPβ phage required overnight incubation at 37°C for plaque formation.

2.8 Protein expression in *E. coli*

Fresh BL21 *E. coli* transformation was carried out for every protein purification. A colony of the transformant was precultured in LB at 37°C upto OD₆₀₀ = 0.8-1.0. A preculture was inoculated in 2l LB-carbenicillin broth to OD₆₀₀ = 0.1 and grown at 37°C to OD₆₀₀ = 0.8. This culture was induced with 0.7 mM IPTG and expressed overnight at 18°C. Cells were harvested by centrifugation at 4° C, 6000 rpm for 15 minutes, washed with buffer T2 (50 mM Tris, 200 mM NaCl, 10 % glycerol, 10 mM imidazole, pH 8.0 / 4° C). At this point cell pellet was either processed directly by lysing or stored under liquid nitrogen at -80° C.

3. Biomolecular DNA techniques

3.1 Site directed mutagenesis (SDM)

SDM approach was used to create point mutations and deletions. First, PCR using the mutagenizing oligonucleotides and plasmid template was carried out as follows:

Table 8. PCR components

Component	For 50 μ L Reaction	Final concentration
5X Phusion GC buffer	10	1X
Plasmid as template	1	<250 ng
10 μ M Primer F	2.5	0.5 μ M
10 μ M Primer R	2.5	0.5 μ M
10 mM dNTP mix	3	
100% DMSO	1.2	2.4%
50 mM MgCl ₂	0.2	0.2 mM
2000 Units/mL Phusion polymerase	0.5	1 unit
ddH ₂ O	Upto 50 μ L	

PCR cycling condition consisted of an initial denaturation of 1 min at 98°C followed by 21 cycles of amplification with 30 seconds denaturing at 98°C, 30 seconds annealing at 55°C, and extension at 1 minute/kb of plasmid length at 72°C. Amplified products were cleaned using PCR cleaning kit from Macherey-Nagel, as per specified instructions. Purified DNA was then digested with 1 μ L DpnI enzyme (NEB) at 37°C for 2 hours, followed by purification and transformation in *E. coli* DH5 α

3.2 Polymerase Chain Reaction (PCR)

PCR for cloning was performed with Phusion DNA polymerase from NEB, as per manufacturer's protocol. For colony PCR, Taq DNA polymerase from Lucigen, was used as per suppliers instructions.

3.3 Agarose gel electrophoresis

Electrophoresis was performed with gels containing 1 % agarose in TAE (40 mM Tris, 1.1 % acetic acid, 1 mM EDTA, pH 8.0 / 25° C) using a BioRad MiniSUBCell GT at 120 volts. Gels were stained with 5 mg/L ethidium bromide. Sizes of DNA-fragments were estimated by exponential fit of a Generuler plus DNA marker from Fermentas (Thermo Scientific).

3.4 DNA digestion with restriction endonucleases

Restriction of DNA with endonucleases was performed under conditions recommended by the distributor (NEB or Fermentas).

3.5 DNA ligation

DNA fragments were ligated at 5-10 ng/mL total DNA with T4 DNA ligase (NEB) either at room temperature for 2 hours or at 4° C overnight.

3.6 Sequencing

DNA sequencing was performed by in-house sequencing facility at Biocenter, LMU.

3.7 Plasmid isolation from *E. coli*

E. coli plasmid isolation was carried out using spin-column kit from Macherey-Nagel, as per instructions provided in the manual.

3.8 DNA isolation from *B. subtilis*

Freshly plated cells were collected with an inoculation loop and suspended in 200 µL sterile water. The cell suspension was mixed with 200 µL phenol (pH 6.5) and incubated for 10 minutes at 65°C in water bath. The cell-phenol suspension was further cooled on ice and vortexed extensively with 200 µL chloroform:isoamylalcohol (24:1) solution. Mixture was centrifuged at 14000 rpm for 6 minutes at 4°C. Supernatant was transferred into a new tube and mixed with 200 µL chloroform:isoamylalcohol (24:1) solution which was subjected to centrifugation. 100 µL of the supernatant containing DNA was collected into a new tube and used for transformation.

4. Biomolecular protein techniques

4.1 Protein purification

For lysis of *E. coli*, the harvested cells (mentioned in Materials and Methods 2.8) were resuspended in 20 ml (usually 5 X volume of cell mass) T2 buffer containing 10 mM imidazole, 0.7 % TX-100, DNase and 1 tablet of Roche Complete Protease Inhibitor (EDTA-free). A homogenous solution of cells prepared by vigorous vortexing was subjected to the cell-disrupter at 100.000-150.000 KPa pressure and lysed cells were centrifuged at 12000 X g for 20 minutes. The obtained lysate was mixed with T2 equilibrated 1.5 ml Qiagen Ni-NTA beads solution and incubated overnight at 4° C on a rolling mixer. On following day, beads were collected by centrifugation at 2000 X g for 10 minutes and washed 4X with T2 (50 mM Tris, 200 mM NaCl, 10% glycerol, pH 8.0 / 4° C) containing 10 mM imidazole. Beads were mixed with appropriate T5 buffer containing 1M imidazole for 1 hr. Solution was made beadless by spinning down as above. The eluate was concentrated and subjected to either further purification.

NiNTA purified protein was further concentrated using a 50k MWCO filter tube containing high recovery Ultracel regenerated cellulose membrane that has protein recovery rate of 94%. Concentration was carried out at 4000 X g with repeated mixing at intervals. Concentrated protein was further subjected to gel filtration. 1 ml concentrated protein was treated with 1 mM DTT and then ultracentrifuged at 10000 rpm for 10 minutes. DTT readily permeates cell membranes and helps reducing disulphide bonds thus promoting proteins to unfold and maximize bonding. Gel filtration was used to estimate the molecular weight of proteins. Gel filtration also known as Size-Exclusion Chromatography separates molecules in a solution according to their size as they pass through a gel filtration medium packed in a column. This separation was performed at room temperature using ÄKTA Explorer (GE Healthcare) and Superdex 200 10/300 GL (Tricorn). An elution profile of eluted protein was analysed. Positive fractions were pooled after testing on 7% SDS gels, aliquoted and flash frozen at -80° C.

4.2 Protein quantification

Protein concentration was estimated using colorimetric bicinchoninic acid (BCA) assay kit purchased from Thermo scientific, as per instructions provided.

4.3 Protein concentration

Protein was concentrated by centrifugation at 3,200 X g in Amicon concentrator tubes (Millipore). Full length DynA was concentrated in MWCO 100,000 (KDa) filters. For D1 and D2 fragments, MWCO 50,000 (KDa) filters were used. The solutions were mixed repeatedly by pipetting during the concentration process.

4.4 SDS Polyacrylamide gel electrophoresis (SDS-PAGE)

SDS-PAGE was performed with resolving gels of 7 % acrylamide/bisacrylamide and stacking gels of 4 % (37.5:1, Rotiphorese Gel 30 solution). Samples were prepared by addition of 4X loading buffer (150 mM Tris/HCl pH 7.0 / 25° C, 12 % SDS, 6 % β -mercaptoethanol, 30 % glycerol, 0.05 % Coomassie G-250) and heating for 5-10 min at 95° C when required. Gels were run in a BioRad Mini-PROTEAN chamber at 200 V using buffer containing 10 mM CAPS and 10% methanol (pH 11.0). Coomassie Brilliant Blue (CBB) staining was performed for 30 minutes in 0.02 % Coomassie G-250, 25 % methanol, 10 % acetic acid with subsequent destaining in 10 % acetic acid and a cellulose tissue. Protein size was determined with PageRuler prestained protein ladder from Fermentas or prestained protein ladder from NEB.

4.5 Immunoblotting

Samples were separated on an SDS-PAGE gel and blotted onto a PVDF transfer membrane for 2 hours at 100 mA or overnight at 20 mA. Blots were blocked for at least one hour in blocking buffer (5 % Milk powder in wash buffer). The blot was incubated with primary antibody (anti-GFP, 1:2,000, anti-His, 1:2000) diluted in blocking buffer at room temperature for at least 1 hour. The blot was then washed four times with washing buffer (8 g NaCl, 0.2 g KCl, 1.44 g Na_2HPO_4 , 0.24 g KH_2PO_4 , 0.1 % (w/v) Tween 20, 1 L ddH₂O, pH 7.4 with KOH) and incubated with the secondary antibody (anti-rabbit conjugated with alkaline phosphatase, 1:10,000, anti-mouse conjugated with alkaline phosphatase, 1:10,000) at room temperature

for at least 1 hour. The blot was again washed four times with washing buffer. Detection was visualized by incubation with Nitro blue tetrazolium chloride (NBT)/ 5-Bromo-4-chloro-3-indolyl phosphate (BCIP). For this, 10 ml of phosphatase buffer (100 mM NaCl, 100 mM Tris, 5 mM MgCl₂, pH 9.5) was mixed with 60 µl NBT and 100 µl BCIP and placed on the gel.

4.6 GTPase assay

GTP hydrolysis was assessed using HPLC with a hydrophobic C18 column (Chromolith Performance HPLC column 100-4.6 mm) in 10 mM tetrabutylammonium bromide, 0.2 mM sodium azide, 100 mM potassium phosphate pH 6.5 and 2 % acetonitrile. Hydrolysis reactions contained 1 mM nucleotide, 50 mM Tris/HCl, 200 mM NaCl, 5 mM MgSO₄ and 2.5 µM protein. GDP and GTP amounts were detected at 254 nm and 285 nm wavelengths in a total volume of 100 µL. The sample was incubated at 37° C for 15 min and filtered before injection onto the column. The chromatogram was analysed in OriginPro 8.0.

4.7 Liposome sedimentation assay

With the aim to study lipid-protein interaction and protein mediated membrane fusion, liposomes from commercially available lipid molecules were prepared as per the manufacturer's protocol.

4.7.1 Liposome preparation

Phosphatidylcholine (PC), phosphatidylethanolamine (PE), phosphatidylglycerol (PG) and cardiolipin (CA) phospholipids from Avanti were used to generate synthetic vesicles using buffer T2 and a mini extruder. Chloroform from the lipid solution was evaporated under nitrogen gas to prevent any vacuum formation. After complete drying, lipids were redissolved in buffer T2, aliquoted and stored at -80° C. For liposome formation, lipids were diluted to 2 mg/ml in T2, vortexed vigorously to get a homogenous solution and then extruded 15-17 times through a Millipore filter of pore size 0.4 µm. Liposomes were used within an hour for the assay.

4.7.2 Lipid-binding assay

Liposome binding experiments were performed at room temperature with 0.2 mg/mL liposomes, T2 (50 mM Tris, 200 mM NaCl, 10 % glycerol, pH 8), 0.5 mM MgSO₄ and 1 mM GTP/GDP/ATP. Reaction and control tubes were incubated for 2-3 hours and ultracentrifuged at 80,000 rpm for 20 minutes. Supernatant and liposome (pellet) fractions were analysed by SDS-PAGE.

4.7.3 Liposome staining

10 µL of pelleted liposomes from sedimentation assay was incubated with Nile red (10 µg/mL) for 2 minutes and observed immediately under a Zeiss AxioImager M1 equipped with a Zeiss AxioCam HRm camera. An EC Plan-Neofluar 100x/1.3 Oil Ph3 objective was used. Red fluorescence was monitored using filter set 43 HE Cy3. Nile red is a lipophilic compound used as membrane stain (Greenspan et al 1985).

4.8 Phage-protein crosslinking *in vitro*

Formaldehyde (FA) was used as a crosslinker between purified DynA protein and phage (Φ29 and SPβ). 1 µM protein was incubated with 30 µL of 10⁻² dilution of the respective phage (having pfu of about 3.8 X 10⁸) in phosphate buffered saline (PBS), at 37°C for 1 hour. FA was then added to the reaction to a final concentration of 0.2 %, incubated for 20 minutes at room temperature. Further, this crosslinking was terminated by adding 150 mM glycine and incubating for 10 minutes. Finally, 15 µL of every reaction was analysed by SDS-PAGE.

4.9 Phage-protein labeling *in vitro*

Purified wild-type DynA protein was labelled *in vitro* with Texas red dye as per manufacturer's protocol (Life Technologies) with appropriate modifications. Protein and dye were incubated at room temperature for 1 hour with constant mild-shaking. For concentrating labelled-protein, 0.5 mL concentrator tubes of 50 KDa pore size were used. Excess dye was washed with PBS. 10 µL of 10⁻² dilution of SPβ was incubated with DAPI (1 µg/mL) stain for 5 minutes for labeling phage DNA. 10 µL of labeled protein was then incubated with 2 µL of labeled phage, incubated for 10 minutes at room temperature and

visualized under light microscope, Zeiss AxioImager M1 equipped with a Zeiss AxioCam HRm camera. Red fluorescence was monitored using filter 43 HE Cy3 and DAPI fluorescence was examined with filter set 49.

5. Microscopy

5.1 Light microscopy

Localisation of fluorophore-tagged proteins in *B. subtilis* was observed under a Zeiss AxioImager M1 equipped with a Zeiss AxioCam HRm camera. An EC Plan-Neofluar 100x/1.3 Oil Ph3 objective was used. GFP fluorescence was monitored using filter set 38 HE eGFP. A loopful of freshly plated cells was used to inoculate 10 ml CH medium. Cells were inoculated in fresh media and grown up to a desired OD. Cells were induced with 0.1% xylose at mid-exponential phase. After 60 minutes of induction 2 μ l of the cell culture (around OD₆₀₀ 1) was placed on agarose bed on a glass slide, covered with a glass slip, and observed under light microscope.

5.2 Fluorescence Loss In Photobleaching (FLIP)

For FLIP analysis, cells were grown in MD medium supplemented with CAA and 0.4% xylose upto an OD₆₀₀ of 1.0. 50 μ l of cells were stained with 1.5 μ M FM4-64 for 10 minutes at RT, washed and resuspended in fresh MD medium. 3 μ l of these stained cells were mounted onto 1% MD-agarose pad as mentioned above, and analysed using the Delta Vision microscope. For FM4-64 bleaching, 405 nm laser was used at 20% power and pulse duration of 0.02 seconds. For image acquisition, mCherry channel (excitation, 575/25, emission, 623/60) from filter set 3 was used with an exposure time of 0.4 seconds. An image was taken every second for a total of 60 seconds. All FRAP/FLIP/time-lapse movies were analysed using Image J program.

Results

1. Functional characterisation of DynA

1.1 DynA confers resistance against membrane stress-inducing antibiotics

Bacterial dynamins are well-characterised proteins. However, no *in vivo* phenotype has been elucidated so far. A $\Delta dynA$ strain showed decreased sensitivity to antibiotics that act within the cytosol by blocking protein biosynthesis (unpublished data from PhD thesis of Suey van Baarle), thus giving rise to the idea that the absence of DynA might alter the transport and/or diffusion of antibiotics across the plasma membrane. To address whether DynA influences antibiotic-susceptibility, growth experiments were performed in the presence of cell-envelope stress inducing antibiotics. Initially, a membrane-pore forming antibiotic, nisin was tested. Nisin is a small cationic antimicrobial peptide that can target cell-wall biosynthesis precursor, lipid II (Hyde et al 2006) and cause permeabilization of the lipid bilayer by forming pores (Sahl et al 1987). Upon addition of nisin (10 $\mu\text{g}/\text{mL}$) to the medium at OD_{600} 1.0, an abrupt decrease in the optical density was observed with wild-type and $\Delta dynA$ culture. However, wild-type cells recovered faster than $\Delta dynA$ from nisin-stress (Figure 3).

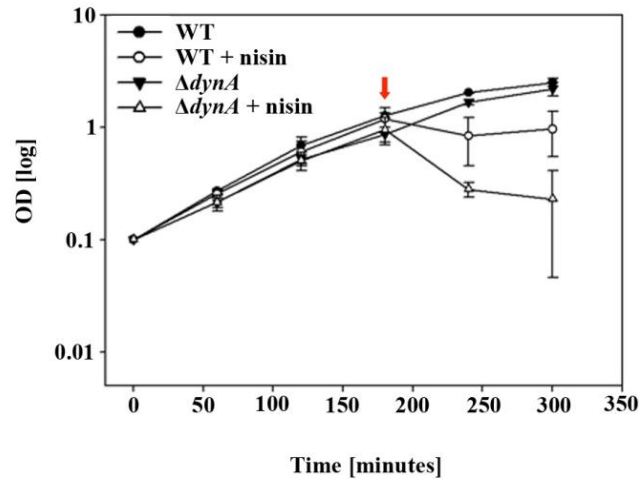


Figure 3. The $\Delta dynA$ strain takes longer to recover from nisin-stress, compared to wild-type. Upon adding 10 $\mu\text{g}/\text{mL}$ of nisin to exponentially growing bacteria, an abrupt decrease in the optical density is observed. Wild-type cells recovered faster than $\Delta dynA$ from this lag phase suggesting that endogenously expressed DynA plays a role in combating nisin induced membrane stress whereas lack of $dynA$ makes the cells more sensitive to nisin-induced membrane stress.

When exponentially growing cultures were diluted in medium containing nisin (30 $\mu\text{g}/\text{mL}$), the growth of $\Delta dynA$ again was impaired in comparison with the wild-type (Figure 4A). Although, nisin is an ideal antibiotic to induce envelope stress in bacteria, it is highly unstable at a high pH, with a maximum activity at an acidic pH of 3 (Ringstad et al 1997, Szaszak et al 2002, Wigge et al 1997). Therefore, another widely used cell envelope-stress causing antibiotic, bacitracin was used for testing susceptibility of $\Delta dynA$. The exact mechanism of action of bacitracin is still not very clear. However, bacitracin is known to induce envelope stress (including cell-wall and cell-membrane stress) in *B. subtilis* by binding to peptidoglycan synthesis precursor, undecaprenyl pyrophosphate (Economou et al 2013, Stone and Strominger 1971). Upon adding the minimal concentration (MIC > 300 $\mu\text{g}/\text{mL}$ for wild-type 25152 with bacitracin-stock tested) of bacitracin required for inducing *B. subtilis* envelope stress (200 $\mu\text{g}/\text{mL}$), no difference in wild-type and $\Delta dynA$ growth was observed. However, an increase in concentration of up to 250 $\mu\text{g}/\text{mL}$ resulted in slow growth of $\Delta dynA$, whereas the wild-type culture was not affected (Figure 4B and 4C). The growth phenotypes

observed with $\Delta dynA$ were significantly complemented in the DynA complementation strain, PSB033. Another cell wall targeting antibiotic, vancomycin was used for studying susceptibility of wild-type and $\Delta dynA$. No difference was observed in the growth and susceptibility of wild-type and $\Delta dynA$ in presence of vancomycin (Figure 4D and 4E), thus indicating, that DynA, expressed in wild-type and PSB033, is likely involved in combating membrane stress that mostly involves pore formation rather than directly inhibiting cell wall synthesis. To further analyse the involvement of DynA in membrane stress response, growth experiments were performed in the presence of linear pentadecapeptide, gramicidin (a mixture of gramicidin A, B, C and D from *Bacillus brevis*) that affects membranes of Gram-positive bacteria by forming well defined transmembrane ion channels for transport of monovalent cations and alkali metals (Burkhart et al 1999, Dubos 1939). However, the channels formed by linear gramicidin merely have a pore diameter of about 4 Å, whereas nisin-induced pores range between 20-25 Å (Kelkar and Chattopadhyay 2007). The growth of wild-type and $\Delta dynA$ in a medium containing gramicidin (10 µg/mL) was, as expected, comparable (Figure 4F), thus indicating that DynA indeed responds to membrane stress that involves lipid-pore formation in *B. subtilis*. Another explanation to these observations would be that pore-forming peptides, such as nisin require negatively charged phospholipids (such as phosphatidylglycerol, PG) for binding to bacterial membranes (Breukink et al 1998), which is also the site for DynA localisation and therefore its function. Hence, daptomycin, which has affinity for negatively charged membranes, was tested. Daptomycin is an anionic lipopeptide that requires the presence of Ca²⁺ ions and especially PG head groups for binding and damaging bacterial membranes. No notable difference in growth with daptomycin (15 µg/mL and 20 µg/mL) was seen between wild-type and $\Delta dynA$, but a striking resistance to daptomycin stress was observed in *B. subtilis* overproducing DynA (Figure 4G and 4H). Taken together, these observations strongly indicate a protective role of DynA against membrane stress in *B. subtilis*.

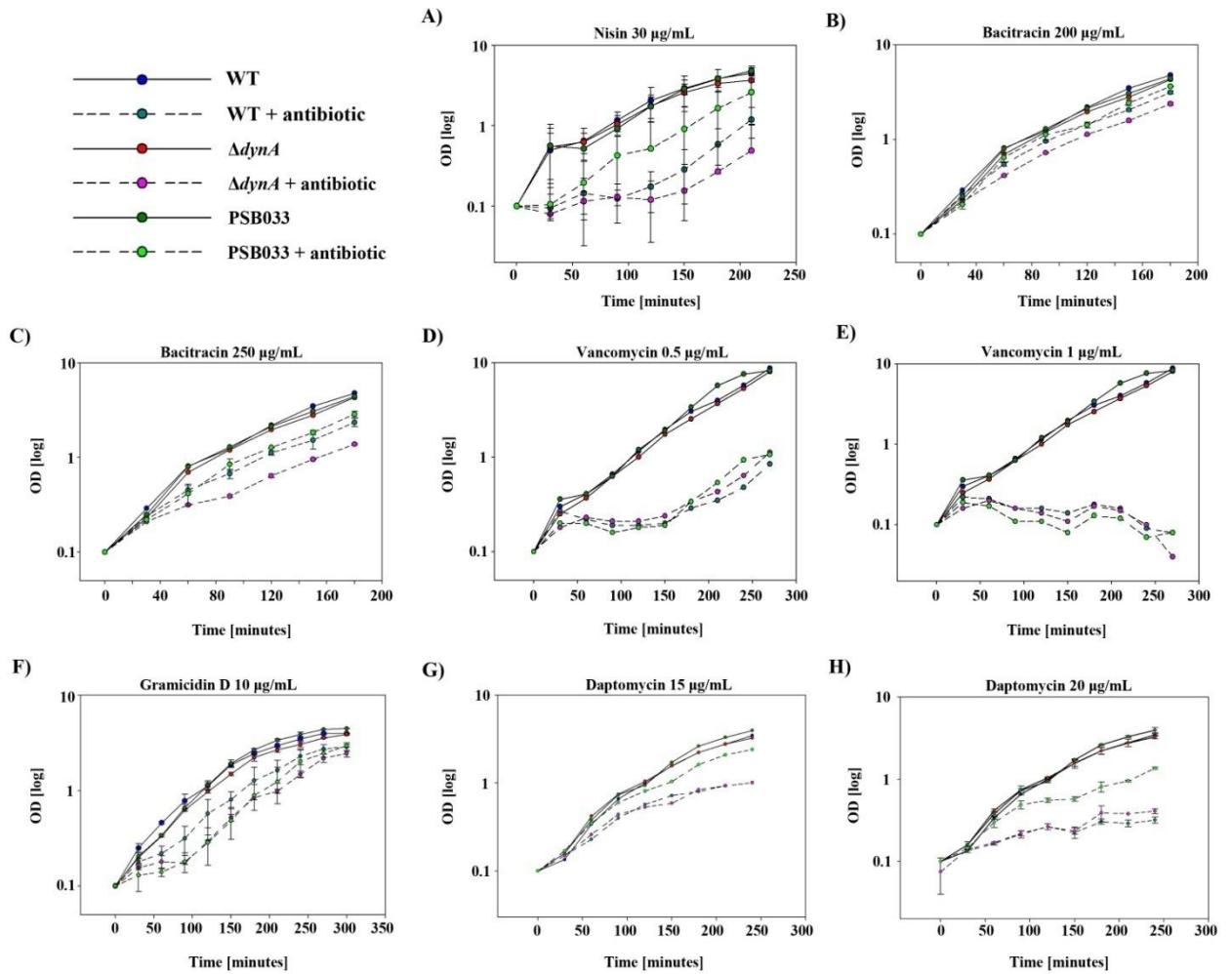


Figure 4. A $\Delta dynA$ strain is more sensitive to antibiotic induced membrane stress. To test whether DynA has a protective function upon membrane stress, growth experiments were performed in the presence of nisin (A), bacitracin (B and C), vancomycin (D and E), gramicidin (F) and daptomycin (G and H). Growth curves from at least two independent experiments were analyzed to evaluate cell sensitivity towards antibiotic-induced envelope stress. The $\Delta dynA$ strain is more sensitive to nisin and increasing concentrations of bacitracin, whereas a strain that over-expresses DynA, PSB033 has enhanced tolerance to daptomycin. No growth phenotype is seen with antibiotic that specifically targets the cell wall, such as vancomycin or antibiotics that fail to produce membrane pores, such as linear gramicidin.

1.2 DynA becomes static under nisin-induced membrane stress

LiaH, a cytoplasmic phage shock protein A (PspA) homolog, was seen to be recruited to the bacterial membrane into static foci upon membrane stress, induced specifically by antibiotics that target the lipid II cycle in *B. subtilis* (Dominguez-Escobar et al 2014). Therefore, the localisation of DynA was analysed *in vivo* in the presence of membrane stress-inducing antibiotic, nisin. DynA is highly dynamic at bacterial membranes (Appendix figure 1A). However, like LiaH, DynA localised into static foci upon adding 1 µg/mL nisin (Figure 5A). Protein dynamics was analysed by FRAP (Appendix figure 1C). The prominent foci formation could hint towards two possibilities, 1) DynA-GFP is recruited to membrane pores caused by nisin or 2) nisin-generated pores create membrane gaps, thus concentrating DynA-GFP to intact regions on the damaged membrane, giving rise to prominent foci. As a control, the localisation of another membrane protein, AtpA-GFP was followed upon nisin treatment. AtpA is an ATP synthase F1 sector subunit alpha that localises to the cell membrane of *B. subtilis* (Johnson et al 2004). Since no difference in AtpA localisation could be seen upon nisin addition (Figure 5B), one could contemplate the phenotype observed with DynA-GFP as a genuine response of the cell against membrane stress.

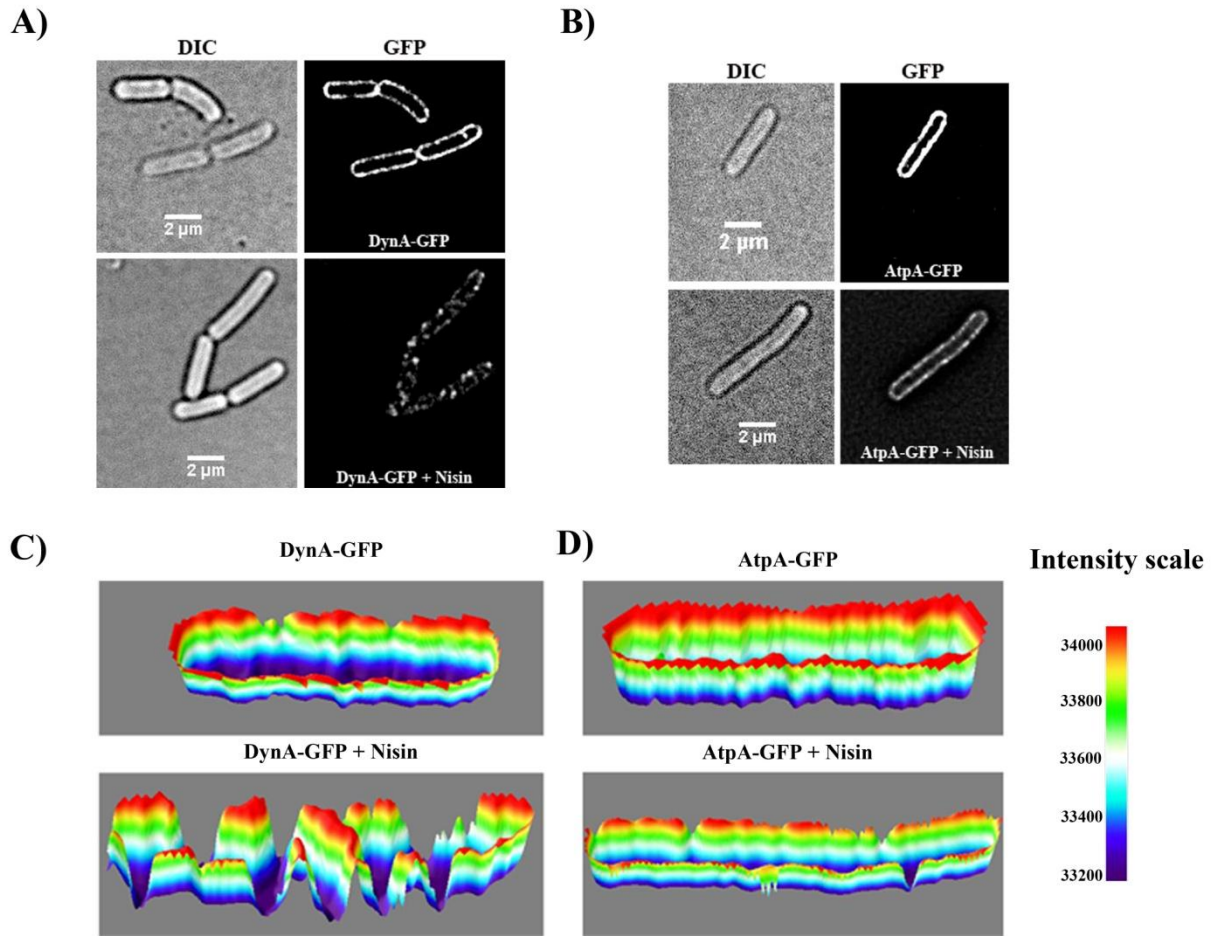


Figure 5. DynA-GFP responds to nisin induced membrane stress. Localisation of DynA-GFP and AtpA-GFP was analysed upon nisin treatment. (A) DynA-GFP, under xylose inducible promoter, P_{xyl} , localises throughout the bacterial membrane. However, in the presence of nisin, DynA-GFP localizes into confined foci on the membrane. (B) Localization of another membrane protein, AtpA-GFP is not affected by nisin and, therefore serves as a control for localisation experiments. Scale bar, 2 μm . (C and D) 3D surface plots representing the distribution of DynA-GFP and AtpA-GFP along the bacterial membrane in the absence and presence of nisin. Surface plots were generated using ImageJ program.

Nisin is known to disturb bacterial membrane potential (Ruhr and Sahl 1985). The localisation of several membrane-associated proteins, especially proteins with C-terminal amphipathic helices, is affected upon loss of membrane potential (Strahl and Hamoen 2010). To analyse whether DynA-GFP concentrates into foci due to dissipation of membrane potential, localisation experiments were performed in the presence of a protonophore,

carbonyl cyanide *m*-chlorophenylhydrazone (CCCP). DynA-GFP mislocalise into static foci upon CCCP (100 μ M) addition, indicating the importance of membrane potential for proper localisation of DynA *in vivo*. However, the pattern of foci formation upon CCCP addition was different to the foci formed upon nisin stress (Figure 6A). On an average about 8 and 5 foci per cell were observed due to nisin and CCCP addition, respectively. Foci due to CCCP were large, covering an area of 0.181 μ m² along the membrane whereas nisin-induced foci were comparatively small, covering an area of 0.104 μ m² along the membrane (Figure 6B). The intensity of DynA-GFP foci due to nisin and CCCP was measured and was about 18% more in the latter case (Figure 6C). This suggested that DynA reacts differently to loss in membrane potential and pore formation. Although DynA responds to loss in membrane potential, which is most likely due to its membrane-binding mechanism via amphiphilicity, its major function is to sense and react to membrane damage, particularly pores. It can be suggested that dissipation of membrane potential might affect proper localisation of DLPs, thus affecting their functionality.

1.3 DynA is not involved in maintaining *B. subtilis* membrane potential

Some stress response proteins in bacteria, such as PspA from *E. coli*, are known to protect the damaged cell membrane from proton leakage (Kleerebezem et al 1996). Since both DynA and phage shock proteins (PSPs) respond to membrane stress in *B. subtilis*, the idea that they might act synergistically was conceivable. To analyse if DynA, too, is involved in maintaining bacterial membrane potential, wild-type, Δ *dynA* and DynA complementation (PSB033) strains were tested against membrane dissipating ionophores, nisin and valinomycin, and a fluorogenic dye DiSC₃(5). DiSC₃(5) accumulates on hyperpolarised membranes and translocates into the lipid bilayer (Sims et al 1974, Síp et al 1990). It reacts to changes in the transmembrane potential and allows fluorescence measurement at excitation/emission wavelengths of 544 nm/660 nm in dimethylformamide (DMF). A control reaction (Figure 6B) was performed to measure the stability of DiSC₃(5)-intensity over time in a plate-reader, in the absence of cells. DiSC₃(5) was stable for the time of the experiment except for slight

fluctuations. Since these experiments were performed in a plate-reader where the experimental plate containing all the samples had to be removed from the plate-reader for adding every component, Disc₃(5), nisin and valinomycin, the fluctuations in Disc₃(5) intensity could be either due to the addition of these components or due to exposure of the plate to light while adding these components. The control experiment shows that the reduced intensity of Disc₃(5) seen in actual experiment is due to quenching of the dye by bacterial membranes. Results from these experiments show no obvious difference in the dissipation of membrane potential between tested strains (Figure 6B) indicating that the loss of DynA has no effect on *B. subtilis* membrane potential. This observation suggests that DLPs and PSPs are involved in different response pathways. Based on these results, one can hypothesize that DLPs are involved in sealing membrane gaps by tethering and potentially fusing the damaged membrane.

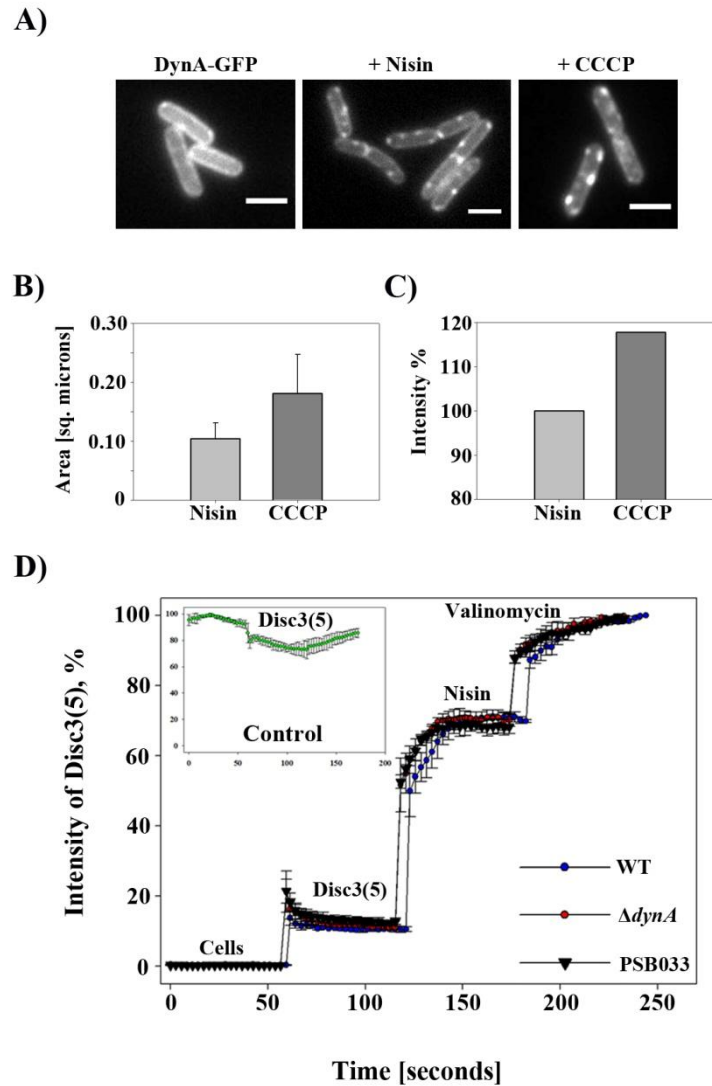


Figure 6. DynA is not involved in maintaining bacterial membrane potential but requires the membrane potential for correct localisation. (A) DynA-GFP localises into static foci upon nisin 10 (10 $\mu\text{g}/\text{mL}$) and CCCP (100 μM) addition, indicating the importance of membrane potential for proper localisation of DynA, *in vivo*. Staticity of the foci was analysed by FRAP (Appendix figure 1D). Scale bar, 2 μM . **(B)** The average area of DynA-GFP foci formed due to nisin is about 0.104 μM^2 , whereas foci formed due to CCCP have an area of about 0.181 μM^2 . The average was taken from 20 foci. **(C)** Bar graph showing the difference (~18%) in the intensity of DynA-GFP foci formed due to nisin and CCCP addition. **(D)** No difference in membrane potential dissipation due to proton ionophores, nisin and valinomycin, was observed between wild-type, ΔdynA and PSB033 (DynA⁺). Disc₃(5), nisin and valinomycin were added after 60, 120 and 180 seconds, respectively. Disc₃(5) intercalates into the cells and is released upon dissipation of membrane potential, which is induced by nisin and valinomycin. Control graph shows the intensity of Disc₃(5) over time in the absence of cells. Results from two independent experiments are summarised here.

1.4 Over-expression of DynA facilitates *B. subtilis* membrane remodelling

Bacterial membrane remodelling is necessary to overcome environmental stress. Time-lapse experiments were performed with nisin-treated wild-type, $\Delta dynA$ and PSB033 strains, where the membrane was fluorescently visualised using FM4-64 dye. Exponentially growing cells were transferred onto a 1% agarose-pad containing medium supplemented with nisin, and their membrane was monitored by fluorescence microscopy. The time-lapse analysis revealed a drastic reduced growth in cells lacking DynA, which is consistent with the results from the corresponding growth curve analysis (Figure 4A). In addition, membrane deformations (as visualised by FM4-64), that were absent in wild-type cells exposed to nisin, clearly show that cells lacking DynA are impaired in combating membrane stress in *B. subtilis*, whereas wild-type cells can efficiently combat nisin-induced membrane stress (Master thesis of Kristina Eissenberger, Appendix figure 2). For a membrane-bound protein that responds to stress by inducing membrane remodelling, a high degree of molecular mobility seems plausible. To analyse movement of DynA, along the bacterial membrane, fluorescence recovery after photobleaching (FRAP) was performed on *B. subtilis* strain, FBB018, expressing DynA-GFP. The GFP signal recovery was strikingly fast, within seconds (half time being 6-7 seconds), thus showing DynA to be highly dynamic at the bacterial membrane (Master thesis of Kristina Eissenberger, Appendix figure 1A).

Since DynA, like eukaryotic DLPs, is shown to exhibit membrane-remodelling behaviour and is found to be highly dynamic at bacterial membrane, it seemed likely that over-expression of DynA might result in an elevated membrane turnover/remodelling rate. Here, membrane turnover/remodelling is referred to as rapid changes occurring in the cellular membrane due to loss, replacement and diffusion of membrane components, either lipids or proteins. For this purpose, wild-type, $\Delta dynA$ and PSB033 (DynA⁺) cells were subjected to fluorescence loss in photobleaching (FLIP) analysis upon FM4-64 membrane staining. The bacterial cell membrane was stained with lipophilic FM4-64, which has been extensively used for microscopically visualising bacterial membranes as well as studying membrane remodelling

processes such as endocytosis in yeast cells (Vida and Emr 1995). After staining with FM4-64, a defined region on the membrane was bleached and the loss of fluorescence from another defined region on the membrane was measured over time (Figure 7A). The rate of loss in intensity was rapid, within seconds for all the three strains, which indicated that bacterial membrane remodelling is an extremely fast process. Figure 7B, 7C and 7 D shows the average loss in intensity over time for the different strains tested, along with the necessary controls ($n \geq 10$ cells for every strain). Controls included unbleached cells and background readings. Unbleached cells were taken into account to analyse the loss in fluorescence intensity over time due to bleaching during imaging and background values were subtracted from every reading taken for FLIP measurement. Figure 7E shows a graph with normalised intensity values. In both, wild-type and PSB033 (DynA⁺) strains, there was a rapid loss after bleaching in FM4-64 intensity, in the area measured, whereas in $\Delta dynA$, this loss was slow, indicating the loss that we measure is indeed due to movements in the membrane. And because these membrane movements are being compromised in cells lacking DynA, the loss in FM4-64 intensity is gradual. Another striking observation is that the intensity is seen to increase and fluctuate over time in cells expressing DynA, which indicates that membrane remodelling is so fast that the dye rapidly comes back to the area being monitored. Such behaviour is not observed with cells lacking DynA. Hence, it is ideal to say that the changing membrane environment or membrane turnover, as monitored via FM4-64, is due to the influence of DynA.

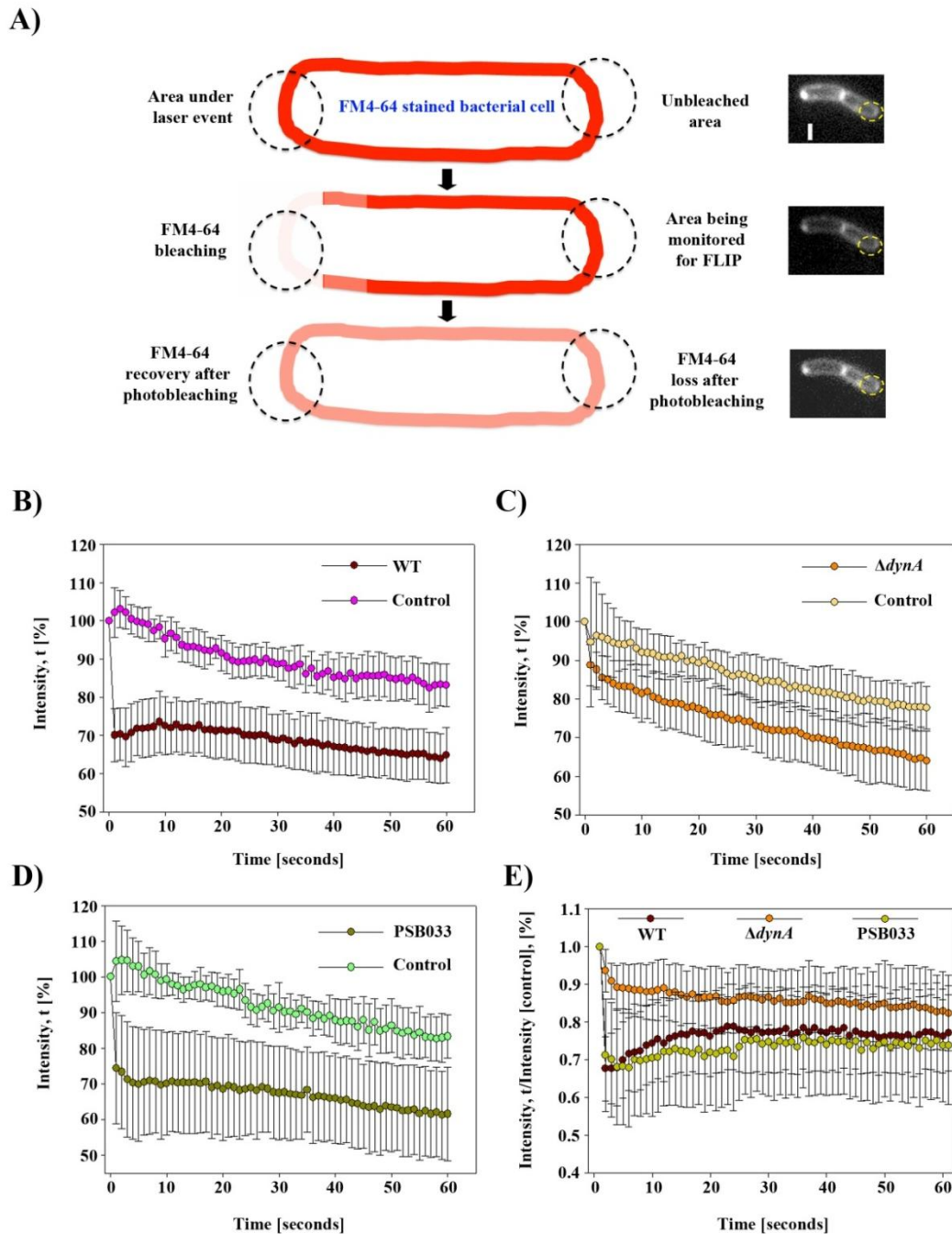


Figure 7. Over-expression of DynA facilitates *B. subtilis* membrane remodelling. (A) A cartoon illustrating fluorescence loss in photobleaching (FLIP) performed on FM4-64 stained bacterial cell. (B, C and D) Loss in intensity of FM4-64 before and after bleaching of wild-type, $\Delta dynA$ and PSB033 (DynA⁺) membranes, respectively. The instant decrease in the intensity of FM4-64 from a non-bleached region in wild-type and PSB033 cells imply faster movement to the bleached region, which is most likely due to rapid bacterial membrane remodelling in the presence of DynA. Controls represent loss in intensity from unbleached cells. (E) Graph showing loss in FM4-64 intensity values over time that were normalised with control values. FM4-64 intensity is seen to recover instantaneously after loss, in wild-type and PSB033, indicating a very high rate of membrane remodelling in these cells.

1.5 *B. subtilis* lacking DynA is sensitive to phage stress

Since DynA is similar to Mx proteins in several aspects, it was reasonable to question if DynA exhibited antiviral activity. In addition, a phage has to penetrate the bacterial membrane and induce pore formation to inject its genetic material. To further investigate the hypothesis that DynA reacts to pore formation, *B. subtilis* wild-type 168 and $\Delta dynA$ 168 strains were subjected to plaque assay to test sensitivity against an infectious phage, $\Phi 29$. The appropriate dilution that could be used to perform quantitative plaque assay (QPA) was determined by spotting 5 μ L of 10-fold dilutions of the phage stock on a lawn of wild-type culture (Appendix figure 3). A $\Delta dynA$ strain showed higher sensitivity to $\Phi 29$ phage infection, with almost 50% more plaques compared to the wild-type strain. The difference in plaque numbers was observed when cells were infected during the late exponential phase (Figure 8A and 8B). A plausible explanation to this observation could be that the presence of DynA, which is expressed mainly during the late vegetative growth phase in wild-type cells, is imparting resistance towards phage infection. Hence, all plaque assays were performed with cells grown to higher optical densities ($OD_{600} > 1.5$). Over-expressing DynA in *B. subtilis* (PSB032/PSB033) could significantly complement the phenotype observed with $\Delta dynA$. To address if DynA was active only against $\Phi 29$ or has an innate property against *B. subtilis* phages, plaque assays were performed with another phage, SP β . SP β phage cannot infect *B. subtilis* 168 wild-type. Hence, an SP β -sensitive *B. subtilis* wild-type 25152 (DSMZ) was used for phage infection assays. Consequently, a $\Delta dynA$ 25152 strain was generated (Appendix figure 4). In this case too, the $\Delta dynA$ strain was more sensitive to phage infection than the wild-type strain, with an average difference of 20% more plaques (Figure 8C). Plaques developed faster in cells lacking *dynA*, indicating faster execution of lytic cycle. Also, a difference was observed in the formation of plaques between wild-type and $\Delta dynA$. The wild-type strain produced single and isolated plaques, whereas clusters of plaques were observed with $\Delta dynA$ (Figure 8D); again indicating cells lacking DynA are more susceptible to phage

infection, thus allowing easy propagation of phages. These results indicate DynA to be a potential candidate of the innate immunity in bacteria.

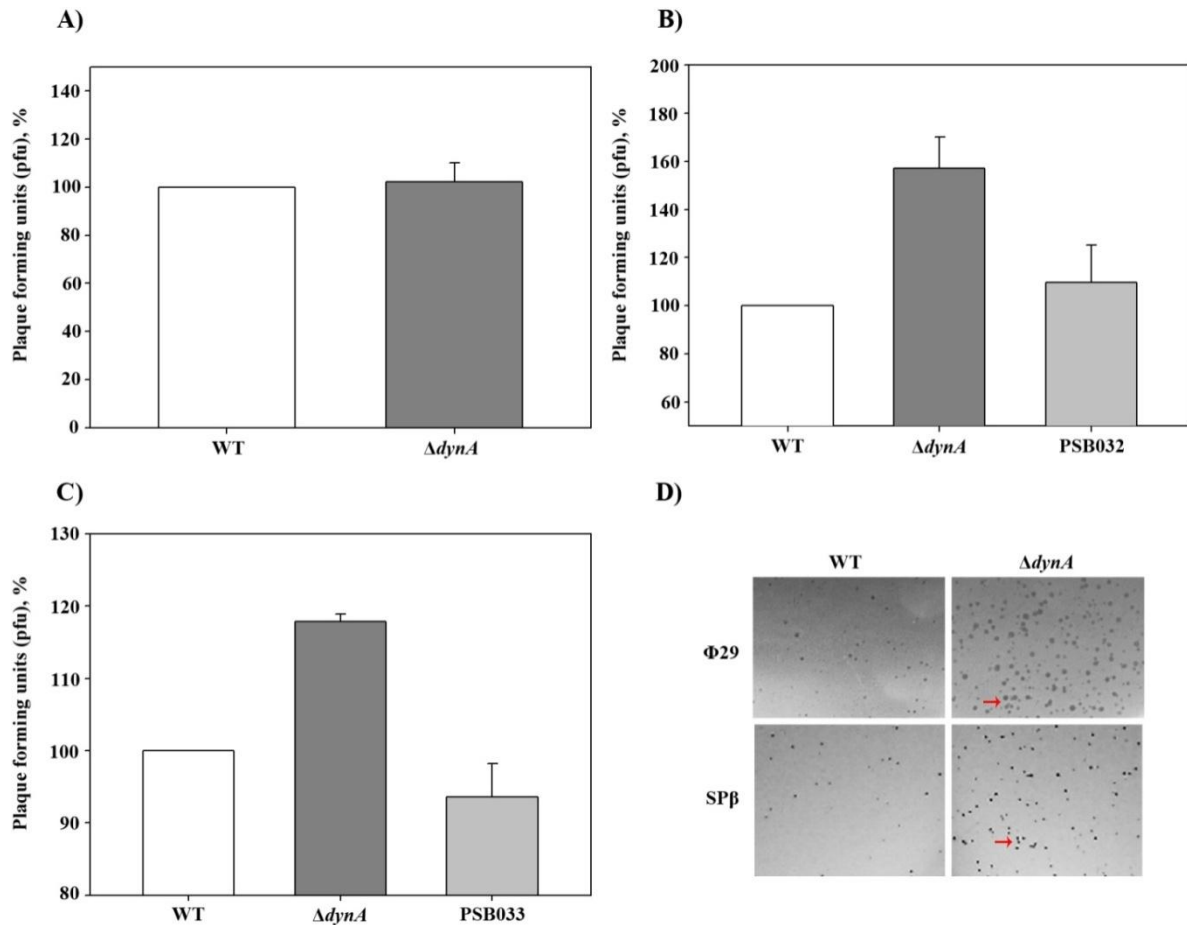


Figure 8. A $\Delta dynA$ strain is more sensitive to phage infection than wild-type. (A) No difference in phage sensitivity was observed during early log growth phase (OD ~ 1). Quantitative plaque assay of $\Phi 29$ (B) and SP β (C) bacteriophage performed on wild-type and mutant strains is indicated in percent plaque forming units (% pfu) per mL. A consistent difference was observed in the number of plaques produced on wild-type and $\Delta dynA$ plates. On an average, cells lacking DynA produced about 50% more plaques with $\Phi 29$ and about 20% more plaques with SP β compared to wild-type. Graphs represent an average taken from 3 independent experiments. (D) Clusters of plaques (indicated by red arrows) were observed with $\Delta dynA$, whereas single-isolated plaques were observed with wild-type, indicating that cells lacking *dynA* are more susceptible to infection, thus allowing the phage to easily propagate within neighbouring cells.

The $\Delta dynA$ strain was constructed by replacing the *ypbR* gene with a tetracycline resistance cassette by double crossover method. Tetracycline targets the 30S ribosomal subunit of

bacteria. Some tetracycline compounds can get trapped within bacterial membranes and make them permeable (Chopra and Roberts 2001), possibly enabling phage particles to easily penetrate bacterial membranes. Hence, it was important to examine another strain containing tetracycline resistance cassette as a control for QPA. This would avoid any possibility of having pleiotropic effects due to replacement by the cassette on genes downstream of *yprB*. To test this idea, a flotillin knockout strain of *B. subtilis*, where the *yqfA* gene was deleted by tetracycline resistance cassette replacement and the *yuaG* (*floT*) gene was disrupted by pMUTIN insertion, was subjected to QPA with $\Phi 29$. The number of plaques observed with wild-type and flotillin (*yqfA* and *yuaG*) mutant were comparable (Figure 9). These results also suggest that flotillins, that can influence membrane fluidity by organising lipid and protein assemblies at the cell membrane (Bach and Bramkamp 2013), are not involved in resistance against phage infection in *B. subtilis*.

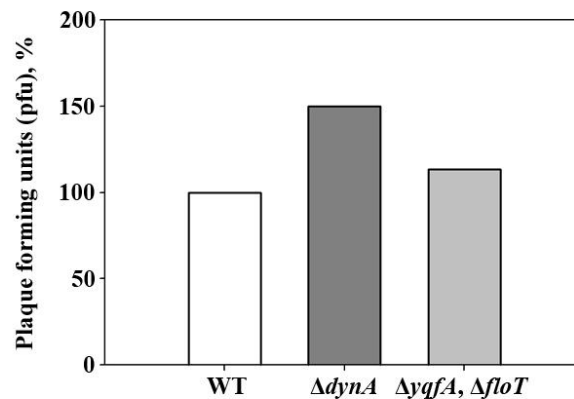


Figure 9. *dynA* deletion by *tet* insertion does not cause pleiotropic effects. Plaque assay of $\Phi 29$, performed on wild-type and mutant 168 strains is indicated in percent plaque forming units (% pfu) per mL. A flotillin knockout strain of *B. subtilis*, where *yqfA* gene was deleted by replacement with *tet* and *yuaG* (*floT*) was disrupted by pMUTIN insertion, was tested for phage susceptibility. The number of plaques observed with wild-type and flotillin mutant was comparable.

1.6 DynA binds to phage particles *in vitro*

Mx proteins can interact with viral nucleocapsid proteins to form membrane-associated perinuclear complexes to block viral replication, thus inhibiting virus activity (Kochs et al 2002). To analyse whether DynA has the ability to bind phage particles, an *in vitro* formaldehyde-crosslinking experiment was performed. Formaldehyde (FA) fixation is one promising method to identify protein complexes and interactions. Here, 0.2% FA was used for fixing phage-DynA reactions to verify an interaction. The experimental set up included necessary control reactions such as 'only protein' and 'only phage'. Results have been summarized in Figure 10, which shows a Commassie-stained SDS gel image with FA fixed samples. A clear shift is observed in DynA upon phage addition (Φ 29 or SP β), indicating interaction between DynA and the respective phage. Since this crosslinking was performed with purified protein and phage (under *in vitro* conditions), it is clear that DynA binds to an outer-exposed component of the phage. These components could be the tail, appendages or capsid surface proteins. Mass peptide fingerprinting (MPF) was used to identify phage-DynA interactions. Table 9 provides a list of peptides, other than DynA, identified from these samples. No phage proteins were detected here and all the other peptides detected have a very low coverage. DynA was purified from *E. coli*, therefore, presence of other non-phage *Bacillus* proteins indicate that these come from the phage stock. These proteins are likely co-purified along with phages, which were ordered from DSMZ. As a result of which this data causes ambiguous interpretation. Another shortcoming of this experiment was low phage concentrations, which prevented detection of any phage proteins by MPF. Therefore, phage propagation and concentration experiments should be performed in the future to have high phage yield. On the other hand, YdjH protein is detected from SP β plus DynA samples, 1 and 2. YdjH is a part of the sigma W-induced *pspA* operon in *B. subtilis*. It is proposed to interact with YwpG, a potential DynA-interacting partner, according to the STRING protein-network database (Version 10) analysis (Szkłarczyk et al 2015). Hence, it would be worth testing DynA-phage interactions in detail.

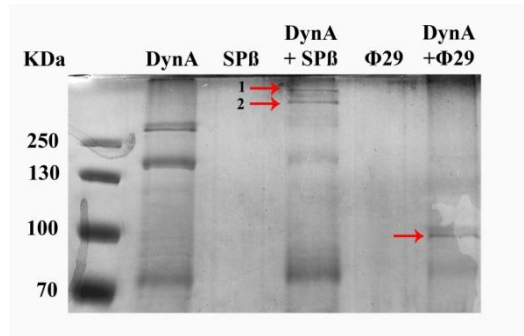


Figure 10. DynA binds to phage particles *in vitro*. Phage-DynA interaction was verified using 0.2% formaldehyde crosslinking *in vitro* and analysed by SDS-PAGE. A clear shift is observed in DynA protein upon incubation with phages, $\Phi 29$ and SP β , indicating DynA has the ability to bind phages.

Table 9. List of proteins detected in mass peptide fingerprinting.

Accession	Coverage	PSMs	Peptides	MW [kDa]	Description
SP β plus DynA-sample 1					
J7JIR6	19.36	26	10	76.6	Elongation factor G, Fusa
J7JVC6	2.34	4	1	41.3	Succinyl-CoA ligase [ADP-forming] subunit beta, SucC
J7JYQ7	2.60	1	1	51.9	Argininosuccinate lyase, ArgH
J7JYZ3	5.70	1	1	18.5	Nucleoside triphosphate phosphohydrolase, YtkD
J7JVL4	2.37	4	1	47.7	Tyrosine--tRNA ligase, TyrS
J7JNQ9	2.09	1	1	38.6	Serine phosphatase, RsbU
J7JPB5	1.43	1	1	55.6	Glucose-6-phosphate 1-dehydrogenase Zwf
J7JP22	5.10	1	1	28.3	Unknown protein, YdjH
J7JV31	3.56	1	1	35.9	Cell-shape determining protein, MreB
J7JS09	2.68	1	1	33.1	Site-determining protein, YlxH
SP β plus DynA-sample 2					
A2QIU1	6.46	4	1	29.0	PaiB

J7JVL4	2.37	2	1	47.7	Tyrosine-tRNA ligase, TyrS
J7JM40	4.00	2	1	31.4	Succinyl-CoA ligase [ADP-forming] subunit alpha, sucD
J7JP22	5.10	1	1	28.3	Unknown protein, YdjH
J7JY59	2.78	1	1	55.8	D-alanine-poly (phosphoribitol) ligase subunit 1, DltA
O05229	1.42	1	1	53.4	Na ⁺ /H ⁺ antiporter subunit D, MrpD
Φ29 plus DynA					
P45939	9.01	1	1	12.4	Uncharacterized protein YqcD
J7JS72	2.52	2	1	72.6	Unknown protein, YvcB
J7JZF7	2.54	1	1	51.0	Secreted cell wall DL-endopeptidase, CwlO
J7JSQ7	3.77	2	1	38.1	Pectin lyase, PelB
J7JS90	0.33	1	1	475.3	Polyketide synthase, PksM

For microscopic visualisation of phage-DynA interaction, phage and DynA protein were labelled *in vitro* with fluorescent dyes. SPβ was labelled with DAPI stain for 5 minutes and DynA with Texas Red according to the manufacturers' protocol. 4',6-diamidino-2-phenylindole (DAPI) is a membrane permeable DNA-binding fluorescent stain (Kapuscinski 1995), whereas Texas red is a bright-red fluorescent dye which is used for labelling protein conjugates (Titus et al 1982). Labelled phage particles and DynA were incubated in phage buffer at 37°C for 30 minutes and mounted on a 1% agarose pads for microscopic analysis. A Delta Vision Elite microscope with an emission wavelength setting for DAPI of 390/18 nm and Cy5 632/22 nm for Texas red was used for co-visualisation. Here, co-localisation was observed between the labelled phages and DynA (Figure 11). DynA has the tendency to form large oligomers and therefore it can be assumed that these oligomers trap phage particles, thus showing co-localisation. Therefore, one has to repeat this experiment with a suitable oligomerisation-mutant protein as control that does not show co-localisation with phage.

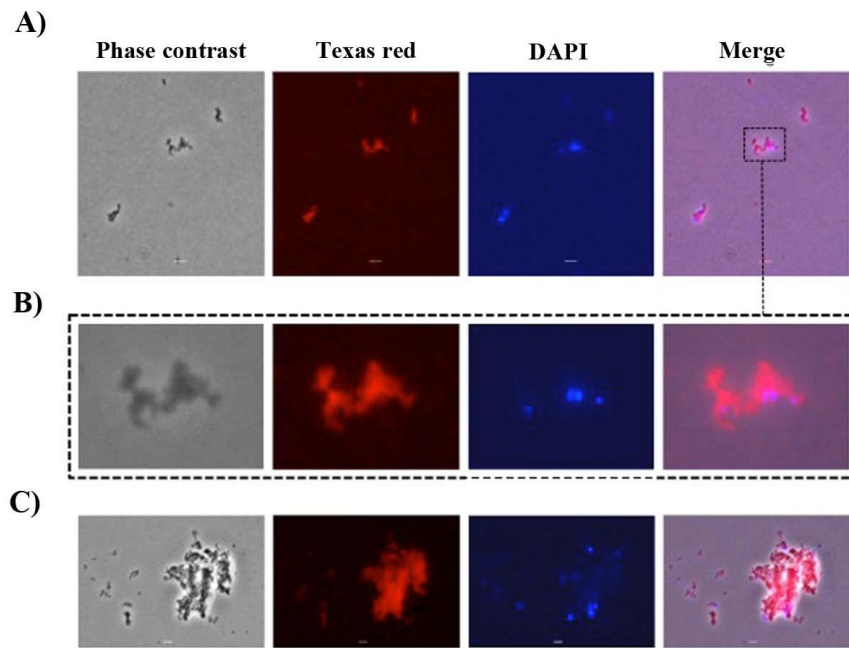


Figure 11. DynA binds to labelled-phage particles *in vitro*. (A, B and C) Co-localisation was observed between Texas red labelled DynA and DAPI stained SP β phage. Scale bar, 2 μ M.

2. Mutational analysis of DynA

2.1 DynA preferentially binds to anionic phospholipids (PLs)

In classical dynamins, a PH domain mediates binding to negatively charged PL (Ferguson et al 1994). However, other DLPs, such as Mx proteins, which lack PH domain, are also known to bind negatively charged PLs (von der Malsburg et al 2011). DLPs such as Mgm1p and Fzo1p require an anchor protein, Ugo1p for membrane association (Wong et al 2003). In *B. subtilis*, DynA was shown to bind bacterial membranes, *in vivo* and *in vitro* (Bürmann et al 2011b). But so far, no membrane anchor has been identified for DynA. To further analyse the membrane-binding behaviour of DynA, liposome sedimentation assays were performed with extruded liposomes composed of different phospholipids, PG, CL and PC, respectively. Purified His-DynA was incubated with liposomes at room temperature. After ultracentrifugation, DynA was mostly recovered from liposomes containing anionic PL (PG) whereas weak binding was observed with CL and no binding with PC, suggesting that like

other DLPs, DynA prefers binding to negatively charged membranes (Figure 12). Reactions were also carried out in the presence of magnesium, since magnesium is known to influence lipid binding behaviour of several proteins (Maffey et al 2001). But the presence of magnesium ions had no influence on the membrane-binding behaviour of DynA (Figure 17B). As shown for other dynamin members (Vallis et al 1999), DynA might initiate binding to negatively charged membranes via positive amino acid residues. This has been shown for yeast mitochondrial DLP, Mgm1, where several positively charged lysine residues (K795 K566 and K724) were found to be important for lipid binding *in vitro* (Meglei and McQuibban 2009, Rujiviphat et al 2009).

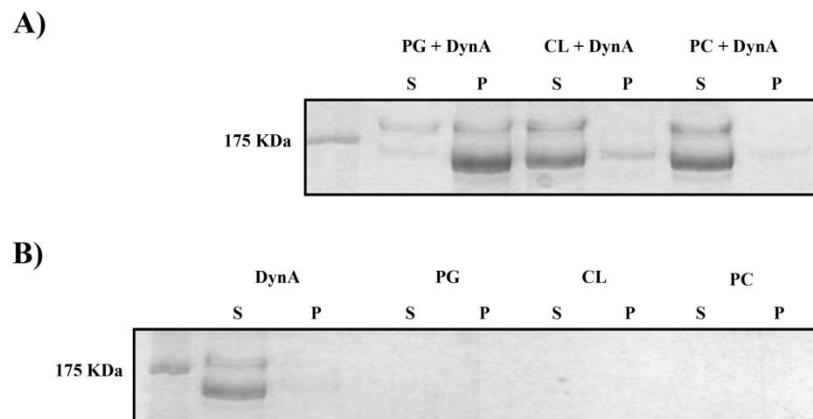


Figure 12. DynA binds to negatively charged membranes. Unilamellar vesicles were extruded from PG, CL and PC phospholipids and incubated with DynA for 1 hour at 25°C. Reactions were analysed by SDS-PAGE. (A) DynA was mostly recovered from liposomes containing anionic phospholipids, PG, whereas weak binding was observed with CL and no binding with PC. (B) Control reactions containing only protein or liposomes. S, supernatant, P, pellet, PG, phosphatidylglycerol, CL, cardiolipin, PC, phosphatidylcholine.

2.2 DynA mediates liposome tethering, tubulation and fusion

BDLP1 from *N. punctiforme* can self-assemble on liposomes to induce tubulation. It forms a compact helical assembly around lipid tubes which is reminiscent of eukaryotic dynamins (Low and Löwe 2006). DynA, too, is able to bind and fuse liposomes (Bürmann et al 2011b). From the above liposome sedimentation experiments, 10 μ L of pelleted DynA-liposomes (PG

and CL), were microscopically examined upon staining with Nile red, a lipophilic dye that stains phospholipids. Microscopic analysis revealed that DynA could induce tethering of liposomes, resulting in the formation of large lipid aggregates (Figure 13A) DynA-induced liposome tethering was found to be independent of Mg^{2+} ions and nucleotides, re-confirming earlier findings (Bürmann et al 2011b). Apart from liposome-tethering, DynA was seen to induce nucleotide-independent tubulation, fusion and fission of liposomes (Figure 13B and 13C) containing PG and CL. DynA-induced fusion was also observed with liposomes prepared from lipid extracts of *B. subtilis* cells (data not shown). When tested with eukaryotic liposomes made from brain polar lipid extract, DynA showed nucleotide-independent liposome binding and tethering, thus phenocopying membrane binding behaviour of eukaryotic DLPs. These observations confirm DynA to have fusogenic properties that are required for inducing membrane-remodelling events.

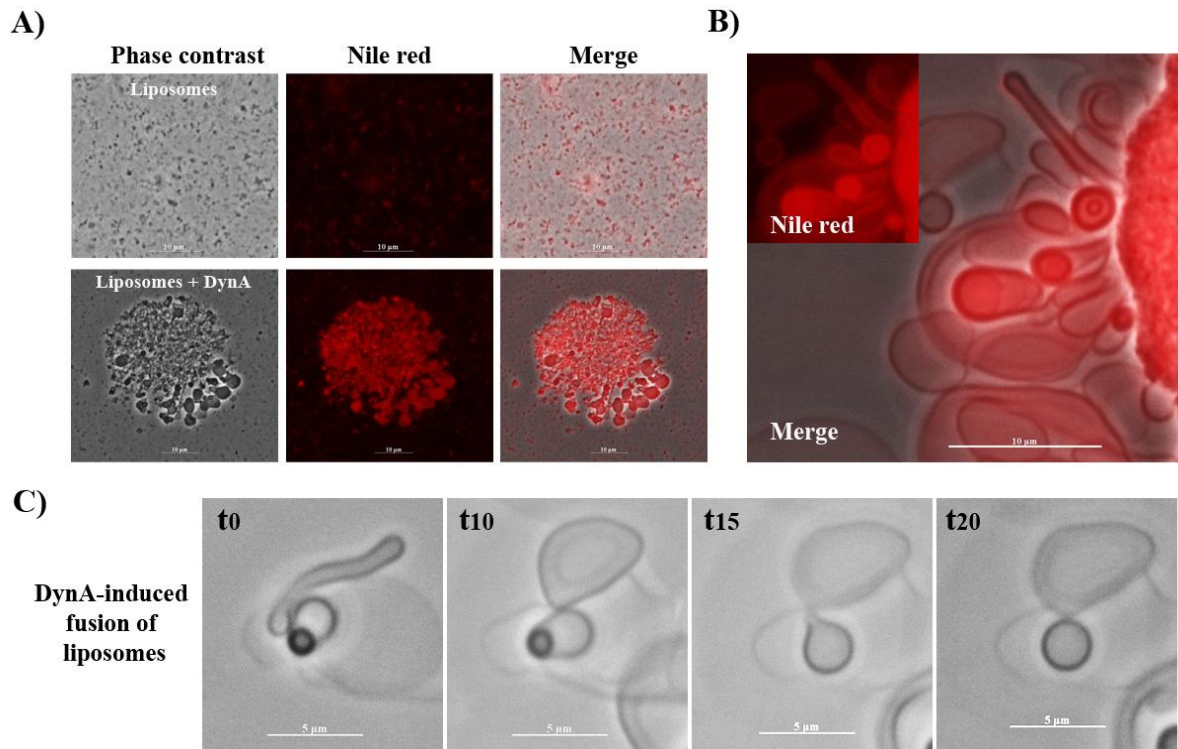


Figure 13. DynA is a membrane remodelling protein. (A) DynA shows nucleotide-independent tethering of liposomes. Aggregation of PG liposomes as well as fusion products was observed upon incubation with DynA. Liposomes were stained with Nile red and reactions were carried out in the absence of GTP and Mg^{2+} ions. Thus, DynA shows nucleotide-independent membrane fusion. Liposome remodelling was not observed in control reactions devoid of DynA. Scale bar, 10 μ M. (B) DynA mediates liposome tubulation. Upon incubation with full-length protein, highly dynamic structural changes (including tubulation and fusion) in PG liposomes were observed under light microscope. Scale bar 10 μ M. (C) Fusion of two PG liposomes induced by DynA observed over time (minutes). Scale bar, 5 μ M.

2.3 Single point mutation, R512A, alters membrane localisation of DynA

Conventional protein-modelling tools, Swiss modelling and iTASSER were used in this study to generate a hypothetical structural model for DynA using BDLP1 (2J68) as a template (Figure 14). The models are in support with our previous results showing the presence of a potential lipid-binding domain (496-500 and 511-522) in D1 subunit, whereas D2 clearly lacks such a domain.

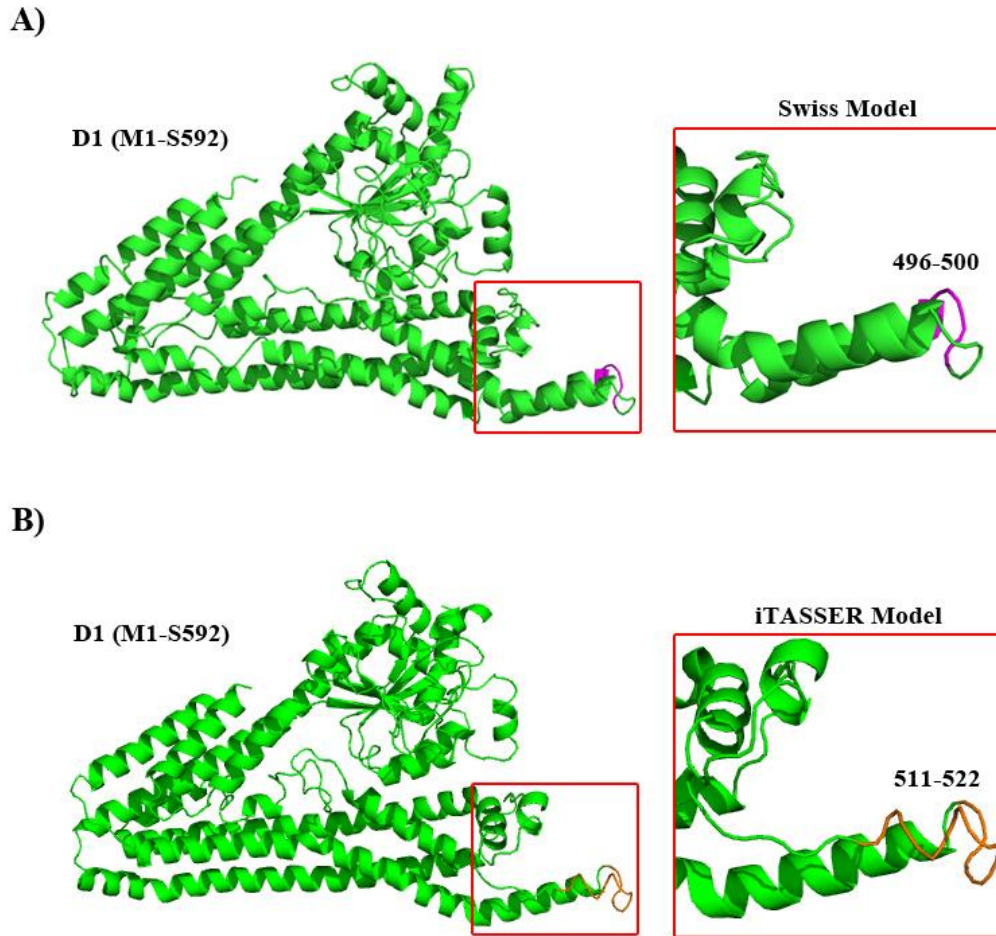


Figure 14. Proposed lipid-binding or paddle loops in subunit D1 of DynA. The D1 (M1-S592) subunit of DynA was aligned on BDLP1 model (2J68) as template using (A) Swiss modelling and (B) iTASSER program to enable the sequence similarities between DynA and BDLP1. The models proposed regions 496-500 and 511-522 to correspond to the lipid-binding paddle domain of BDLP1 (amino acids 576-583).

To identify and verify the lipid-binding region, a site-directed mutagenesis (SDM) approach was adopted to generate DynA mutants. Since DynA binds preferably to negative PLs, it can be hypothesized that positively charged amino-acid residues mediate lipid binding. Hence, regions E496-F500 and A511-W522, along with positively charged amino acid residues were targeted for deletion or point mutation. For localisation studies, plasmid PSC 19 or FBE152 was used as template to generate GFP tagged mutants by SDM. The generated plasmids (PSC

20-29) were used to integrate the DynA mutants into $\Delta dynA$ *B. subtilis* genome, at an amylase-encoding gene, *amyE*, by double-crossover. The resultant colonies had spectinomycin resistance and failed to hydrolyse starch (ie amylase negative). Wild-type DynA-GFP localises throughout the bacterial membrane as well as distinct foci. Similarly, $\Delta 496-500$ DynA-GFP, $\Delta 518-522$ DynA-GFP, K497E DynA-GFP, L498Q DynA-GFP, V499Q DynA-GFP, R506A DynA-GFP and W536A DynA-GFP localise to the membrane, indicating that these regions are not essential for membrane binding (Figure 15A and 15B). Unlike wild-type, $\Delta 511-522$ DynA-GFP and R512A DynA-GFP failed to show membrane localisation suggesting this region with the arginine residue to be important for membrane binding. An important argument against this observation could be the inability to produce a full-length protein, protein instability or low protein expression in the presence of a mutation, thus preventing membrane localisation. To rule out these possibilities, wild-type DynA-GFP and the DynA mutant variants ($\Delta 496-500$, $\Delta 511-522$, V499Q, R506A and R512A DynA-GFP) were analysed by immunoblotting using an anti-GFP antibody. All strains were grown in CH medium and induced with 0.1% xylose for one hour at OD₆₀₀ 1.0. Cells were then harvested and boiled in SDS buffer at 95°C for 10 minutes. In all cases, the full-length monomeric form of the protein was detected (Figure 15C).

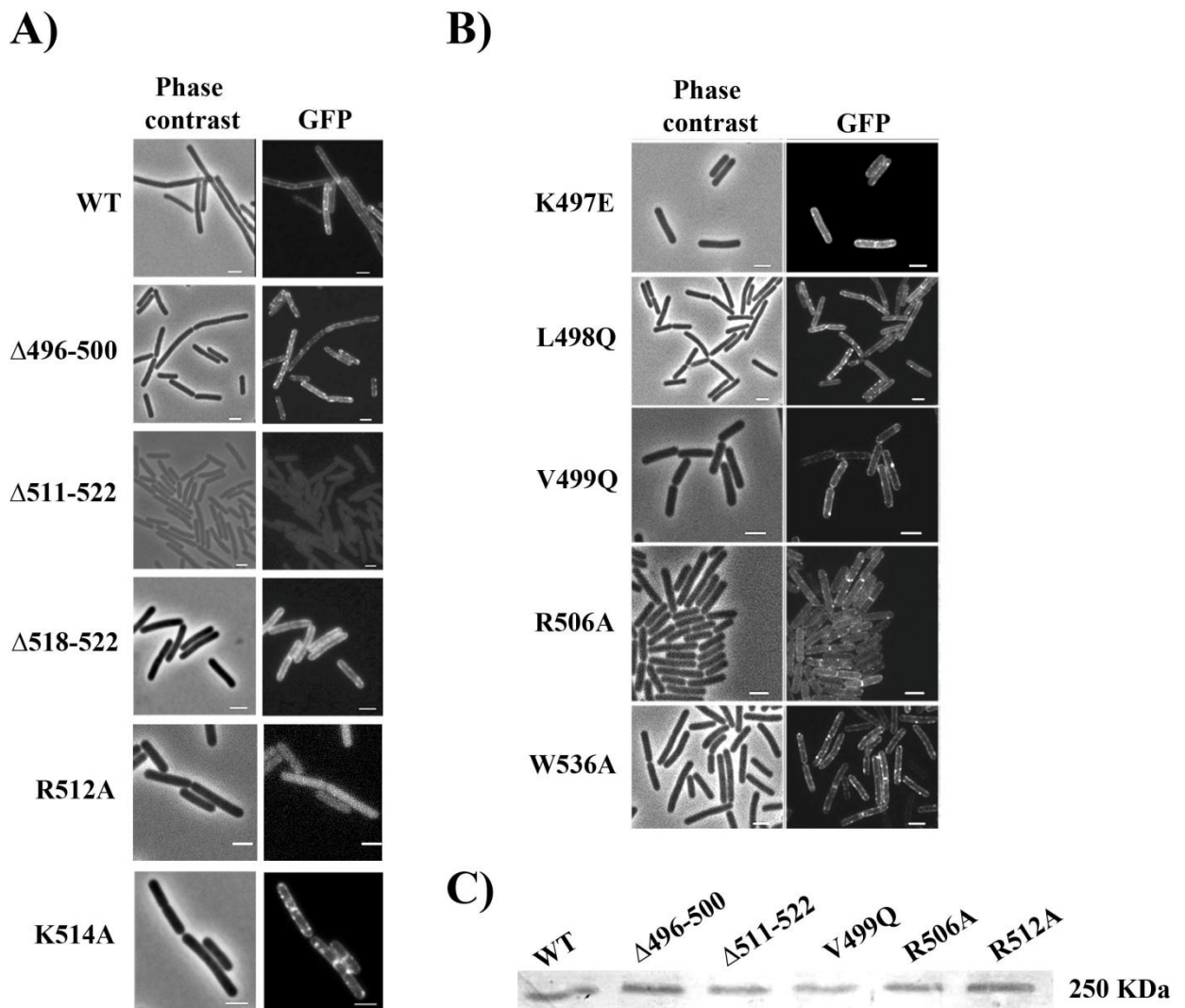


Figure 15. Localisation of wild-type and mutant DynA-GFP in a $\Delta dynA$ background. (A and B) The localization wild-type and mutant DynA-GFP translational fusions were analysed *in vivo*. Like wild-type DynA-GFP, $\Delta 496-500$ DynA-GFP, $\Delta 518-522$ DynA-GFP, K514A DynA-GFP, K497E DynA-GFP, L498Q DynA-GFP, V499Q DynA-GFP, R506A DynA-GFP and W536A DynA-GFP localise to the membrane. $\Delta 511-522$ DynA-GFP and R512A DynA-GFP failed to localise to the membrane. Scale bar 2 μ M. (C) Analysis of mutant-protein stability *in vivo*. wild-type and mutant DynA-GFP proteins are produced as full length proteins, *in vivo*. Cell lysates of the corresponding strains were analysed by immunoblotting using an anti-GFP antibody. Like wild-type protein, mutant proteins form full-length products indicating protein stability in spite of harbouring respective mutations in their coding gene.

Further, liposome sedimentation assays were performed to analyse R512A DynA membrane binding behaviour *in vitro*. Like wild-type DynA-His, $\Delta 511-522$ DynA-His and R512A DynA-His proteins were recovered from liposome sediments demonstrating their membrane-binding ability (Figure 16), thus contradicting the *in vivo* localization data. It seems that altering arginine amino acid somehow alters the *in vivo* lipid binding affinity of DynA. On the other hand, R512A lipid binding was analysed only with PG-liposomes. Hence, it would be ideal to analyse the affinity of this protein for different phospholipids to resolve the ambiguous lipid-binding behaviour *in vivo* and *in vitro*.

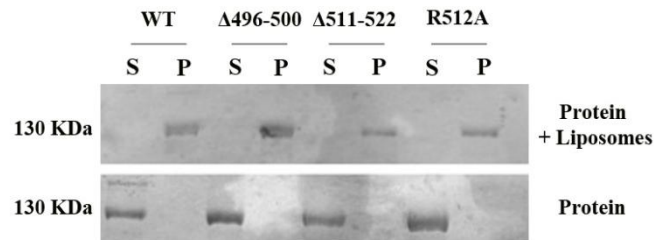


Figure 16. R512A DynA-His binds to membrane *in vitro*. Unilamellar vesicles were prepared from PG and tested with 2 μ M wild-type DynA-His, $\Delta 496-500$ DynA-His, $\Delta 511-522$ DynA-His and R512 DynA-His, respectively, to analyse lipid-binding capability. Reactions were ultracentrifuged prior to SDS PAGE analysis of the supernatant and pellet fractions. Like wild-type DynA-His, a considerable amount of the mutant proteins were recovered from sedimented liposomes indicating lipid-protein interaction. S, supernatant, P, pellet.

Further, GTP hydrolysis of wild-type DynA-His, $\Delta 511-522$ DynA-His and R512A DynA-His was studied by HPLC method. The overall GTP hydrolysis rate of R512A DynA-His was comparable to wild-type protein whereas $\Delta 511-522$ DynA-His lacked GTPase activity (Figure 17A). Thus, it can be concluded that R512A DynA is catalytically active but unlike WT, it fails to form membrane foci *in vivo*. These results confirm that unlike other DLPs, membrane binding and GTPase activity of DynA are independent of each other. Next, lipid binding of R512A DynA-His was analysed in the presence of GTP and Mg^{2+} (Figure 17B). Here, a fraction of protein was recovered in the supernatant, upon GTP addition, indicating R512A DynA has

an altered lipid-binding behaviour which may be influenced either by binding or hydrolysis of nucleotide. It is also possible that GTP hydrolysis mediates disassembly of R512A DynA oligomers that may have assembled on lipid bilayers *in vitro*. And the disassembled free protein remains in the supernatant.

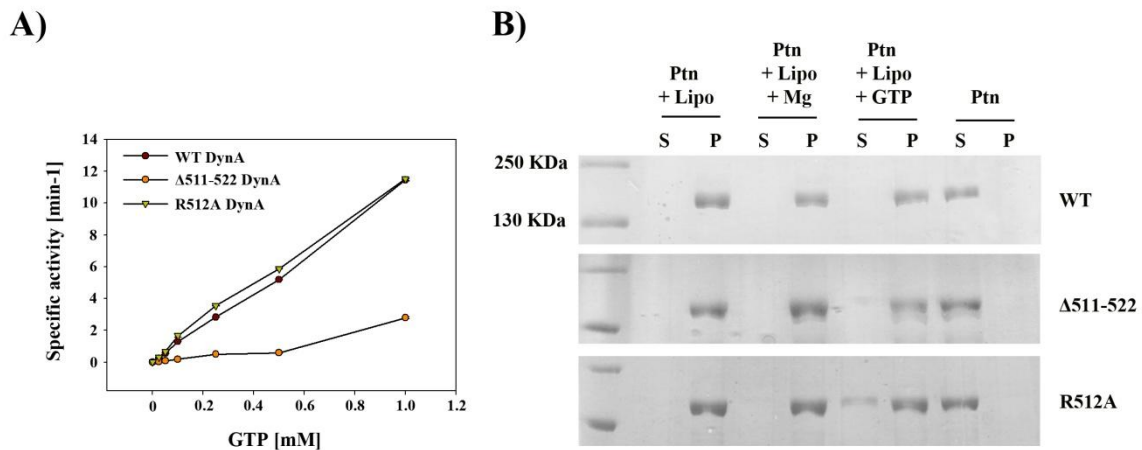


Figure 17. R512A mutation influences lipid-binding behaviour of DynA. (A) Mutation of R512 of DynA does not abolish GTPase activity. The specific activity of 2.5 μ M wild-type DynA and mutants was assayed with increasing GTP concentrations. (B) Lipid-binding behaviour of R512A is influenced by GTP. 2 μ M protein was subjected to PG-liposome binding assays in the presence of nucleotide (1 mM) or MgSO₄ (0.5 mM).

2.4 Amino acid region 591-620 of DynA is required for dimerisation

MxA and other DLPs preferential binding to negatively charged phospholipids is mediated by a positively charged L4 loop in the stalk region (von der Malsburg et al 2011). The L4 loop was also described to be essential for the specificity of the antiviral activity in primate species (Mitchell et al 2012). Protein sequence comparison of DynA with three different Mx molecules (MxA, Mx1 and Mx2) highlighted a common conserved region (Figure 18A), which in Mx proteins is responsible for the antiviral activity as well as inter-molecular interactions. Region 591-620 of DynA was aligned with the C-terminal domains, containing the leucine zipper including part of the L4 loop, of different Mx proteins. The leucine residues and positive amino acids within this region of DynA were found to be conserved. Hence, Δ 591-

620 bacterial clones were generated using SDM approach to study *in vivo* and *in vitro* properties of DynA lacking region 591-620.

For biochemical analysis, Δ 591-620 DynA-His protein was purified in parallel with wild-type DynA-His. Size exclusion chromatography was used to estimate the apparent molecular weight of wild-type and mutant protein. The wild-type DynA-His elution profile revealed peaks corresponding to an oligomer, dimer, monomer and degradation products, whereas Δ 591-620 DynA-His eluted as an oligomer, monomer and degradation products (Figure 18B). The oligomer fraction of Δ 591-620 DynA-His protein, under denaturing conditions (SDS-PAGE), failed to produce a dimer band, which was contrasting to the wild-type protein (Bachelor thesis, Nadine Germ, 2014). In every successive purification, the Δ 591-620 DynA-His elution profile clearly lacked a peak corresponding to a dimer product indicating that some or all amino acids in the 591-620 region of DynA are required for dimer formation. Similarly, region 579-581 was shown to be important for DynA dimer formation, as per the size exclusion elution profiles (Figure 18B), indicating that the C-terminal region of D1 subunit is essential for inter-molecular interactions. Molecular weights of the eluted peaks were estimated by comparing the elution profiles to an elution profile obtained with known-standards (Appendix figure 5, table 1 and 2).

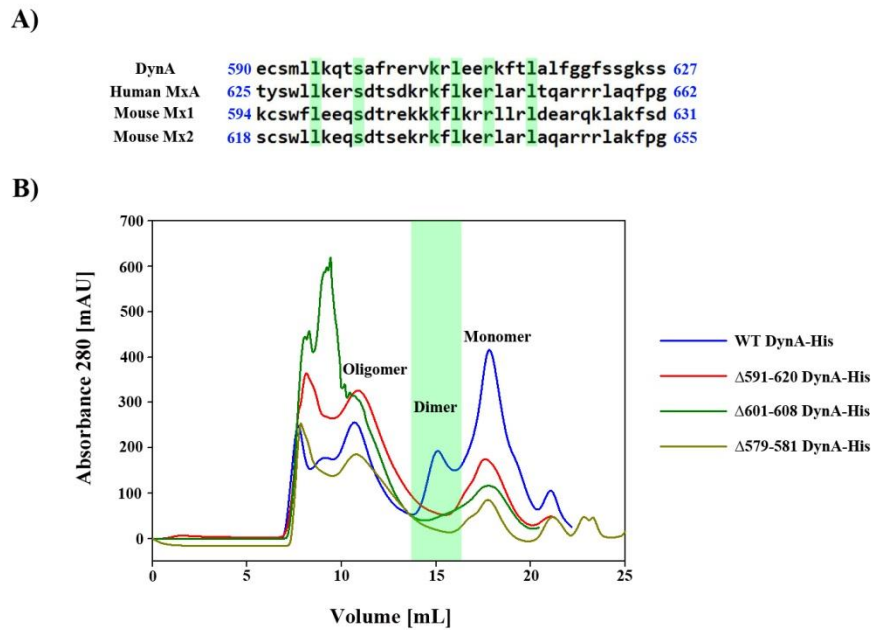


Figure 18. Characterisation of DynA stalk domain, 591-620. (A) DynA-Mx alignment. Alignment of the C-terminal end of DynA D1 subunit (E590-627S) with the C-terminal ends of different Mx members revealed several conserved leucines and positively charged residues (green). (B) Molecular weight determination of wild-type and mutant DynA proteins by size exclusion chromatography. Affinity purified His-tagged wild-type and mutant DynA protein variants were separated on a Superose 6, 10/300 GL column. Elution profiles show the lack of a dimer peak (corresponding to 250 KDa) for mutants, Δ591-620 DynA-His, Δ601-608 DynA-His and Δ579-581 DynA-His, thus indicating their inability to form dimers.

During localisation studies, Δ591-620 DynA-GFP was seen to localise only as foci to the *B. subtilis* membrane (Figure 19), and failed to spread throughout the membrane. Immunoblotting and subsequent probing with an anti-GFP antibody demonstrated that full-length Δ591-620 DynA-GFP was expressed *in vivo*. Further, *in vitro* liposome sedimentation assay showed that Δ591-620 DynA-His binds lipids (Appendix figure 6, Bachelor thesis, Nadine Germ, 2014) in a nucleotide-independent way. However, FRAP analysis revealed that the mobility of Δ591-620 DynA-GFP was impaired compared to wild-type DynA. For wild-type DynA-GFP the majority of the signal recovered in the bleached area within seconds resulting in a saturation-like curve with increasing GFP signal, whereas the loss of the 591-

620 region led to slower recovery resulting in a more linear curve. These findings suggest that DynA is highly dynamic and its C-terminal region is required for mobility across the membrane (Appendix figure 1A, Master thesis of Kristina Eissenberger).

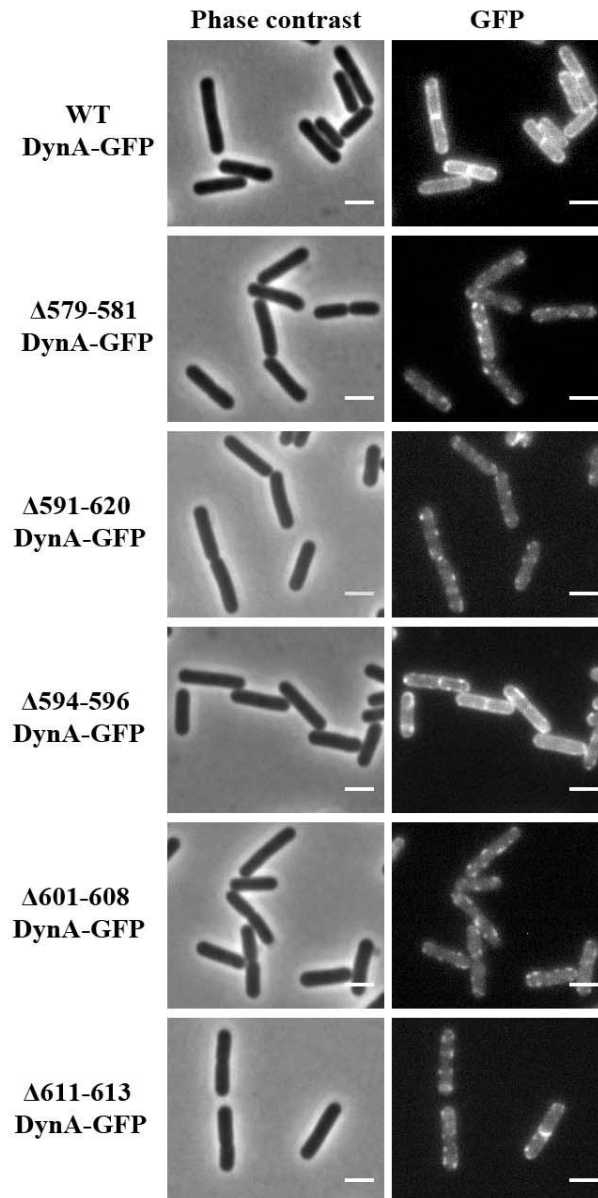


Figure 19. *In vivo* membrane-binding analysis of wild-type and mutant DynA. *ΔdynA* strains expressing translational GFP fusions of wild-type and mutant DynA were microscopically analysed on 1% agarose pads using Zeiss Axiolmager M1. Like wild-type DynA-GFP, $\Delta 579-581$ DynA-GFP, $\Delta 591-620$ DynA-GFP, $\Delta 594-596$ DynA-GFP, $\Delta 601-608$ DynA-GFP and $\Delta 611-613$ DynA-GFP exhibited membrane binding. However, unlike wild-type, all the mutants showed patchy membrane localisation (except $\Delta 594-596$ DynA-GFP) and failed to spread across the membrane. Scale bar 2 μ M.

3. Characterisation of potential DynA-interacting partners identified in a bacterial two-hybrid screen

3.1 Potential DynA-interacting partners localise to the bacterial membrane

DynA localises throughout the *B. subtilis* membrane and to the site of septation. Sequence analysis of DynA show that this protein lacks a transmembrane region, which is necessary for membrane integration. Classical dynamin members bind lipid membranes via PH domain or paddle/L4 loop or anchor proteins. DynA lacks a PH-like domain or L4 loop; however, it can bind to membranes. The fact that DynA can bind to membranes on its own does not nullify the hypothesis that it can interact with mediator proteins under certain conditions to carry out its functions and influence their localisation *in vivo*. Bacterial two-hybrid (BTH) screening was conducted previously to unravel the physical interaction partners of DynA. The screen identified YneK, YmdA and YwpG as potential candidates. YmdA is an essential RNase protein involved in processing of glycolytic mRNA (Commichau et al 2009), whereas YneK and YwpG are proteins of unknown function. To begin with, the localization of the putative DynA interaction partners was analysed individually in *B. subtilis* cells. Thereby, strains expressing C-terminal translational GFP fusions of YneK, YmdA and YwpG, expressed from a xylose-inducible (P_{xyI}) promoter and integrated into the *amyE* locus, were analysed. Like DynA, YneK, YmdA and YwpG tagged to GFP appeared as distinct foci on the *B. subtilis* membrane and sites of septation (Figure 20).

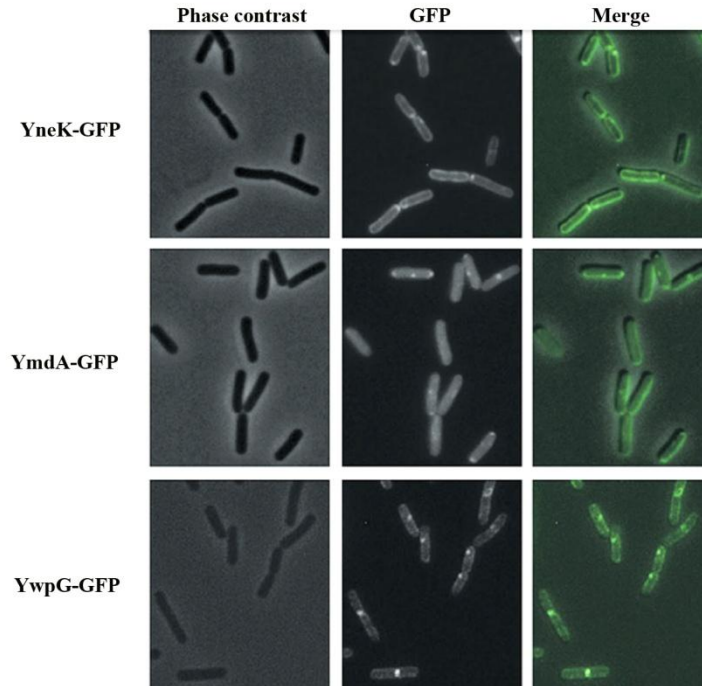


Figure 20. YneK-GFP, YwpG-GFP and YmdA-GFP localise as foci to the bacterial membrane. YneK, YwpG, YmdA (RNase Y) genes were C-terminally tagged to GFP in plasmid pSG1154 and expressed in *B. subtilis* under P_{xyI} promoter. All proteins showed localisation to the membrane as distinct foci and also to the site of septation (Bürmann et al 2012).

The localization of YneK, YmdA and YwpG was also analysed in a $\Delta dynA$ background. No significant difference in the localisation was observed. However, a two-fold decrease in the number of YmdA foci, at the division site, per cell was observed in $\Delta dynA$ strain. Also, the foci formation of YneK-GFP seems to be influenced by DynA, since more than one YneK-GFP focus per cell was observed in the absence of DynA (Table 10). Table 10 provides a statistical analysis on foci formation of the DynA interacting partners.

MinJ forms a novel part of the division site-selection machinery (Bramkamp et al 2008b). Deletion of MinJ alters DynA localisation in *B. subtilis* (Bürmann et al 2011b). Since DynA could demonstrate MinJ-dependent localisation to the division site, the localisation of DynA-interaction partners was analysed in a $\Delta minJ$ background. In the absence of MinJ, foci formation of YneK and YmdA was affected indicating collaboration between DynA and its

identified partners. There is also a possibility that these proteins might function at the septum.

Table 10. Statistical analysis of the localisation of YneK, YmdA and YwpG into foci associated with the cell membrane in a wild-type and $\Delta dynA$ background. Foci formation of YneK and RNaseY in *B. subtilis*, may be DynA-dependent (Bürmann et al 2012).

	YneK-GFP (n = 142)	YneK-GFP $\Delta dynA$ (n = 200)	YwpG-GFP (n = 113)	YwpG $\Delta dynA$ (n = 259)	RNaseY-GFP (n = 331)	RNaseY $\Delta dynA$ (n = 219)
with foci	95.1%	97.5%	97.3%	95.0%	90.6%	91.8%
without foci	4.9%	2.5%	2.7%	5.0%	9.4%	8.2%
with foci at division site	28.9%	35.5%	25.7%	30.9%	72.5%	39.7%
> 1 foci/cell	0%	13%	37.9%	10.4%	7.6%	12.3%

3.2 Interaction matrix of potential DynA-interacting proteins

The BTH system was used to test interaction of the identified DynA-binding proteins with individual subunits, D1 and D2, and their GTPase mutant (M) forms, D1M (K56A) and D2M (K625A), respectively (Bürmann et al 2012). Here, YneK which is a transmembrane protein was found to interact with D1 and D1M subunits. YwpG interacted with both wild-type and mutant subunits, D1, D1M, D2 and D2M, whereas YmdA failed to give a positive reaction with individual subunits (Figure 21). Taken together, these results suggest that YneK, YmdA and YwpG have different patterns of interaction with DynA.

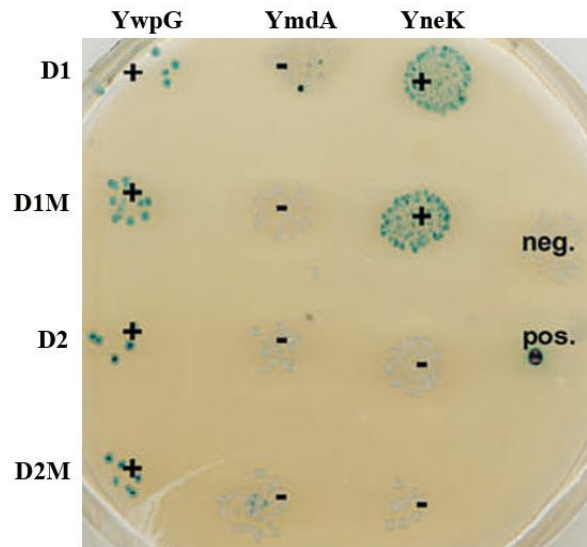


Figure 21. Interaction matrix of YwpG, RNaseY, and YneK with D1 and D2 subunits of DynA and their GTPase mutants (D1M and D2M). D1M harbors the K56A mutation and D2M the K625R mutation, respectively (Bürmann et al 2012).

4. Characterisation of potential DynA-interacting partners identified in a synthetic lethal screen

A synthetic lethal screen (SLS) was performed previously to explore if there is any sick/lethal phenotype in bacteria in combination with deletion of *dynA* (Master thesis of Nina Ebert). The screen identified four genes, *mfd*, *yukF*, *yflN* and *albD* that upon mutation with transposon insertion gave rise to a sick/lethal phenotype in cells lacking DynA. Mfd encodes a 133 KDa transcription-repair coupling factor that functions by promoting strand-specific DNA repair by displacing RNA polymerase stalled at a nucleotide lesion and directing the exonuclease to the RNA damage site (Ayora et al 1996). AlbD is a 49 KDa ABC transporter that is required for the export of antilisterial bacteriocin, subtilosin (Zheng et al 1999). YukF also known as AdeR is a transcription factor required for the expression of alanine dehydrogenase gene *ald* (Lin et al 2012) which is necessary for sporulation in *B. subtilis* (Siranosian et al 1993). YflN is an unknown protein.

4.1 Identified partners fail to produce synthetic lethal/sick phenotype with DynA

During this PhD thesis, the above genes were targeted for deletion using primers, PSP 106-121 and plasmids, PSC 37-39, respectively. Deletion of the respective gene was verified by PCR (Appendix figure 7). Confirmed strains, Δmfd , $\Delta yukF$ and $\Delta yflN$ were subjected to growth experiments along with wild-type, $\Delta dynA$ and DynA complementation strain (PSB032). No significant growth phenotype was observed with the mutants. Genomic DNA from the above-confirmed strains was isolated and transformed in $\Delta dynA$ background. $\Delta mfd\Delta dynA$, $\Delta yukF\Delta dynA$ and $\Delta yflN\Delta dynA$ double mutants were found to grow normally, thus eliminating our hypothesis that cells lacking Mfd, YukF or YflN in combination with DynA are synthetically lethal (Figure 22). Further, microscopic analysis of the deletion strains did not reveal any morphological phenotype, thus verifying our above results.

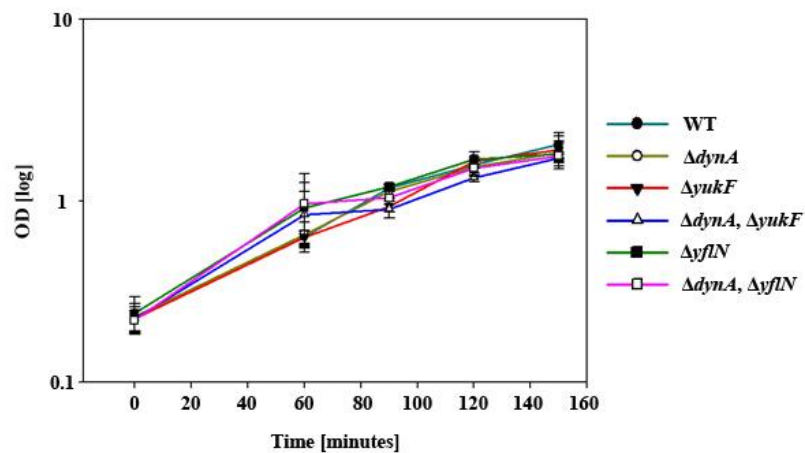


Figure 22. Deletion of putative partners, identified in SLS, fail to produce a synthetic lethal/sick phenotype with $\Delta dynA$. Growth curves from two independent experiments were analysed to verify the synthetic lethality of predicted synthetic lethal partners of DynA. $\Delta yukF$, $\Delta yflN$, $\Delta yukF \Delta dynA$ and $\Delta yflN \Delta dynA$ growth was comparable to $\Delta dynA$ and wild-type. Hence, one can rule out the hypothesis that the absence of YukF and YflN is synthetically lethal with $\Delta dynA$ under normal growth conditions.

4.2 DynA-GFP localisation is not affected in strains lacking the identified potential partner/s

For DynA localisation studies in the absence of Mfd, YukF and YflN, gDNA from Δmfd , $\Delta yukF$ and $\Delta yflN$ strains was isolated and transformed into strain NEB006 (*dynA-prom::tet, amyE::pSG1154_dynA-prom-gfp*). Cells were cultivated in CH medium and induced with 0.5% xylose for microscopic analysis. DynA-GFP, expressed from its native promoter, localised to the cell membrane in the absence of Mfd, YukF and YflN, thus indicating that membrane localisation of DynA is independent of the above-identified candidates (Figure 23). However, patchier membrane localisation of DynA-GFP is observed in the absence of YflN and Mfd, respectively (see figure 23), indicating that these proteins might influence membrane-binding behaviour of DynA, which needs further testing.

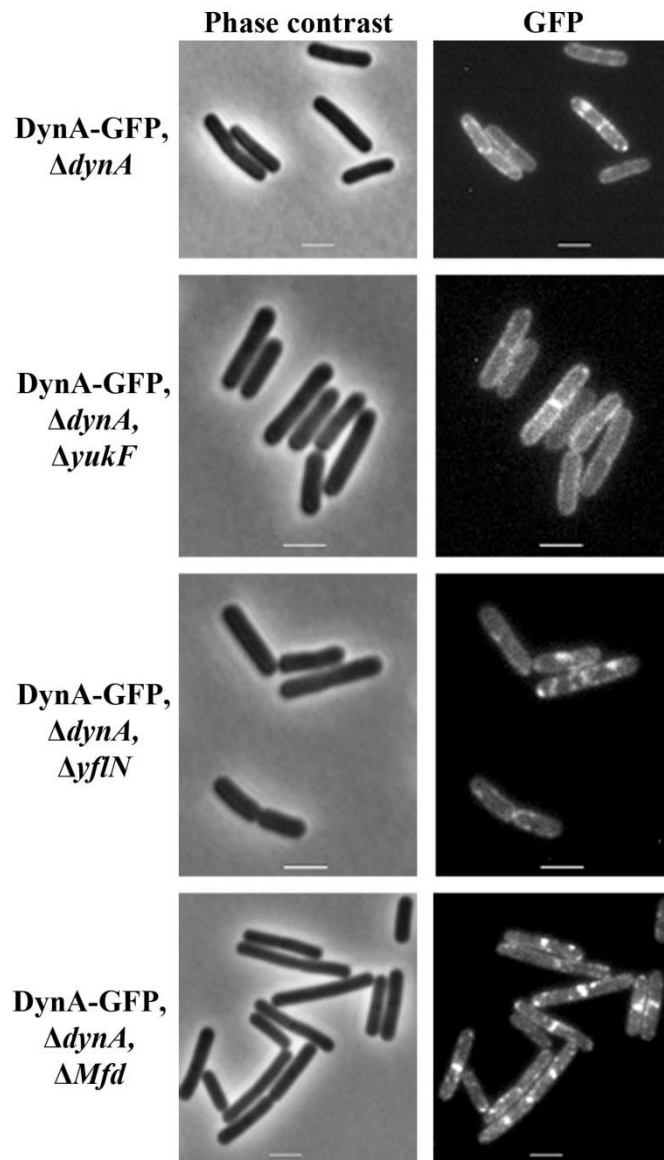


Figure 23. DynA-GFP localisation is not affected in strains lacking the identified potential partner/s. Strains PSB057, PSB054 and PSB053 were grown in CH medium and analysed microscopically using AxioImager M1 equipped with a Zeiss AxioCam HRm camera and GFP filter settings. DynA-GFP localised to the bacterial membrane as well as division sites in cells lacking YukF, YflN and Mfd. Scale bar, 2 μ M.

5. Localisation studies of DynA

5.1 Lack of flotillins does not disturb membrane localisation of DynA

Lipid rafts are micro-domains on the cell membranes, important for cellular functions such as signal transduction and membrane transportation (Bramkamp and Lopez 2015). In eukaryotes, flotillin-1 is an important component of micro-domains co-ordinating the formation of lipid rafts (Bach and Bramkamp 2013). *B. subtilis* encodes for two flotillin-like proteins, YuaG and YqfA that belong to the family of proteins containing SPFH domain. Flotillins can influence membrane fluidity by organising lipid and protein assemblies at the cell membrane. Hence, it was hypothesised that flotillins might influence DynA localisation. For this purpose, gDNA from strain NEB006 (*dynA-prom::tet, amyE::pSG1154_dynA-prom-gfp*) was extracted and transformed into a $\Delta yuaG \Delta yqfA$ *B. subtilis* strain. Spectinomycin resistant and amylase negative colony was selected as a positive transformant (strain PSB086). Strains NEB006 and PSB086 were grown in CH medium for microscopy. DynA-GFP localised to the bacterial membrane even in the absence of both flotillins (Figure 24), YuaG and YqfA, thus eliminating our hypothesis that flotillins might influence DynA localisation.

5.2 DynA-GFP localises into distinct foci and fails to spread across the cell membrane in the absence of YpbQ and YpbS.

The immediate neighbours of DynA-encoding gene, *ypbR* are *ypbQ* and *ypbS*. *ypbQ* is a 504 bps-long gene that encodes a putative integral membrane protein which is homologous to isoprenylcysteine carboxymethyltransferase, however its function in *B. subtilis* has not been characterised. *ypbS* is a 255 bps gene, encoding a protein with unknown function. To analyse if the absence of YpbQ and YpbS has an influence on the localisation of DynA, a $\Delta ypbQRS$ strain was generated (PSB072). gDNA from strain FBB018 was isolated and transformed into competent PSB072 to generate strain PSB085. Microscopic examination of strain PSB085 revealed that DynA, when expressed under a xylose-inducible promoter, localises only as foci on the membrane (Figure 24) in the absence of YpbQ and YpbS. This pattern of foci formation looks different from the foci formation under wild-type background, thus indicating that the neighbouring genes might have an influence on the localisation pattern of DynA. Recent

experiments suggest that DynA localisation is mostly influenced by YpbS since DynA was seen to localise throughout the membrane in the absence of YpbQ (Currently ongoing Master thesis of Laurence Karier).

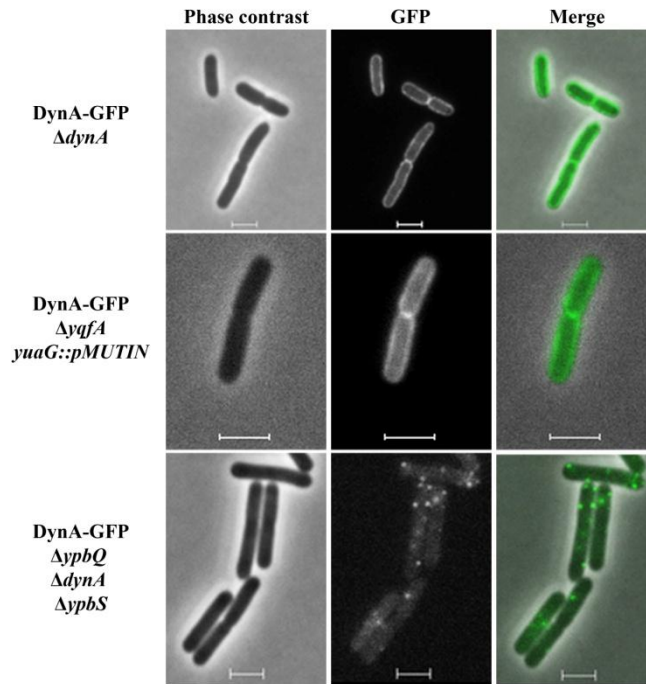


Figure 24. Membrane localisation pattern of DynA-GFP is altered in strain lacking the *yqbQ* and *ypbRS* operon. DynA-GFP localised around the bacterial cell membrane as well as at the division site. DynA-GFP localises throughout the membrane in a flotillin knockout strain, $\Delta yuaG \Delta yqfA$ (strain from Juri Bach) thus showing a similar pattern of localisation like in the wild-type background. In a strain lacking YpbQ, YpbR (DynA) and YpbS, ectopically expressed DynA-GFP was seen to form prominent foci in the membrane, thus showing a different pattern of localisation. Shown are different channels as indicated. Scale bar, 2 μ M.

Discussion

During evolution the process of endosymbiosis has played a major role in the distribution of gene pool from prokaryotes to eukaryotes. Several eukaryotic cell organelles, such as mitochondria and plastids, are known to have bacterial origin. The endosymbiotic theory seems to be a plausible explanation for the conservation of genes and proteins between different species of organisms (Timmis et al 2004). The dynamin family is one such class of protein that may have evolved from bacteria to eukaryotes, where these proteins have turned out to be essential for different cellular functions. Members of this protein family can be sub-classified into dynamins or dynamin-like proteins (DLPs), on the basis of their domain content (Praefcke and McMahon 2004). In eukaryotes, dynamins or DLPs participate in endocytosis, organelle division, intracellular cargo trafficking and in defence against viruses. In bacteria, DLPs often exist as two copies in an operon and are known to induce membrane remodelling *in vitro*. Though BDLPs have been characterised in some bacteria, their actual mechanism of action still remains ethereal.

The aim of this PhD thesis was to characterise a BDLP, DynA from *B. subtilis*. To fulfil this aim, mutational analysis on DynA was carried out to have a better understanding of its structural assembly. Site-directed mutagenesis approach was used to truncate regions and generate point mutations within DynA. Generated mutants were then subjected to biochemical analysis. Apart from mutational studies, functional characterisation of DynA was a priority to ascertain its role in the rod-shaped, Gram-positive bacterium, *B. subtilis*. So far, different aspects of *B. subtilis* cell biology have been tested to identify the function of DynA. These include growth, cell division, sporulation, sensitivity to antibiotics and susceptibility to phage infection. Since DynA is a membrane-bound DLP, any alterations in cell membrane synthesis and composition might adversely affect the localisation and in turn the function of DynA or other membrane-binding proteins (and/or protein complexes). On the other hand, the absence of a membrane-bound protein, such as DynA, may lead to pleotropic effects on membrane remodelling events. These events could be associated with cell growth and

division. However, no major growth phenotype was observed with $\Delta dynA$ strain indicating that this protein is not essential under normal laboratory growth conditions. Interestingly, a striking difference was observed in the susceptibility of wild-type and $\Delta dynA$ strains to different antibiotics (PhD thesis of Van Baarle, 2009). A $\Delta dynA$ strain showed decreased sensitivity to tetracycline, chloramphenicol and kanamycin compared to the wild-type strain. These antibiotics are active within the cytosol and block protein synthesis. However, no difference in sensitivity pattern between wild-type and $\Delta dynA$ could be observed with spectinomycin which also targets 30S ribosome to block protein synthesis. Thus suggesting that decreased sensitivity to antibiotics might be caused due to differences in transport and/or diffusion pathway of these compounds and not due to abrogated protein synthesis. A $\Delta dynA$ strain was also found to be sensitive to salt stress and defective in septa formation upon salt stress, which was analysed by electron microscopy (PhD thesis of Van Baarle, 2009). All these observations hinted towards a role of DynA in bacterial cell membrane remodelling under stress conditions. Eukaryotic DLPs are known to participate in several cellular processes, their common characteristic being lipid membrane remodelling. Membrane remodelling in bacteria is required for transport of substrates in and out of the cell and to maintain cellular integrity, when exposed to environmental stress. *B. subtilis* is a soil bacterium and hence, exposed to environmental stress factors, commonly antibiotics and bacteriophages. DLPs such as bacterial IniA and eukaryotic Mx proteins have been proposed to provide protection against antibiotics and phage infection, respectively. This idea led to testing whether DynA is required by *B. subtilis* under stress conditions, since deletion of *dynA* in strain 168, failed to produce any major phenotype under standard laboratory conditions.

1. Functional characterisation of DynA

1.1 DynA is a bacterial membrane remodelling system

Membrane remodelling is one of the many defence strategies used by bacteria to tackle environmental stress. Membrane defences against antimicrobial agents is well studied in Gram-negative bacteria, which can remodel their outer membrane and LPS to decrease the

overall negative charge on their membrane, thus repelling several cationic antimicrobial peptides (Roy et al 2009). Gram-positive bacteria lack an outer membrane, but possess a thicker peptidoglycan layer along with a plasma membrane that pack in teichoic acid and lipoteichoic acid polymers, and together provide resistance to harsh environmental conditions (Brown et al 2013). Surrounding the cell surface and in the membrane, lie several proteins that provide envelope integrity to bacteria. This thesis has unravelled a novel membrane-defence strategy in bacteria, acting at the site of stress induced membrane damage, and it involves the activity of a DLP, DynA. Growth experiments with cell envelope-targeting antibiotics revealed $\Delta dynA$ to be more sensitive to membrane stress (Figure 4). In particular, antibiotics that induce membrane pore formation or directly interact with lipids and distort the membrane (such as nisin and bacitracin) triggered elevated sensitivity. This shows that DynA plays a role in combating the detrimental impact of membrane-targeting antibiotics in *B. subtilis*. Pore formation is one of the most deleterious mechanisms of action of antimicrobial peptides. Nisin is a 3.4 KDa posttranslationally modified peptide produced by *Lactobacillus lactis*. It contains 5 intramolecular rings made up of strong thioether amino acids, lanthionine and 3-methylanthionine. Of these 5 rings, the first two are responsible for binding to lipid II and the last two are intertwined together and can flip in the membrane to form pores. Nisin can follow two mechanisms to form membrane pores. Firstly it can bind to anionic PLs and form nisin aggregates that permeabilise the membrane. However, the pores formed are short-lived. Secondly, nisin can bind to lipid II to form nisin-lipid II (in 2:1 ratio) complexes that together give rise to larger (2-2.5 nM diameter) and more stable membrane pores (Hasper et al 2004, Hsu et al 2004, Piper et al 2011, Van de Ven et al 1991, van Heusden et al 2002, Wiedemann et al 2001). These different pore-forming mechanisms of nisin would therefore depend on the anionic PL content and lipid II concentration in bacterial membranes. This also means that the severity of nisin may fluctuate between different experiments and in different bacteria. Under nisin stress, cell division is compromised in bacteria because; the main target for majority of antibiotic agents, including nisin, is the

newly synthesized cell envelope at the division septa. Addition of nisin to a growing culture of *B. subtilis* was also shown to disturb membrane potential, leading to de-localisation of several proteins, including the FtsZ-assembly-inhibiting Min system and the cell shape determinant protein, Mbl. This causes accelerated division-septa formation, which ultimately leads to generation of shorter cells and several morphological defects (Shahbadian et al 2009). The fact that an external stress-inducing agent acts on bacterial division septa would explain why a stress-response protein such as DynA localises with division-site proteins (PhD thesis of Van Baarle). Further, an increased resistance to membrane-targeting daptomycin upon over-expression of DynA is comparable to the phenotype observed with another BDLP, IniA from *M. tuberculosis*. Over-expression of IniA in *M. bovis* provided an enhanced resistance to cell envelope-targeting antibiotics, isoniazid (INH) and ethambutol (EMB) (Colangeli et al 2005). The results from growth experiments suggest DynA to induce a protective response upon sensing membrane stress caused by antibiotics. The fact that cells expressing DynA, too, take time to combat stress, is indicative of involvement of other stress-response proteins that might be required prior to the action of a DLP.

Since lack of DynA is seen to enhance resistance to antibiotics that act internally (such as chloramphenicol and kanamycin) and aid membrane-targeting antibiotics, it can be assumed that DynA is involved in either maintaining the bacterial membrane potential or PL integrity or inhibiting diffusion through the membrane. One of the well-known stress-response pathways in bacteria is the phage shock protein (PSP) system. In *E. coli*, the PSP response is induced by filamentous phage infection and is known to prevent proton leakage from bacterial membrane. *In vitro*, higher-order PspA oligomers were shown to bind to PG containing liposomes and prevent proton leakage (Kobayashi et al 2007). This oligomer-forming behaviour of PspA is similar to lipid-bilayer induced higher-order assembly formation of DLPS (Low and Löwe 2006). Like LiaH, a PspA homolog in *B. subtilis*, DynA localised in static foci, staticity analysed by FRAP (Appendix figure 1C, Master thesis of Kristina Eissenberger), upon membrane stress (induced by nisin, in the case of DynA). Hence,

it was assumed that PSPs and DLPs have similar functions. Loss of membrane potential due to nisin is a well-known fact, which hinted towards the possibility that static foci formation by DynA could be induced due to loss of electric potential over the membrane. Therefore, the localisation of DynA was analysed upon addition of another ionophore, CCCP. Like nisin, addition of CCCP also led to formation of static foci by DynA-GFP (Appendix figure 1D). However, the pattern of foci formation of DynA by nisin and CCCP was different, in terms of foci number and size. About 5 large foci per cell were observed with CCCP, whereas 8 small foci per cell were observed with nisin, suggesting that DynA indeed reacts differently to nisin-induced pore formation and CCCP-induced loss of membrane potential. Since it reacted to CCCP, it was ideal to analyse if DynA, like *E. coli* PspA, is involved in maintaining bacterial membrane potential. Membrane potential dissipation experiments with nisin and valinomycin, however, nullify the assumption that DLPs act towards maintaining membrane potential (see figure 6). This shows that PSPs and DLPs follow different membrane-protection pathways during stress, at least in *B. subtilis*. One could propose PSPs to be involved in regulating the proton motive force across the membrane, and DLPs to be involved in sealing membrane gaps by tethering the damaged membrane. This proposition can be well supported with our previous study demonstrating membrane fusion properties of DynA (Bürmann et al 2011b). Given that DynA binds to lipid membranes and can induce membrane tethering and fusion, it is imaginable that this protein functions by acting like a fusogenic agent when recruited to a damaged site, in particular pores on the bacterial membrane. It is likely that DynA forms large polymers that fill up membrane gaps, induced by nisin, to prevent cytoplasmic leakage. This hypothesis was further verified by time-lapse microscopic experiments (Master thesis by Kristina Eissenberger), which showed that cells lacking DynA are impaired in recovering from membrane stress that involved pore formation by nisin. For time-lapse microscopy with nisin, cells were stained with FM4-64 dye. This lipophilic dye is membrane non-permeable, indicating that it is most likely binding to phospholipid head groups on the outside of the membrane. Heavy membrane deformations are observed in the

presence of nisin in $\Delta dynA$, which are located towards the cytoplasmic side of the cell (Appendix figure 2). One can imagine that bacteria have to undergo rapid membrane or lipid rearrangement to internalize and then dissolve these deformations. Several membrane-remodelling proteins, including DynA, are expected to participate in such processes.

The membrane remodelling behaviour of DynA was further analysed by FRAP and FLIP experiments. Since, DynA, like eukaryotic DLPs, was shown to exhibit membrane remodelling behaviour and found to be highly dynamic at bacterial membrane, it seemed likely that over-expression of DynA might result in an elevated membrane turnover rate. For this purpose, WT, $\Delta dynA$ and PSB033 (DynA⁺) bacterial cells were subjected to FRAP analysis upon membrane staining (Master thesis by Kristina Eissenberger). The cell membrane was stained with lipophilic FM4-64, bleached at a defined region and lipid recovery was measured over time. After bleaching one cell pole, recovery of the signal was measured within seconds for all the three strains. The time for half maximum recovery was calculated on the basis of best-fit trend lines; $\tau/2(\text{WT}) = 26.62 \text{ sec}$; $\tau/2(\Delta dynA) = 32.75 \text{ sec}$; $\tau/2(\text{PSB033}) = 4.42 \text{ sec}$. Although, the difference in membrane dynamics between wild-type and $\Delta dynA$ was minor, DynA over-expressing strain exhibited dramatically faster recovery. The data revealed a 23% extended recovery time in $\Delta dynA$ compared to wild-type strain. In contrast, the recovery in PSB033 (DynA⁺) was six times faster compared to wild-type. The data not only showed that DynA can undergo a highly dynamic subunit exchange across the membrane but also indicates a role of DynA in membrane turnover (at least upon DynA over-expression). To avoid ambiguity due to possible photo-switching of FM4-64, FLIP experiments were performed to compare the mobility of FM4-64 in membranes in the presence and absence of DynA. FLIP results show that the rate of membrane remodelling in bacteria is indeed very high and facilitated in cells expressing DynA (Figure 7).

Taken together, the results from antibiotic growth experiments, time-lapse analysis, stress-induced localisation studies and FLIP analysis; it is conclusive that DynA is engaged in functions that involve membrane remodelling when bacteria are exposed to stress. It is clear

that DynA mostly recognises membrane stress that includes pore formation and likely responds by repairing the damaged membrane with its fusogenic ability. Although not essential for growth, DynA seems to be involved in a novel bacterial defence strategy under membrane stress. Also one cannot ignore the fact that the bacterium contains several lines of defence during stress that might be dominant over the activity of DynA. But the conservation of such a large DLP by the bacterium indeed justifies that this protein is important during some stage of the bacterial life cycle.

1.2 DynA phenocopies Mx proteins by providing defence against bacteriophages

DynA's membrane protection function was further analysed using another membrane-stress inducing agent called bacteriophage. A bacteriophage has to undergo adsorption onto the bacterial surface, through receptors, which is then followed by bacterial membrane penetration to inject the phage genetic material into the cell cytoplasm. Membrane penetration by phages can induce several stress-response systems in bacteria. This PhD thesis has unravelled one such phage-response system, DynA, in *B. subtilis*. Recent experiments have shown a $\Delta dynA$ strain to be more sensitive to bacteriophage infections. Initially, wild-type and $\Delta dynA$ (168) strains were tested for susceptibility towards an infectious phage, $\Phi 29$, with plaque forming assay. The latter strain was found to be highly susceptible to phage stress, hinting towards a role of DynA in providing resistance to bacteria during $\Phi 29$ infection. Next, it was ideal to test if DynA acts specifically against $\Phi 29$ or phage infections in general. Therefore, a wild-type and $\Delta dynA$ (25152) strain were tested for susceptibility to another bacteriophage, SP β . SP β is a prophage but can be excised from the bacterial genome by adding mitomycin C to a growing culture. Since 168 strain background is lysogenic for SP β , all plaque assays were performed with prophage-free *B. subtilis* 25152 strain background. The 25152 strain lacking DynA was again found to be more sensitive to SP β than wild-type, thus verifying our idyllic hypothesis that DynA has a common function of protecting bacteria from phage infections. Over-expressing DynA in a $\Delta dynA$ strain (PSB032 and PSB033) could significantly reverse the *dynA* deletion mutant phenotype. This phenotype

is in support with the proposed function of DynA and that is membrane protection upon extracytoplasmic stress (Figure 25). This phenotype also makes DynA, the Mx equivalent in bacteria. Similar to Mx proteins, DynA shows oligomerisation and membrane tethering properties. Furthermore, like MxA (von der Malsburg et al 2011), DynA prefers binding to negatively charged phospholipids and shares common amino acid residues with the C-terminal region of different Mx molecules. These C-terminal regions in Mx constitute the leucine zipper, which is required for Mx oligomerisation (Melen et al 1992). Mutational analysis of the region containing these common leucine residues, 591-620, has further shed light on oligomerisation behavior of DynA (see below, 2.2).

Further aims of this project were to unravel the importance of DynA in antiviral defence. Like Mx, DynA could possibly be targeting a viral protein to promote antiviral activity. GTP-binding, sub-cellular localisation and homo-oligomerisation are considered to be the pre-requisite determinants for Mx antiviral activity. Hence, a detailed study of GTP hydrolysis and oligomerisation of DynA would enable us to unravel the fate of DLPs in antiviral activity. It would be ideal to test the antiviral activity of different DynA mutants, a non-dimer forming Δ 591-620 DynA (see below, 2.2) and a GTPase mutant (K56A, K625A DynA). This would not only tell us whether dimerisation influences antiviral activity, but also explain whether GTPase activity is necessary for its function against phages. Further, testing a non-membrane binding DynA mutant would help clarify if membrane association is required for inhibiting viruses. Like MxA, DynA assemblies are found on lipid membranes. Such assemblies are known to promote protein stability and protect MxA from degradation (Mitchell et al 2012). Another important study would be to identify structural motifs that are crucial for the binding of DynA to viral components. In the case of MxA-expressing cells, stacks of filaments have been observed, that comprise MxA and viral nucleoprotein. Such an interaction is also observed with DynA and phage particles, *in vitro*. Also, *in vitro* labelling experiments could show co-localisation of DAPI-labelled phages with Texas red-labelled DynA. The binding of phage particles and purified protein *in vitro* would suggest that DynA interacts with an

exposed component of the phage, which could be the head, collar, tail or collar appendages. However, these *in vitro* experiments have certain drawbacks. Therefore, it would be ideal to have a control where a mutant DynA fails to show binding to phage particles *in vitro*. Since Mx proteins have been shown to co-sediment with viral nucleo-capsid proteins (Haller and Kochs 2002), it is conceivable that a BDLP follows the same path for acting against bacteriophages. However, the most important question of whether DynA shows a direct interaction with the phage particle *in vivo*, still persists. To resolve this ambiguity, one can perform microscopic analysis on DynA-labelled cells infected with labelled-phage.

Host cell membrane remodelling is required for the attachment of a phage particle to the host cell and for release of viral DNA. Since DynA can tether membranes *in vitro*, a role in membrane remodelling, for example sealing damaged bacterial membrane upon phage penetration, seem plausible. Indeed, DynA would serve as a suitable model for unravelling the molecular details of antiviral defence of homologous eukaryotic DLP counterparts, for example Mx proteins. Recent studies have also focused on the co-evolution of viruses to cope with Mx proteins (Breukink et al 1999, Wiedemann et al 2001). Also, the conservation of a positive selection on amino acids in the antiviral specific L4 loop of Mx molecules sheds light upon the evolution of Mx proteins in different primate species (Bonev et al 2004). Further mutational and structural studies with DynA will ensure a better understanding of the conservation and mechanism of antiviral proteins in bacteria.

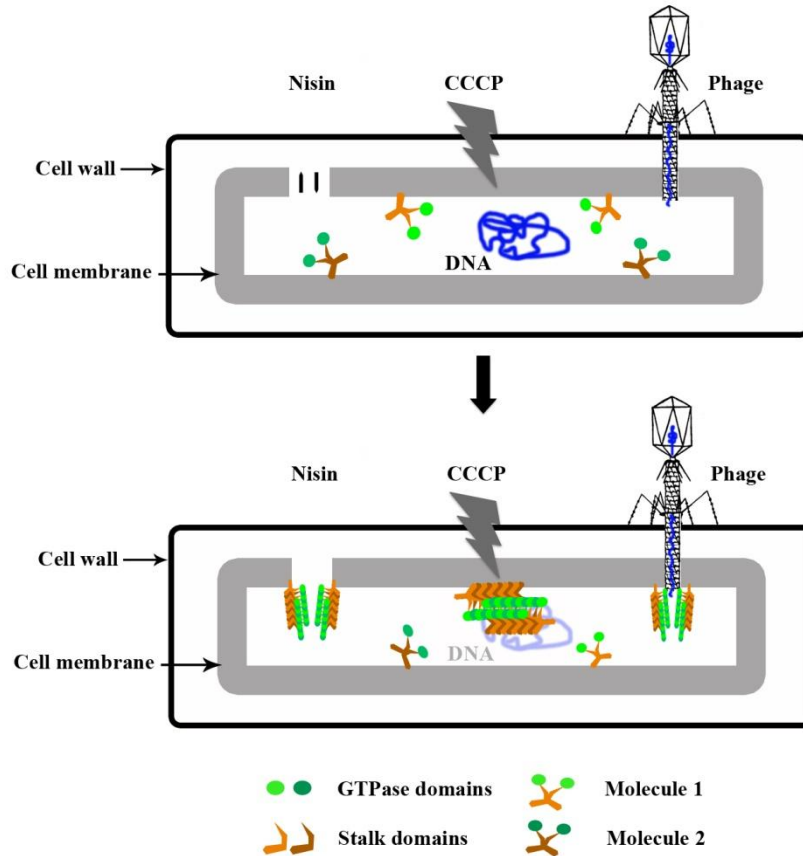


Figure 25. Proposed model for membrane protection by DynA. Upon membrane stress, induced by an extracytoplasmic factor, such as phage or antibiotic, DynA is recruited to the damaged membrane site. At this site, DynA polymerises into large assemblies and seals membrane gaps by inducing lipid-bilayer fusion.

2. Mutational analysis of DynA

2.1 Membrane-foci formation is oligomerisation-dependent and GTP hydrolysis is required for disassembly of oligomers

DynA is a membrane associated protein but lacks any transmembrane region. Therefore, it is likely that binding to membranes is due to its affinity for lipids and/or is mediated by other membrane-binding proteins. Previous studies have shown DynA to be capable of inducing membrane tethering and fusion (Bürmann et al 2011b). Hence, DynA could be assumed as a force-generating fusogen on bacterial membranes. This assumption is concurrent with its

proposed membrane-sealing function. When tested for interaction with phospholipids, DynA sedimented with PG, CL, *E. coli* total lipids and eukaryotic folsch liposomes. DynA showed preference for binding to negatively charged phospholipids; PG and CL. PG and CL are anionic lipids at neutral pH that may undergo structural changes with a change in pH and presence of divalent cations (Mg^{2+}) or fusogenic molecules, thus inducing changes in membrane structure. Anionic lipids are enriched on the inner layer of the bacterial lipid bilayer as well as at the site of septation and their interaction with positively charged amino acids can influence the topology of proteins, including DynA. In classical dynamin, the pleckstrin homology (PH) domain is responsible for mediating membrane interaction whereas in BDLP1, a paddle-binding loop has been characterised comprising of L576, L577 and F583 residues (Low et al 2009). No such membrane-binding domain or loop has been identified in DynA.

With the aim to identify the DynA paddle loop, structural modelling of DynA was carried out using I-TASSER and Swiss modelling software systems. The crystal structure of BDLP1 (2J68.pdb model of BDLP1) was used as a template to generate structural models of individual subunits (D1 and D2) of DynA. Two putative membrane-binding loops (496-500 and 511-522) were proposed through these models. Also, these regions contain several positively charged amino acids that were predicted to mediate interaction with negatively charged phospholipids. To identify the true lipid-binding loop, mutagenesis of the proposed paddle domains was targeted to study membrane-DynA interactions *in vivo* and *in vitro*. For *in vivo* localisation studies, wild-type DynA-GFP and mutant DynA-GFP were expressed in $\Delta dynA$ background. Of all the mutants tested so far, $\Delta 511-522$ DynA-GFP failed to show membrane localisation, though it was produced as a full-length protein, judged by immunoblotting. In addition, $\Delta 511-522$ DynA-His protein failed to hydrolyse GTP (Appendix figure 8) suggesting that this region might also lie in the GED region, which is known to affect GTP hydrolysis of DLPs. It is also possible that deletion of region 511-522 might affect appropriate folding of the protein, thus abrogating GTP binding and hydrolysis. *In vitro*,

Δ511-522 DynA-His could mediate binding to liposomes, thus discarding the possibility of this region being the paddle domain of DynA. Further, single point mutation analysis within this region could show R512A substitution to inhibit membrane foci formation of DynA, *in vivo*. However, *in vitro* experiments revealed that R512A DynA-His protein binds to PG-liposomes but this binding is altered in the presence of GTP, when compared to wild-type protein. DLPs can mediate nucleotide-dependent oligomerisation and membrane-binding. Since DynA can mediate nucleotide-independent oligomerisation and membrane-binding *in vitro*, it can be speculated that this protein might need nucleotide hydrolysis for the disassembly of its oligomers. Hence, an increased GTPase activity would trigger disassembly of DynA oligomers, which appear as foci on the membrane. Our results show arginine at position 512 to be a potential regulator of membrane-binding behaviour of DynA. The membrane-binding behaviour of R512A was tested *in vitro* with liposome sedimentation assay performed in the presence of GTP. Here, a fraction of protein was recovered in the supernatant, upon GTP addition, indicating GTP binding prevents R512A DynA from localising membrane or GTP hydrolysis certainly mediates disassembly of DynA oligomers that may have assembled on lipid bilayers *in vitro*. This also suggests that R512A DynA binding to liposomes is weaker than wild-type protein. The disassembled free protein remains in the supernatant. However, it would be ideal to quantify the amount of free and liposome-bound protein to get a comprehensive insight about membrane binding of mutant proteins compared to the wild-type. Since R512A DynA-GFP fails to localise into foci on the membrane, it could be suggested that this amino acid residue is required for formation of stable higher-order oligomers, which is a pre-requisite for focal-assembly on bacterial membrane.

2.2 Region 591-620 of DynA is required for dimerisation

The stalk region of MxA comprises of a major portion of its middle domain and the amino terminal region of GED (amino acids 366-633), which together give rise to a four-helix bundle symmetry. Mutational analysis of the stalk region of MxA has provided a structural

framework to understand the membrane binding behaviour as well as the antiviral activity of MxA. These mutations include L617D, D377K, K614D, L620D, I376D, M527D, F602D, R408D, G392D and Δ 533-561 (L4 loop). These mutations resulted in the disruption of MxA tetramers (equivalent to DynA dimers), but the formation of stable dimers (equivalent to DynA monomer) suggesting that they are important in oligomer formation. Moreover, these mutants were found to hydrolyse GTP but failed to show liposome binding. Also, these mutants failed to co-localise with La Crosse virus (LACV) nucleoproteins and lacked antiviral activity against H5N1 influenza thus indicating that MxA oligomerisation is essential for viral recognition and antiviral activity (Verhelst et al 2013). Protein sequence comparison of DynA with three different Mx molecules (MxA, Mx1 and Mx2) highlighted a common conserved region, which in Mx proteins is responsible for oligomerisation and function. This region of DynA, 591-620, was targeted for deletion and analysed for *in vivo* localization as well as *in vitro* membrane binding. Δ 591-620 DynA-GFP was produced as a full-length copy, as detected by western blot and was found to localise to the bacterial membrane in distinct polar foci and rarely at the division septa. *In vitro*, Δ 591-620 DynA-His could bind to liposomes, but failed to show GTP binding and hydrolysis, which was contrary to the Mx stalk mutants that failed to show lipid binding but GTP hydrolysis. This could very well suggest that, in spite of sequence and structural similarities, molecular assembly and GTPase activity of DynA and Mx is different. Size exclusion chromatography revealed that Δ 591-620 DynA-His did not assemble into dimers (likely a functional equivalent of Mx tetramer). However, similar to wild-type DynA, higher-ordered Δ 591-620 DynA-His oligomers were detected, which under denaturing conditions (SDS-PAGE) produced fragments equivalent to monomeric state, indicating that lack of region 591-620 could still induce oligomerisation. The fact that Δ 591-620 DynA-His failed to bind and hydrolyse GTP (Bachelor thesis of Nadine Germ) indicated that this region is also required, as a GED, for appropriate folding of the molecule to expose the nucleotide-binding pocket in GTPase domain. Such a phenotype was previously observed with Mx proteins. The C-terminal region of Mx molecules is considered to be the GED because of its

ability to interact with the N-terminal GTPase domain, to form the enzymatically active site of Mx proteins. Mx proteins are known to mediate inter-molecular interactions via the stalk and GTPase domains (Gao et al 2010). Hence, it is conceivable that lack of 591-620 stalk might prevent inter-molecular stalk interactions but allow GTPase domains to interact, thus giving rise to high-molecular weight oligomers. All results taken together suggest region 591-620 to be important for dimer formation. However the importance of this region in biological function of DynA still has to be tested.

DLPs can oligomerise to form helical ring structures around lipid tubes (Hinshaw and Schmid 1995). The MxA structural model proposed by Gao et al. suggests that the GTPase domain is not required for ring formation around lipid tubes, but for establishing inter-ring contacts (Haller et al 2007b). Based on the available data on Mx DLPs and results from this thesis, it can be proposed (Figure 26) that in presence of a lipid bilayer, the $\Delta 591-620$ DynA-His protein can induce membrane-binding via the uncharacterised paddle loop and induce higher assemblies via inter-GTPase domain interactions. These assemblies appear on the membrane as static foci as they fail to disassemble due to lack of GTP hydrolysis. Since the non-dimer forming protein fails to assemble throughout the membrane, it can be assumed that dimerisation is essential for lateral movement of DynA along the bacterial membrane. FRAP analysis showed $\Delta 591-620$ DynA-GFP to have impaired membrane-mobility, thus supporting our assumption (Master thesis of Kristina Eissenberger). Future crystallisation studies will further enlighten the actual mechanism of oligomer formation of DynA. Another method to verify the dimerisation phenotype of DynA via region 591-620 is a bacterial two-hybrid (BTH) screen. A BTH screen was previously performed to identify the interaction matrix of DynA and its subunits (Manz et al 2013). DynA subunits, D1 and D2 were shown to induce homotypic interactions. Hence, it is clear that one DynA molecule will interact with another molecule through D1-D1 and D2-D2 contacts. Region 591-620 lies towards the C-terminal end of D1. If this region is responsible for dimerisation, then $\Delta 591-620$ D1 and wild-type D1

should fail to give a positive reaction in BTH test. However, this idea could not be implemented due to time constraints and could be tested in the future.

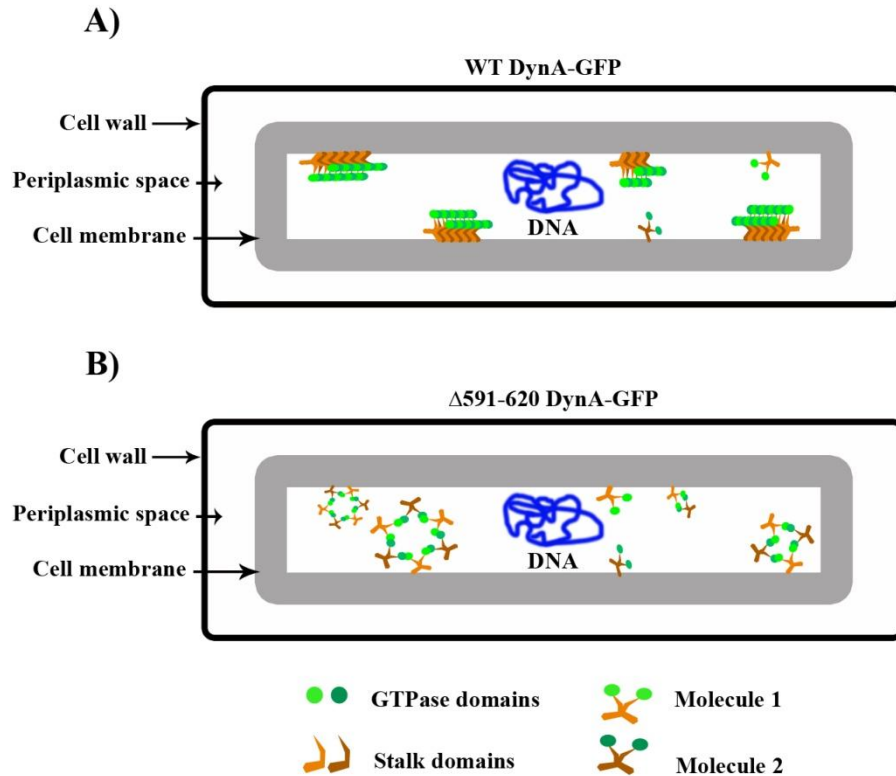


Figure 26. Model for $\Delta 591-620$ DynA oligomerisation and localisation *in vivo*. (A) Wild-type DynA can dimerise through stalk and G domains to form high-order assemblies and localise to the bacterial membrane via D1 paddle loop whereas (B) DynA lacking the stalk domain, $\Delta 591-620$ DynA-GFP, can still induce inter-molecular interactions via its G domain and localise to the bacterial membrane via D1 paddle loop.

3. Potential interaction partners YneK, YmdA and YwpG have different patterns of interaction with DynA

The function of DynA in *B. subtilis* was enigmatic. To unravel the *in vivo* function, it was important to identify the interacting partners of DynA. For this purpose, 1) a *B. subtilis* genomic library was generated and subjected to bacterial two-hybrid (BTH) screening and 2) a synthetic lethal screen (SLS) was performed with the help of a transposon. The BTH screen

identified YmdA, YwpG and YneK as putative DynA interaction partners (Bürmann et al 2012). The importance of these potential interactions still remains unwarranted. However, previous studies have shown dynamin members to interact with other proteins. Classical dynamins have a proline-rich domain, which enables them to bind proteins containing SH3 domains (Shpetner et al 1996). But DLPs that lack proline-rich domain have also been shown to interact with other proteins. YmdA and YneK are membrane associated, whereas YwpG is a soluble protein. The best example of a DLP interacting with soluble as well as transmembrane proteins is Dnm1. Dnm1 is a cytosolic DLP in yeast that upon initiation of mitochondrial fission translocates to the outer mitochondrial membrane. It interacts with Fis1 present on the outer mitochondrial membrane. Soluble adaptor proteins, Mdv1 and Caf4 mediate Dnm1-Fis1 interaction. In humans, mitochondrial fission requires the interaction of cytosolic Drp1 (homolog of Dnm1) with outer mitochondrial membrane protein Mff (Low et al 2009). *In vitro* studies have revealed Dnm1/Drp1 to form dynamin-like assemblies that wrap around the mitochondrial tubule. This assembly constricts and severs the tubule upon GTP hydrolysis.

YmdA (also known as RNaseY) is an endoribonuclease that participates in mRNA metabolism. It contains a RNA-binding KH domain (Otera and Mihara 2011) and a highly conserved HD region. It participates in nucleic acid metabolism by processing prematurely terminated mRNA transcripts (Ingerman et al 2005, Smirnova et al 2001, Yoon et al 2001). YmdA exhibits a transmembrane region, which explains its membrane localisation. YneK and YwpG proteins have unknown functions. Localisation studies showed YneK-GFP, YwpG-GFP and YmdA-GFP to localise to bacterial membranes. YwpG is a soluble protein, mostly localised in the cytoplasm, but is also seen to localise into membrane foci. The different localisation patterns seem to be growth-phase and medium dependent and needs further evaluation. Medium-dependent expression of *ywpG* and its neighbouring single-stranded DNA binding (*ssb*) gene, *ywpH* has been described previously (Lindner et al 2004). About 38% cells expressing YwpG-GFP contained more than one foci per cell. In the absence of DynA, this

number was reduced to 10% suggesting that DynA indeed helps to recruit YwpG to the membrane. It could very well be that YwpG has additional potential interacting partners that regulate its membrane-binding behaviour. DynA is also seen to regulate the division-site localisation of YmdA, since YmdA-GFP localisation at the division site was reduced by 50% in cells lacking DynA. The fact that DynA interacts with different proteins suggests that it could be involved in more than one membrane associated functions. A possible role of these interactions could be in cell division, since DynA and its partners are seen to assemble at the site of septation. Also, localisation of DynA, YneK and YmdA was affected in cells lacking a division-site regulating protein, MinJ. A positive interaction of DynA with MinJ as well as EzrA was observed in a BTH screen (PhD thesis of Van Baarle). EzrA is a negative regulator of FtsZ (Levin et al 1999) whereas MinJ is a topological determinant of medial FtsZ positioning and acts as an intermediary between DivIVA and MinD (Bramkamp et al 2008a). The majority of cells lacking EzrA can form a central or polar FtsZ ring, but only a small percentage of these polar rings actually form mini-cells (Levin et al 1999). In the absence of MinJ, cells fail to produce FtsZ rings and thus are filamentous (Bramkamp et al 2008a). The significance of the interaction of EzrA/MinJ with DynA is yet to be analysed. However, in the absence of DynA, cells do not show any division phenotype, which points out the fact that there may be surrogate systems that play similar roles in *B. subtilis*. In the future, it would be informative to generate knockouts of YneK, YmdA and YwpG and study the effect on DynA localisation as well as on *B. subtilis* growth and behaviour. To further define these interactions, a second BTH was performed to identify the DynA subunit (D1 or D2) that mediates interaction with YneK, YmdA and YwpG. The screen revealed interaction of YneK with D1, YwpG with both D1 and D2 and YmdA with none of the subunits alone suggesting that an intact molecule of DynA is required for interacting with YmdA. YneK and YwpG were also found to interact with the GTPase mutants indicating that GTPase activity is not essential for interaction. The consequence of these interactions remains to be elucidated. Since DynA is proposed to act

upon membrane stress, it can be presumed that DynA-YneK/YwpG/YmdA interactions might be important during certain environmental stress conditions.

A synthetic lethal screen (SLS) was performed previously (Master thesis of Nina Ebert, 2009) to identify genes in the bacterial genome that would, upon mutation or deletion, result in a sick or lethal phenotype in cells lacking DynA. Such a screen was predicted to identify potential genomic partners that would act in similar pathways with DynA. However, of the four candidates identified in the screen as potential interaction partners, Mfd, YukF and YflN, were found to be false positives, since their absence along with or without DynA, had no effect on bacterial growth and morphology. A *albD* deletion strain could not be generated. Since DynA is found to be important during membrane stress, it could be hypothesized that its interaction with predicted partners is stress induced. Hence, it would be ideal to perform a SLS or BTH under phage or membrane stress. Another idea would be to test Δmfd , $\Delta yukF$, $\Delta yflN$, $\Delta mfd \Delta dynA$, $\Delta yukF \Delta dynA$ and $\Delta yflN \Delta dynA$ strains against phage infection and resistance to nisin. From all the interaction studies done so far, it is conceivable that DynA has a large interaction network and therefore, it might be involved in more than one function.

4. Outlook

A combination of molecular genetics, biochemical methods and microscopy has revealed the potential membrane protective function of a DLP, DynA, in *B. subtilis*. This PhD thesis has successfully shown DynA to be similar to eukaryotic DLPs since it demonstrated similar structural, biochemical and functional properties. These results also indicate that DLP family has a bacterial origin. Mutational analysis on DynA has successfully enabled identification of its stalk domain, 591-620, and a self-stimulating GTPase regulator, R512. Liposome sedimentation assays have demonstrated the affinity of DynA for anionic phospholipids, thus shedding light on membrane binding behaviour of DynA. Plaque assays and growth experiments have proposed a membrane-protective function for DynA upon extracytoplasmic

stress. Observations such as localisation of DynA at the sites of septation and its interaction with division proteins could be justified with the fact that the main target of any stress-inducing agent would be the newly synthesized envelope at the division site. Taken together, all results have enabled a detailed understanding of both biochemical and functional properties of DynA. However, further investigations to elucidate the role played by DynA in viral inhibition will be of prime concern. DynA has evolved as a distinct and novel candidate for anti-bacteriophage study. The following few experiments will provide a further understanding of the correlation between eukaryotic and bacterial DLPs;

1. Performing a BTH screen or SLS under stress-induced conditions to identify potential DynA interacting partners.
2. Performing phage infection and antibiotic-induced stress studies to identify the functional correlation of DynA with its predicted interaction partners.
3. Performing a native PAGE study on $\Delta 591-620$ DynA-His to compare its oligomerisation behaviour with wild-type DynA-His.
4. Analysing the susceptibility of $\Delta 591-620$ DynA against phage and antibiotics to identify whether dimerisation is necessary for membrane-protection function.
5. Studying membrane-binding and oligomerisation behaviour of DynA by electron microscopic analysis of liposomes decorated with DynA.
6. Resolving the crystal structure of DynA to unravel the structural features of a novel protein, which is an assembly of two fused DLPs.

This thesis indeed enlightens an important membrane-remodelling role for bacterial DLPs. Although the question of essentiality of DLPs in bacteria is still unsolved, their symbiotic transfer to eukaryotes during evolution is well justified here. Further information on characteristics that are pre-requisite for a membrane remodelling candidate, such as nucleotide-binding, membrane-binding, GTPase activity, oligomerisation, disassembly of oligomers and conformational changes brought due to nucleotide and membrane binding, will provide information on DynA-mediated membrane fusion mechanisms.

References

Anderson DL, Hickman DD, Reilly BE (1966). Structure of Bacillus subtilis bacteriophage phi 29 and the length of phi 29 deoxyribonucleic acid. *J Bacteriol* 91: 2081-2089.

Anderson DL, Mosharrafa ET (1968). Physical and biological properties of phage phi 29 deoxyribonucleic acid. *J Virol* 2: 1185-1190.

Aravind L, Koonin EV (1998). The HD domain defines a new superfamily of metal-dependent phosphohydrolases. *Trends Biochem Sci* 23: 469-472.

Ayora S, Rojo F, Ogasawara N, Nakai S, Alonso JC (1996). The Mfd protein of Bacillus subtilis 168 is involved in both transcription-coupled DNA repair and DNA recombination. *Journal of Molecular Biology* 256: 301-318.

Bach JN, Bramkamp M (2013). Flotillins functionally organize the bacterial membrane. *Mol Microbiol* 88: 1205-1217.

Barna JC, Williams DH (1984). The structure and mode of action of glycopeptide antibiotics of the vancomycin group. *Annu Rev Microbiol* 38: 339-357.

Bhattacharya A, Jain R, Shrimal S, Bhattacharya S (2010). Identification and Partial Characterization of a Dynamin-Like Protein, EhDLP1, from the Protist Parasite Entamoeba histolytica. *Eukaryot Cell* 9: 215-223.

Bijisma JJE, Groisman EA (2003). Making informed decisions: regulatory interactions between two-component systems. *Trends Microbiol* 11: 359-366.

Bonev BB, Breukink E, Swiezewska E, De Kruijff B, Watts A (2004). Targeting extracellular pyrophosphates underpins the high selectivity of nisin. *Faseb J* 18: 1862-1869.

Bramkamp M, Emmins R, Weston L, Donovan C, Daniel RA, Errington J (2008a). A novel component of the division-site selection system of Bacillus subtilis and a new mode of action for the division inhibitor MinCD. *Mol Microbiol* 70: 1556-1569.

Bramkamp M, Emmins R, Weston L, Donovan C, Daniel RA, Errington J (2008b). A novel component of the division-site selection system of Bacillus subtilis and a new mode of action for the division inhibitor MinCD. *Molecular Microbiology* 70: 1556-1569.

Bramkamp M (2012a). Structure and function of bacterial dynamin-like proteins. *Biol Chem* 393: 1203-1214.

Bramkamp M (2012b). Structure and function of bacterial dynamin-like proteins. *Biological Chemistry* 0: 1-12.

Bramkamp M, Lopez D (2015). Exploring the existence of lipid rafts in bacteria. *Microbiol Mol Biol Rev* 79: 81-100.

Breukink E, van Kraaij C, van Dalen A, Demel RA, Siezen RJ, de Kruijff B *et al* (1998). The orientation of nisin in membranes. *Biochemistry* 37: 8153-8162.

Breukink E, Wiedemann I, van Kraaij C, Kuipers OP, Sahl HG, de Kruijff B (1999). Use of the cell wall precursor lipid II by a pore-forming peptide antibiotic. *Science* 286: 2361-2364.

Brissette JL, Russel M, Weiner L, Model P (1990). Phage shock protein, a stress protein of *Escherichia coli*. *Proc Natl Acad Sci U S A* 87: 862-866.

Brown S, Maria JPS, Walker S (2013). Wall Teichoic Acids of Gram-Positive Bacteria. *Annual Review of Microbiology, Vol 67* 67: 313-336.

Bugg TDH, Walsh CT (1992). Intracellular Steps of Bacterial-Cell Wall Peptidoglycan Biosynthesis - Enzymology, Antibiotics, and Antibiotic-Resistance. *Nat Prod Rep* 9: 199-215.

Burkhart BM, Gassman RM, Langs DA, Pangborn WA, Duax WL, Pletnev V (1999). Gramicidin D conformation, dynamics and membrane ion transport. *Biopolymers* 51: 129-144.

Bürmann F, Ebert N, van Baarle S, Bramkamp M (2011a). A bacterial dynamin-like protein mediating nucleotide-independent membrane fusion. *Mol Microbiol* 79: 1294-1304.

Bürmann F, Ebert N, van Baarle S, Bramkamp M (2011b). A bacterial dynamin-like protein mediating nucleotide-independent membrane fusion. *Mol Microbiol* 79: 1294-1304.

Bürmann F, Sawant P, Bramkamp M (2012). Identification of interaction partners of the dynamin-like protein DynA from *Bacillus subtilis*. *Communicative & Integrative Biology* Volume 5: 362 - 369.

Butcher BG, Helmann JD (2006). Identification of *Bacillus subtilis* sigma(W)-dependent genes that provide intrinsic resistance to antimicrobial compounds produced by Bacilli. *Molecular Microbiology* 60: 765-782.

Cao M, Kobel PA, Morshedi MM, Wu MF, Paddon C, Helmann JD (2002). Defining the *Bacillus subtilis* sigma(W) regulon: a comparative analysis of promoter consensus search, run-off transcription/microarray analysis (ROMA), and transcriptional profiling approaches. *J Mol Biol* 316: 443-457.

Chan DC, Song ZY, Ghochani M, McCaffery JM, Frey TG (2009). Mitofusins and OPA1 Mediate Sequential Steps in Mitochondrial Membrane Fusion. *Mol Biol Cell* 20: 3525-3532.

Chen H, Detmer SA, Ewald AJ, Griffin EE, Fraser SE, Chan DC (2003). Mitofusins Mfn1 and Mfn2 coordinately regulate mitochondrial fusion and are essential for embryonic development. *J Cell Biol* 160: 189-200.

Chopra I, Roberts M (2001). Tetracycline antibiotics: Mode of action, applications, molecular biology, and epidemiology of bacterial resistance. *Microbiol Mol Biol R* 65: 232-+.

Colangeli R, Helb D, Sridharan S, Sun JC, Varma-Basil M, Hazbon MH *et al* (2005). The Mycobacterium tuberculosis iniA gene is essential for activity of an efflux pump that confers drug tolerance to both isoniazid and ethambutol. *Molecular Microbiology* 55: 1829-1840.

Commichau FM, Rothe FM, Herzberg C, Wagner E, Hellwig D, Lehnik-Habrink M *et al* (2009). Novel activities of glycolytic enzymes in Bacillus subtilis: interactions with essential proteins involved in mRNA processing. *Mol Cell Proteomics* 8: 1350-1360.

Costa V, Giacomello M, Hudec R, Lopreiato R, Ermak G, Lim D *et al* (2010). Mitochondrial fission and cristae disruption increase the response of cell models of Huntington's disease to apoptotic stimuli. *EMBO Mol Med* 2: 490-503.

Damper PD, Epstein W (1981). Role of the membrane potential in bacterial resistance to aminoglycoside antibiotics. *Antimicrob Agents Chemother* 20: 803-808.

Danese PN, Snyder WB, Cosma CL, Davis LJ, Silhavy TJ (1995). The Cpx two-component signal transduction pathway of Escherichia coli regulates transcription of the gene specifying the stress-inducible periplasmic protease, DegP. *Genes Dev* 9: 387-398.

Darwin AJ (2005). The phage-shock-protein response. *Mol Microbiol* 57: 621-628.

de Kruijff B, van Dam V, Breukink E (2008). Lipid II: a central component in bacterial cell wall synthesis and a target for antibiotics. *Prostaglandins Leukot Essent Fatty Acids* 79: 117-121.

Delcour AH (2009). Outer membrane permeability and antibiotic resistance. *Biochim Biophys Acta* 1794: 808-816.

Dominguez-Escobar J, Wolf D, Fritz G, Hofler C, Wedlich-Soldner R, Mascher T (2014). Subcellular localization, interactions and dynamics of the phage-shock protein-like Lia response in Bacillus subtilis. *Mol Microbiol* 92: 716-732.

Dubnau D (1991). Genetic Competence in Bacillus-Subtilis. *Microbiol Rev* 55: 395-424.

Dubos RJ (1939). Studies on a Bactericidal Agent Extracted from a Soil Bacillus : Ii. Protective Effect of the Bactericidal Agent against Experimental Pneumococcus Infections in Mice. *J Exp Med* 70: 11-17.

Economou NJ, Cocklin S, Loll PJ (2013). High-resolution crystal structure reveals molecular details of target recognition by bacitracin. *Proc Natl Acad Sci U S A* 110: 14207-14212.

Eichenberger P, Fujita M, Jensen ST, Conlon EM, Rudner DZ, Wang ST *et al* (2004). The program of gene transcription for a single differentiating cell type during sporulation in *Bacillus subtilis*. *PLoS Biol* 2: e328.

Engl C, Jovanovic G, Lloyd LJ, Murray H, Spitaler M, Ying L *et al* (2009). In vivo localizations of membrane stress controllers PspA and PspG in *Escherichia coli*. *Mol Microbiol* 73: 382-396.

Erickson JW, Gross CA (1989). Identification of the sigma E subunit of *Escherichia coli* RNA polymerase: a second alternate sigma factor involved in high-temperature gene expression. *Genes Dev* 3: 1462-1471.

Faelber K, Posor Y, Gao S, Held M, Roske Y, Schulze D *et al* (2011). Crystal structure of nucleotide-free dynamin. *Nature*.

Ferguson KM, Lemmon MA, Schlessinger J, Sigler PB (1994). Crystal structure at 2.2 Å resolution of the pleckstrin homology domain from human dynamin. *Cell* 79: 199-209.

Fischer K, Weber A, Brink S, Arbinger B, Schunemann D, Borchert S *et al* (1994). Porins from plants. Molecular cloning and functional characterization of two new members of the porin family. *J Biol Chem* 269: 25754-25760.

Friedman L, Alder JD, Silverman JA (2006). Genetic changes that correlate with reduced susceptibility to daptomycin in *Staphylococcus aureus*. *Antimicrob Agents Ch* 50: 2137-2145.

Gao S, von der Malsburg A, Paeschke S, Behlke J, Haller O, Kochs G *et al* (2010). Structural basis of oligomerization in the stalk region of dynamin-like MxA. *Nature* 465: 502-506.

Gebhard S (2012). ABC transporters of antimicrobial peptides in Firmicutes bacteria - phylogeny, function and regulation. *Mol Microbiol* 86: 1295-1317.

Georgopapadakou NH (1993). Penicillin-binding proteins and bacterial resistance to beta-lactams. *Antimicrob Agents Chemother* 37: 2045-2053.

Gimpel M, Brantl S (2012). Construction of a modular plasmid family for chromosomal integration in *Bacillus subtilis*. *J Microbiol Methods* 91: 312-317.

Gonzalez-Huici V, Salas M, Hermoso JM (2004). The push-pull mechanism of bacteriophage O29 DNA injection. *Mol Microbiol* 52: 529-540.

Gonzalez-Jamett AM, Momboisse F, Haro-Acuna V, Bevilacqua JA, Caviedes P, Cardenas AM (2013). Dynamin-2 function and dysfunction along the secretory pathway. *Front Endocrinol (Lausanne)* 4: 126.

Greenspan P, Mayer EP, Fowler SD (1985). Nile Red - a Selective Fluorescent Stain for Intracellular Lipid Droplets. *Journal of Cell Biology* 100: 965-973.

Griffin EE, Graumann J, Chan DC (2005). The WD40 protein Caf4p is a component of the mitochondrial fission machinery and recruits Dnm1p to mitochondria. *Journal of Cell Biology* 170: 237-248.

Gu C, Yaddanapudi S, Weins A, Osborn T, Reiser J, Pollak M *et al* (2010). Direct dynamin-actin interactions regulate the actin cytoskeleton. *EMBO J* 29: 3593-3606.

Haeusser DP, Schwartz RL, Smith AM, Oates ME, Levin PA (2004). EzrA prevents aberrant cell division by modulating assembly of the cytoskeletal protein FtsZ. *Mol Microbiol* 52: 801-814.

Hales KG, Fuller MT (1997). Developmentally regulated mitochondrial fusion mediated by a conserved, novel, predicted GTPase. *Cell* 90: 121-129.

Haller O, Kochs G (2002). Interferon-induced mx proteins: dynamin-like GTPases with antiviral activity. *Traffic* 3: 710-717.

Haller O, Kochs G, Weber F (2007a). Interferon, Mx, and viral countermeasures. *Cytokine Growth Factor Rev* 18: 425-433.

Haller O, Staeheli P, Kochs G (2007b). Interferon-induced Mx proteins in antiviral host defense. *Biochimie* 89: 812-818.

Haller O, Staeheli P, Schwemmler M, Kochs G (2015). Mx GTPases: dynamin-like antiviral machines of innate immunity. *Trends Microbiol* 23: 154-163.

Hasper HE, de Kruijff B, Breukink E (2004). Assembly and stability of nisin-Lipid II pores. *Biochemistry* 43: 11567-11575.

Hemphill HE, Whiteley HR (1975). Bacteriophages of *Bacillus subtilis*. *Bacteriol Rev* 39: 257-315.

Hermann GJ, Thatcher JW, Mills JP, Hales KG, Fuller MT, Nunnari J *et al* (1998). Mitochondrial fusion in yeast requires the transmembrane GTPase Fzo1p. *J Cell Biol* 143: 359-373.

Herzog IM, Fridman M (2014). Design and synthesis of membrane-targeting antibiotics: from peptides- to aminosugar-based antimicrobial cationic amphiphiles. *Medchemcomm* 5: 1014-1026.

Hinshaw JE, Schmid SL (1995). Dynamin Self-Assembles into Rings Suggesting a Mechanism for Coated Vesicle Budding. *Nature* 374: 190-192.

Ho TD, Ellermeier CD (2012). Extra cytoplasmic function sigma factor activation. *Curr Opin Microbiol* 15: 182-188.

Hoch JA (2000). Two-component and phosphorelay signal transduction. *Curr Opin Microbiol* 3: 165-170.

Hoepfner D, van den Berg M, Philippsen P, Tabak HF, Hettema EH (2001). A role for Vps1p, actin, and the Myo2p motor in peroxisome abundance and inheritance in *Saccharomyces cerevisiae*. *J Cell Biol* 155: 979-990.

Hoppins S, Lackner L, Nunnari J (2007). The machines that divide and fuse mitochondria. *Annu Rev Biochem* 76: 751-780.

Horisberger MA (1992). Interferon-Induced Human Protein Mxa Is a Gtpase Which Binds Transiently to Cellular Proteins. *Journal of Virology* 66: 4705-4709.

Hsu STD, Breukink E, Tischenko E, Lutters MAG, de Kruijff B, Kaptein R *et al* (2004). The nisin-lipid II complex reveals a pyrophosphate cage that provides a blueprint for novel antibiotics. *Nature Structural & Molecular Biology* 11: 963-967.

Hyde AJ, Parisot J, McNichol A, Bonev BB (2006). Nisin-induced changes in *Bacillus* morphology suggest a paradigm of antibiotic action. *Proc Natl Acad Sci U S A* 103: 19896-19901.

Ingerman E, Perkins EM, Marino M, Mears JA, McCaffery JM, Hinshaw JE *et al* (2005). Dnm1 forms spirals that are structurally tailored to fit mitochondria. *Journal of Cell Biology* 170: 1021-1027.

Ishihara N, Nomura M, Jofuku A, Kato H, Suzuki SO, Masuda K *et al* (2009). Mitochondrial fission factor Drp1 is essential for embryonic development and synapse formation in mice. *Nat Cell Biol* 11: 958-U114.

Jahn R (2008). Some classic papers in the field of membrane fusion--a personal view. *Nat Struct Mol Biol* 15: 655-657.

Johnson AS, van Horck S, Lewis PJ (2004). Dynamic localization of membrane proteins in *Bacillus subtilis*. *Microbiology* 150: 2815-2824.

Joly N, Engl C, Jovanovic G, Huvet M, Toni T, Sheng X *et al* (2010). Managing membrane stress: the phage shock protein (Psp) response, from molecular mechanisms to physiology. *FEMS Microbiol Rev* 34: 797-827.

Jones BA, Fangman WL (1992). Mitochondrial DNA maintenance in yeast requires a protein containing a region related to the GTP-binding domain of dynamin. *Genes Dev* 6: 380-389.

Jordan S, Hutchings MI, Mascher T (2008). Cell envelope stress response in Gram-positive bacteria. *FEMS Microbiol Rev* 32: 107-146.

Kadner RJ (1996). *Escherichia coli and Salmonella, Cellular and Molecular Biology*. ASM Press, Washington, DC.

Kahan FM, Kahan JS, Cassidy PJ, Kropp H (1974). The mechanism of action of fosfomycin (phosphonomycin). *Ann N Y Acad Sci* 235: 364-386.

Kapuscinski J (1995). DAPI: a DNA-specific fluorescent probe. *Biotech Histochem* 70: 220-233.

Kelkar DA, Chattopadhyay A (2007). The gramicidin ion channel: a model membrane protein. *Biochim Biophys Acta* 1768: 2011-2025.

Kleerebezem M, Crielaard W, Tommassen J (1996). Involvement of stress protein PspA (phage shock protein A) of *Escherichia coli* in maintenance of the protonmotive force under stress conditions. *EMBO J* 15: 162-171.

Kobayashi R, Suzuki T, Yoshida M (2007). *Escherichia coli* phage-shock protein A (PspA) binds to membrane phospholipids and repairs proton leakage of the damaged membranes. *Mol Microbiol* 66: 100-109.

Kochs G, Haller O (1999). GTP-bound human MxA protein interacts with the nucleocapsids of Thogoto virus (Orthomyxoviridae). *J Biol Chem* 274: 4370-4376.

Kochs G, Janzen C, Hohenberg H, Haller O (2002). Antivirally active MxA protein sequesters La Crosse virus nucleocapsid protein into perinuclear complexes. *P Natl Acad Sci USA* 99: 3153-3158.

Kohanski MA, Dwyer DJ, Collins JJ (2010). How antibiotics kill bacteria: from targets to networks. *Nat Rev Microbiol* 8: 423-435.

Kunst F, Ogasawara N, Moszer I, Albertini AM, Alloni G, Azevedo V *et al* (1997). The complete genome sequence of the gram-positive bacterium *Bacillus subtilis*. *Nature* 390: 249-256.

Kutschera U, Niklas KJ (2005). Endosymbiosis, cell evolution, and speciation. *Theory Biosci* 124: 1-24.

Labrousse AM, Zappaterra MD, Rube DA, van der Bliek AM (1999). *C. elegans* dynamin-related protein DRP-1 controls severing of the mitochondrial outer membrane. *Mol Cell* 4: 815-826.

Lazarevic V, Dusterhoft A, Soldo B, Hilbert H, Mauel C, Karamata D (1999). Nucleotide sequence of the *Bacillus subtilis* temperate bacteriophage SPbetac2. *Microbiology* 145 (Pt 5): 1055-1067.

Leipe DD, Wolf YI, Koonin EV, Aravind L (2002). Classification and evolution of P-loop GTPases and related ATPases. *J Mol Biol* 317: 41-72.

Levin PA, Kurtser IG, Grossman AD (1999). Identification and characterization of a negative regulator of FtsZ ring formation in *Bacillus subtilis*. *Proc Natl Acad Sci U S A* 96: 9642-9647.

Lin TH, Wei GT, Su CC, Shaw GC (2012). AdeR, a PucR-Type Transcription Factor, Activates Expression of L-Alanine Dehydrogenase and Is Required for Sporulation of *Bacillus subtilis*. *JOURNAL OF BACTERIOLOGY* 194: 4995-5001.

Linden M, Andersson G, Gellerfors P, Nelson BD (1984). Subcellular distribution of rat liver porin. *Biochim Biophys Acta* 770: 93-96.

Lindner C, Nijland R, van Hartskamp M, Bron S, Hamoen LW, Kuipers OP (2004). Differential expression of two paralogous genes of *Bacillus subtilis* encoding single-stranded DNA binding protein. *J Bacteriol* 186: 1097-1105.

Liu J, Sun Y, Drubin DG, Oster GF (2009). The mechanochemistry of endocytosis. *PLoS Biol* 7: e1000204.

Liu Z, Pan Q, Ding S, Qian J, Xu F, Zhou J *et al* (2013). The interferon-inducible MxB protein inhibits HIV-1 infection. *Cell Host Microbe* 14: 398-410.

Low HH, Löwe J (2006). A bacterial dynamin-like protein. *Nature* 444: 766-769.

Low HH, Sachse C, Amos LA, Löwe J (2009). Structure of a bacterial dynamin-like protein lipid tube provides a mechanism for assembly and membrane curving. *Cell* 139: 1342-1352.

Lunde CS, Hartouni SR, Janc JW, Mammen M, Humphrey PP, Benton BM (2009). Telavancin Disrupts the Functional Integrity of the Bacterial Membrane through Targeted Interaction with the Cell Wall Precursor Lipid II. *Antimicrob Agents Ch* 53: 3375-3383.

Maffey KG, Keil LB, DeBari VA (2001). The influence of lipid composition and divalent cations on annexin V binding to phospholipid mixtures. *Ann Clin Lab Sci* 31: 85-90.

Manstein DJ, Reubold TF, Eschenburg S, Becker A, Leonard M, Schmid SL *et al* (2005). Crystal structure of the GTPase domain of rat dynamin 1. *P Natl Acad Sci USA* 102: 13093-13098.

Manz B, Dornfeld D, Gotz V, Zell R, Zimmermann P, Haller O *et al* (2013). Pandemic Influenza A Viruses Escape from Restriction by Human MxA through Adaptive Mutations in the Nucleoprotein. *Plos Pathog* 9.

Mascher T, Margulis NG, Wang T, Ye RW, Helmann JD (2003). Cell wall stress responses in *Bacillus subtilis*: the regulatory network of the bacitracin stimulon. *Mol Microbiol* 50: 1591-1604.

Mascher T, Zimmer SL, Smith TA, Helmann JD (2004). Antibiotic-inducible promoter regulated by the cell envelope stress-sensing two-component system LiaRS of *Bacillus subtilis*. *Antimicrob Agents Chemother* 48: 2888-2896.

Meeusen S, DeVay R, Block J, Cassidy-Stone A, Wayson S, McCaffery JM *et al* (2006). Mitochondrial inner-membrane fusion and crista maintenance requires the dynamin-related GTPase Mgm1. *Cell* 127: 383-395.

Meglei G, McQuibban GA (2009). The dynamin-related protein Mgm1p assembles into oligomers and hydrolyzes GTP to function in mitochondrial membrane fusion. *Biochemistry* 48: 1774-1784.

Meijer WJJ, Horcajadas JA, Salas M (2001). phi 29 family of phages. *Microbiol Mol Biol R* 65: 261-+.

Melen K, Ronni T, Broni B, Krug RM, von Bonsdorff CH, Julkunen I (1992). Interferon-induced Mx proteins form oligomers and contain a putative leucine zipper. *J Biol Chem* 267: 25898-25907.

Mendez E, Ramirez G, Salas M, Vinuela E (1971). Structural proteins of bacteriophage phi 29. *Virology* 45: 567-576.

Mendez R, Gutierrez A, Reyes J, Marquez-Magana L (2012). The Extracytoplasmic Function Sigma Factor SigY Is Important for Efficient Maintenance of the Sp beta Prophage That Encodes Sublancin in *Bacillus subtilis*. *DNA Cell Biol* 31: 946-955.

Mercier R, Kawai Y, Errington J (2013). Excess membrane synthesis drives a primitive mode of cell proliferation. *Cell* 152: 997-1007.

Mitchell PS, Patzina C, Emerman M, Haller O, Malik HS, Kochs G (2012). Evolution-guided identification of antiviral specificity determinants in the broadly acting interferon-induced innate immunity factor MxA. *Cell Host Microbe* 12: 598-604.

Model P, Jovanovic G, Dworkin J (1997). The Escherichia coli phage-shock-protein (psp) operon. *Mol Microbiol* 24: 255-261.

Morrison DC, Jacobs DM (1976). Binding of polymyxin B to the lipid A portion of bacterial lipopolysaccharides. *Immunochemistry* 13: 813-818.

Munoz-Espin D, Daniel R, Kawai Y, Carballido-Lopez R, Castilla-Llorente V, Errington J *et al* (2009). The actin-like MreB cytoskeleton organizes viral DNA replication in bacteria. *Proc Natl Acad Sci U S A*.

Nakae T (1976). Identification of the outer membrane protein of E. coli that produces transmembrane channels in reconstituted vesicle membranes. *Biochemical and Biophysical Research Communications* 71: 877-884.

Nikaido H (1996). *Escherichia coli and Salmonella, Cellular and Molecular Biology*. ASM Press, Washington, DC.

Nikaido H (2003). Molecular basis of bacterial outer membrane permeability revisited. *Microbiol Mol Biol R* 67: 593-+.

Nothwehr SF, Conibear E, Stevens TH (1995). Golgi and vacuolar membrane proteins reach the vacuole in vps1 mutant yeast cells via the plasma membrane. *J Cell Biol* 129: 35-46.

Olichon A, Baricault L, Gas N, Guillou E, Valette A, Belenguer P *et al* (2003). Loss of OPA1 perturbs the mitochondrial inner membrane structure and integrity, leading to cytochrome c release and apoptosis. *J Biol Chem* 278: 7743-7746.

Osteryoung KW, Pyke KA (2014). Division and dynamic morphology of plastids. *Annu Rev Plant Biol* 65: 443-472.

Otera H, Mihara K (2011). Molecular mechanisms and physiologic functions of mitochondrial dynamics. *J Biochem* 149: 241-251.

Pai EF, Krengel U, Petsko GA, Goody RS, Kabsch W, Wittinghofer A (1990). Refined Crystal-Structure of the Triphosphate Conformation of H-Ras P21 at 1.35 Å Resolution - Implications for the Mechanism of Gtp Hydrolysis. *Embo Journal* 9: 2351-2359.

Patrick JE, Kearns DB (2008). MinJ (YvjD) is a topological determinant of cell division in Bacillus subtilis. *Molecular Microbiology* 70: 1166-1179.

Pavlovic J, Schroder A, Blank A, Pitossi F, Staeheli P (1993). Mx proteins: GTPases involved in the interferon-induced antiviral state. *Ciba Found Symp* 176: 233-243; discussion 243-237.

Peschel A, Vuong C, Otto M, Gotz F (2000). The D-alanine residues of *Staphylococcus aureus* teichoic acids alter the susceptibility to vancomycin and the activity of autolytic enzymes. *Antimicrob Agents Ch* 44: 2845-2847.

Pfanner N, Wiedemann N, Meisinger C (2004). Cell biology. Double membrane fusion. *Science* 305: 1723-1724.

Piper C, Hill C, Cotter PD, Ross RP (2011). Bioengineering of a Nisin A-producing *Lactococcus lactis* to create isogenic strains producing the natural variants Nisin F, Q and Z. *Microb Biotechnol* 4: 375-382.

Praefcke GJ, McMahon HT (2004). The dynamin superfamily: universal membrane tubulation and fission molecules? *Nat Rev Mol Cell Biol* 5: 133-147.

Prakash B, Praefcke GJ, Renault L, Wittinghofer A, Herrmann C (2000). Structure of human guanylate-binding protein 1 representing a unique class of GTP-binding proteins. *Nature* 403: 567-571.

Prost LR, Sanowar S, Miller SI (2007). Salmonella sensing of anti-microbial mechanisms to promote survival within macrophages. *Immunol Rev* 219: 55-65.

Raivio TL, Silhavy TJ (2001). Periplasmic stress and ECF sigma factors. *Annual Review of Microbiology* 55: 591-624.

Ramachandran R (2011). Vesicle scission: dynamin. *Semin Cell Dev Biol* 22: 10-17.

Ramirez G, Mendez E, Salas M, Vinuela E (1972). Head-neck connecting protein in phage phi29. *Virology* 48: 263-265.

Rapaport D, Brunner M, Neupert W, Westermann B (1998). Fzo1p is a mitochondrial outer membrane protein essential for the biogenesis of functional mitochondria in *Saccharomyces cerevisiae*. *J Biol Chem* 273: 20150-20155.

Ringstad N, Nemoto Y, De Camilli P (1997). The SH3p4/Sh3p8/SH3p13 protein family: binding partners for synaptojanin and dynamin via a Grb2-like Src homology 3 domain. *Proc Natl Acad Sci U S A* 94: 8569-8574.

Rothman JH, Stevens TH (1986). Protein Sorting in Yeast - Mutants Defective in Vacuole Biogenesis Mislocalize Vacuolar Proteins into the Late Secretory Pathway. *Cell* 47: 1041-1051.

Roy A, Kucukural A, Zhang Y (2010). I-TASSER: a unified platform for automated protein structure and function prediction. *Nat Protoc* 5: 725-738.

Roy H, Dare K, Ibba M (2009). Adaptation of the bacterial membrane to changing environments using aminoacylated phospholipids. *Molecular Microbiology* 71: 547-550.

Rubio V, Salas M, Vinuela E, Usobiaga P, Saiz JL, Llopis JF (1974). Biophysical properties of bacteriophage phi29. *Virology* 57: 112-121.

Ruhr E, Sahl HG (1985). Mode of Action of the Peptide Antibiotic Nisin and Influence on the Membrane-Potential of Whole Cells and on Cytoplasmic and Artificial Membrane-Vesicles. *Antimicrob Agents Ch* 27: 841-845.

Rujiviphat J, Meglei G, Rubinstein JL, McQuibban GA (2009). Phospholipid association is essential for dynamin-related protein Mgm1 to function in mitochondrial membrane fusion. *J Biol Chem* 284: 28682-28686.

Sahl HG, Kordel M, Benz R (1987). Voltage-dependent depolarization of bacterial membranes and artificial lipid bilayers by the peptide antibiotic nisin. *Arch Microbiol* 149: 120-124.

Salas M, Vasquez C, Mendez E, Vinuela E (1972). Head fibers of bacteriophage phi 29. *Virology* 50: 180-188.

Samson JE, Moineau S (2013). Bacteriophages in food fermentations: new frontiers in a continuous arms race. *Annu Rev Food Sci Technol* 4: 347-368.

Schneiderschaulies S, Schneiderschaulies J, Schuster A, Bayer M, Pavlovic J, Termeulen V (1994). Cell-Type-Specific Mxa-Mediated Inhibition of Measles-Virus Transcription in Human Brain-Cells. *Journal of Virology* 68: 6910-6917.

Schumacher B, Staeheli P (1998). Domains mediating intramolecular folding and oligomerization of MxA GTPase. *J Biol Chem* 273: 28365-28370.

Sesaki H, Jensen RE (2004). Ugo1p links the Fzo1p and Mgm1p GTPases for mitochondrial fusion. *J Biol Chem* 279: 28298-28303.

Sever S (2002). Dynamin and endocytosis. *Curr Opin Cell Biol* 14: 463-467.

Shahbadian K, Jamalli A, Zig L, Putzer H (2009). RNase Y, a novel endoribonuclease, initiates riboswitch turnover in *Bacillus subtilis*. *EMBO J* 28: 3523-3533.

Shpetner HS, Herskovits JS, Vallee RB (1996). A binding site for SH3 domains targets dynamin to coated pits. *J Biol Chem* 271: 13-16.

Sims PJ, Waggoner AS, Wang CH, Hoffman JF (1974). Studies on the mechanism by which cyanine dyes measure membrane potential in red blood cells and phosphatidylcholine vesicles. *Biochemistry*.

Síp M, Herman P, Plásek J, Hrouda V (1990). Transmembrane potential measurement with carbocyanine dye diS-C3-(5): fast fluorescence decay studies. *Journal of Photochemistry and Photobiology B: Biology*.

Siranosian KJ, Ireton K, Grossman AD (1993). Alanine Dehydrogenase (Ald) Is Required for Normal Sporulation in *Bacillus-Subtilis*. *JOURNAL OF BACTERIOLOGY* 175: 6789-6796.

Smirnova E, Griparic L, Shurland DL, van der Blik AM (2001). Dynamin-related protein Drp1 is required for mitochondrial division in mammalian cells. *Mol Biol Cell* 12: 2245-2256.

Souza BM, Castro TL, Carvalho RD, Seyffert N, Silva A, Miyoshi A *et al* (2014). sigma(ECF) factors of gram-positive bacteria: a focus on *Bacillus subtilis* and the CMNR group. *Virulence* 5: 587-600.

Standar K, Mehner D, Osadnik H, Berthelmann F, Hause G, Lunsdorf H *et al* (2008). PspA can form large scaffolds in *Escherichia coli*. *FEBS Lett* 582: 3585-3589.

Stock AM, Robinson VL, Goudreau PN (2000). Two-component signal transduction. *Annu Rev Biochem* 69: 183-215.

Stone KJ, Strominger JL (1971). Mechanism of action of bacitracin: complexation with metal ion and C 55 -isoprenyl pyrophosphate. *Proc Natl Acad Sci U S A* 68: 3223-3227.

Storm DR, Strominger JI (1973). Complex-Formation between Bacitracin Peptides and Isoprenyl Pyrophosphates - Specificity of Lipid-Peptide Interactions. *J Biol Chem* 248: 3940-3945.

Strahl H, Hamoen LW (2010). Membrane potential is important for bacterial cell division. *P Natl Acad Sci USA* 107: 12281-12286.

Straus SK, Hancock RE (2006). Mode of action of the new antibiotic for Gram-positive pathogens daptomycin: comparison with cationic antimicrobial peptides and lipopeptides. *Biochim Biophys Acta* 1758: 1215-1223.

Studier FW, Moffatt BA (1986). Use of Bacteriophage-T7 Rna-Polymerase to Direct Selective High-Level Expression of Cloned Genes. *Journal of Molecular Biology* 189: 113-130.

Szaszak M, Gaborik Z, Turu G, McPherson PS, Clark AJ, Catt KJ *et al* (2002). Role of the proline-rich domain of dynamin-2 and its interactions with Src homology 3 domains during endocytosis of the AT1 angiotensin receptor. *J Biol Chem* 277: 21650-21656.

Szklarczyk D, Franceschini A, Wyder S, Forslund K, Heller D, Huerta-Cepas J *et al* (2015). STRING v10: protein-protein interaction networks, integrated over the tree of life. *Nucleic Acids Res* 43: D447-452.

Thoms S, Erdmann R (2005). Dynamin-related proteins and Pex11 proteins in peroxisome division and proliferation. *FEBS J* 272: 5169-5181.

Timmis JN, Ayliffe MA, Huang CY, Martin W (2004). Endosymbiotic gene transfer: organelle genomes forge eukaryotic chromosomes. *Nat Rev Genet* 5: 123-135.

Titus JA, Haugland R, Sharrow SO, Segal DM (1982). Texas Red, a hydrophilic, red-emitting fluorophore for use with fluorescein in dual parameter flow microfluorometric and fluorescence microscopic studies. *J Immunol Methods* 50: 193-204.

Tosi M, Anderson DL (1973). Antigenic properties of bacteriophage phi 29 structural proteins. *J Virol* 12: 1548-1559.

Trias J, Jarlier V, Benz R (1992). Porins in the cell wall of mycobacteria. *Science* 258: 1479-1481.

Tuma PL, Collins CA (1994). Activation of Dynamin Gtpase Is a Result of Positive Cooperativity. *J Biol Chem* 269: 30842-30847.

Typas A, Banzhaf M, Gross CA, Vollmer W (2012). From the regulation of peptidoglycan synthesis to bacterial growth and morphology. *Nat Rev Microbiol* 10: 123-136.

Vallis Y, Wigge P, Marks B, Evans PR, McMahon HT (1999). Importance of the pleckstrin homology domain of dynamin in clathrin-mediated endocytosis. *Curr Biol* 9: 257-260.

Van de Ven FJ, Van den Hooven HW, Konings RN, Hilbers CW (1991). NMR studies of lantibiotics. The structure of nisin in aqueous solution. *Eur J Biochem* 202: 1181-1188.

van der Blik AM, Meyerowitz EM (1991). Dynamin-like protein encoded by the *Drosophila* shibire gene associated with vesicular traffic. *Nature* 351: 411-414.

van Heijenoort J (1998). Assembly of the monomer unit of bacterial peptidoglycan. *Cell Mol Life Sci* 54: 300-304.

van Heijenoort J (2001). Formation of the glycan chains in the synthesis of bacterial peptidoglycan. *Glycobiology* 11: 25R-36R.

van Heusden HE, de Kruijff B, Breukink E (2002). Lipid II induces a transmembrane orientation of the pore-forming peptide lantibiotic nisin. *Biochemistry* 41: 12171-12178.

Verhelst J, Hulpiau P, Saelens X (2013). Mx Proteins: Antiviral Gatekeepers That Restrain the Uninvited. *Microbiol Mol Biol R* 77: 551-566.

Vetter IR, Wittinghofer A (2001). The guanine nucleotide-binding switch in three dimensions. *Science* 294: 1299-1304.

Vida TA, Emr SD (1995). A new vital stain for visualizing vacuolar membrane dynamics and endocytosis in yeast. *J Cell Biol* 128: 779-792.

Vizeacoumar FJ, Vreden WN, Fagarasanu M, Eitzen GA, Aitchison JD, Rachubinski RA (2006). The dynamin-like protein Vps1p of the yeast *Saccharomyces cerevisiae* associates with peroxisomes in a Pex19p-dependent manner. *J Biol Chem* 281: 12817-12823.

von der Malsburg A, Abutbul-Ionita I, Haller O, Kochs G, Danino D (2011). Stalk domain of the dynamin-like MxA GTPase protein mediates membrane binding and liposome tubulation via the unstructured L4 loop. *J Biol Chem* 286: 37858-37865.

Wakabayashi J, Zhang ZY, Wakabayashi N, Tamura Y, Fukaya M, Kensler TW *et al* (2009). The dynamin-related GTPase Drp1 is required for embryonic and brain development in mice. *Journal of Cell Biology* 186: 805-816.

Wang H, Song P, Du L, Tian W, Yue W, Liu M *et al* (2011). Parkin ubiquitinates Drp1 for proteasome-dependent degradation: implication of dysregulated mitochondrial dynamics in Parkinson disease. *J Biol Chem* 286: 11649-11658.

Wang X, Su B, Fujioka H, Zhu X (2008). Dynamin-like protein 1 reduction underlies mitochondrial morphology and distribution abnormalities in fibroblasts from sporadic Alzheimer's disease patients. *Am J Pathol* 173: 470-482.

Ward JB (1984). Biosynthesis of peptidoglycan: points of attack by wall inhibitors. *Pharmacol Ther* 25: 327-369.

Warner FD, Kitos GA, Romano MP, Hemphill E (1977). Characterization of SP β : a temperate bacteriophage from *Bacillus subtilis* 168M. *Canadian Journal of Microbiology*.

Warnock DE, Hinshaw JE, Schmid SL (1996). Dynamin self-assembly stimulates its GTPase activity. *J Biol Chem* 271: 22310-22314.

Weidenmaier C, Peschel A, Kempf VA, Lucindo N, Yeaman MR, Bayer AS (2005). DltABCD- and MprF-mediated cell envelope modifications of *Staphylococcus aureus* confer resistance to platelet microbicidal proteins and contribute to virulence in a rabbit endocarditis model. *Infect Immun* 73: 8033-8038.

Wenzel M, Chiriac AI, Otto A, Zweytick D, May C, Schumacher C *et al* (2014). Small cationic antimicrobial peptides delocalize peripheral membrane proteins. *Proc Natl Acad Sci U S A* 111: E1409-1418.

Wiedemann I, Breukink E, van Kraaij C, Kuipers OP, Bierbaum G, de Kruijff B *et al* (2001). Specific binding of nisin to the peptidoglycan precursor lipid II combines pore formation and inhibition of cell wall biosynthesis for potent antibiotic activity. *J Biol Chem* 276: 1772-1779.

Wiegert T, Homuth G, Versteeg S, Schumann W (2001). Alkaline shock induces the *Bacillus subtilis* sigma(W) regulon. *Mol Microbiol* 41: 59-71.

Wigge P, Vallis Y, McMahon HT (1997). Inhibition of receptor-mediated endocytosis by the amphiphysin SH3 domain. *Curr Biol* 7: 554-560.

Wolf D, Kalamorz F, Wecke T, Juszczak A, Mader U, Homuth G *et al* (2010). In-depth profiling of the LiaR response of *Bacillus subtilis*. *J Bacteriol* 192: 4680-4693.

Wong ED, Wagner JA, Scott SV, Okreglak V, Holewinski TJ, Cassidy-Stone A *et al* (2003). The intramitochondrial dynamin-related GTPase, Mgm1p, is a component of a protein complex that mediates mitochondrial fusion. *J Cell Biol* 160: 303-311.

Yoon Y, Pitts KR, McNiven MA (2001). Mammalian dynamin-like protein DLP1 tubulates membranes. *Mol Biol Cell* 12: 2894-2905.

Zahler SA, Korman RZ, Rosenthal R, Hemphill HE (1977). *Bacillus subtilis* bacteriophage SPbeta: localization of the prophage attachment site, and specialized transduction. *J Bacteriol* 129: 556-558.

Zhang Y, Chan DC (2007). Structural basis for recruitment of mitochondrial fission complexes by Fis1. *Proc Natl Acad Sci U S A* 104: 18526-18530.

Zhang YM, Rock CO (2008). Membrane lipid homeostasis in bacteria. *Nat Rev Microbiol* 6: 222-233.

Zhao C, Denison C, Huibregtse JM, Gygi S, Krug RM (2005). Human ISG15 conjugation targets both IFN-induced and constitutively expressed proteins functioning in diverse cellular pathways. *P Natl Acad Sci USA* 102: 10200-10205.

Zheng G, Yan LZ, Vederas JC, Zuber P (1999). Genes of the *sbo-alb* locus of *Bacillus subtilis* are required for production of the antilisterial bacteriocin subtilisin. *J Bacteriol* 181: 7346-7355.

Appendix

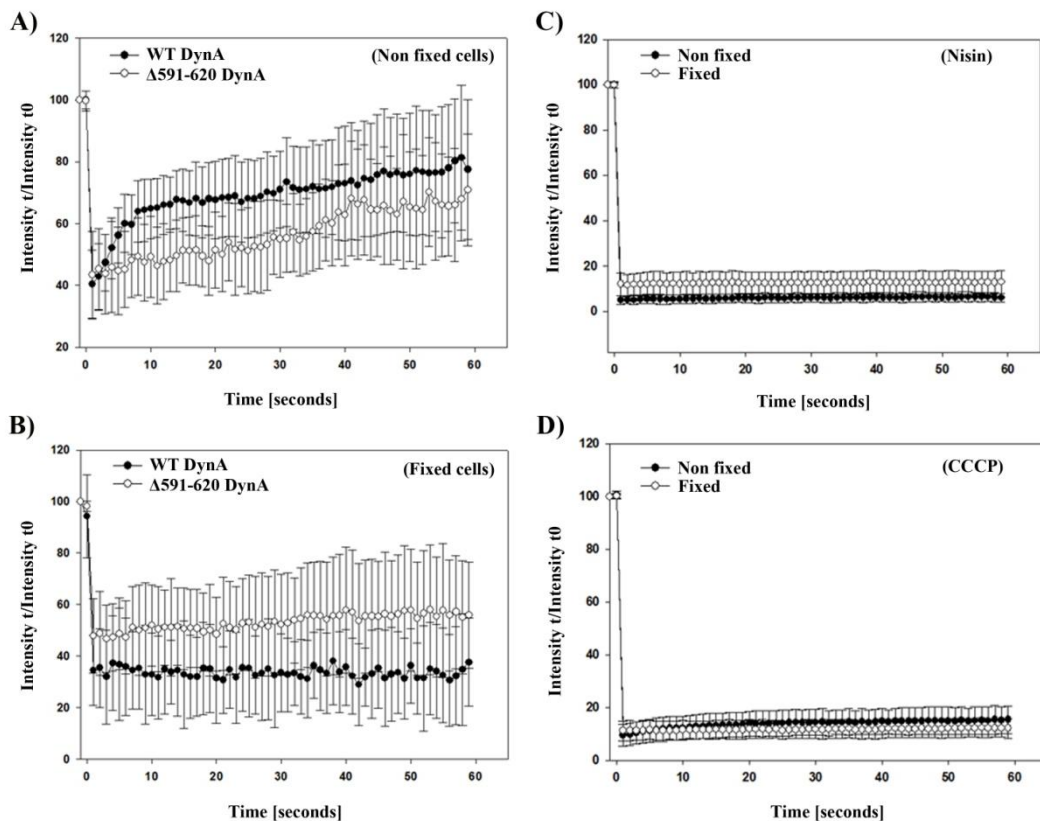


Figure 1. FRAP analysis of wild-type and $\Delta 591-620$ DynA-GFP. For FRAP studies, a Delta Vision Elite microscope equipped with a CoolSnap HQ2 CCD camera was used. Images were taken with a 100X oil PSF U-Plan S-Apo 1.4 NA objective using a FITC filter set for observing GFP signals and analysed using Softworx (GE Healthcare, Applied Precision). GFP-bleaching was performed at a defined region on bacterial pole with 488 laser at 10% power and a pulse duration of 0.05 seconds and GFP recovery was measured over time. For visualising GFP we used 475/28nm excitation and 525/48nm emission wavelengths. Pictures were taken every second. **(A)** GFP signal recovery was strikingly fast, within seconds (half time being 6-7 seconds), thus showing DynA to be highly dynamic at the bacterial membrane. Compared to the full-length protein, $\Delta 591-620$ DynA-GFP exhibited slower recovery with a lower maximum of fluorescence resulting in a more linear curve **(B)** Further to avoid any possibility of photo-switching of GFP, cells were fixed with formaldehyde and exposed to FRAP. **(C and D)** FRAP analysis of cells treated with nisin and CCCP revealed that DynA becomes highly static upon membrane stress. All the necessary controls for analysing and normalising FRAP measurements were taken into consideration.

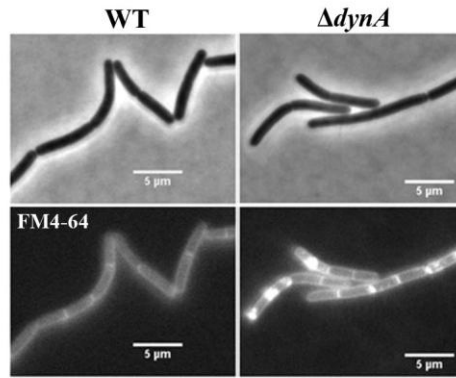


Figure 2. Membrane deformations are observed in $\Delta dynA$ upon nisin-exposure. Microscopic images with nisin and the lipophilic FM4-64 dye show $\Delta dynA$ cells to produce membrane deformations, which are absent in wild-type cells, indicating that DynA relieves cells from membrane stress (Master thesis of Kristina Eissenberger). Scale bar, 5 μm .

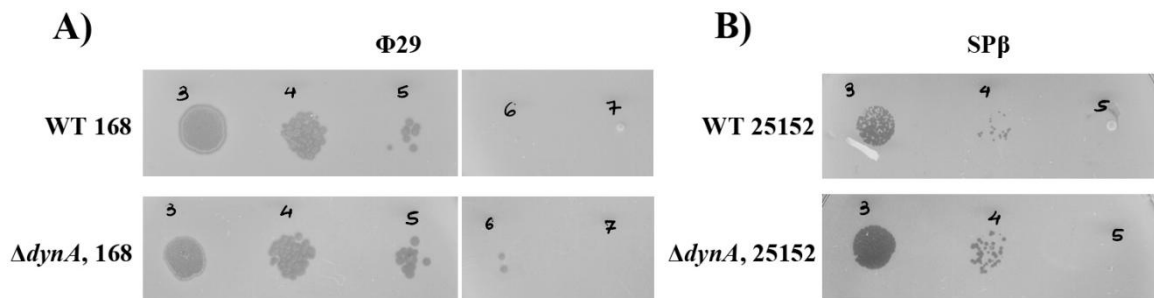


Figure 3. Spot assay with phages, $\Phi 29$ and SP β . 5 μL of 10-fold serially diluted phage stocks were spotted on a lawn of wild-type 168, $\Delta dynA$ 168, wild-type 25152 and $\Delta dynA$ 25152 bacteria, respectively. The dilution that produced single and isolated plaques was used for performing quantitative plaque assays (QPAs).

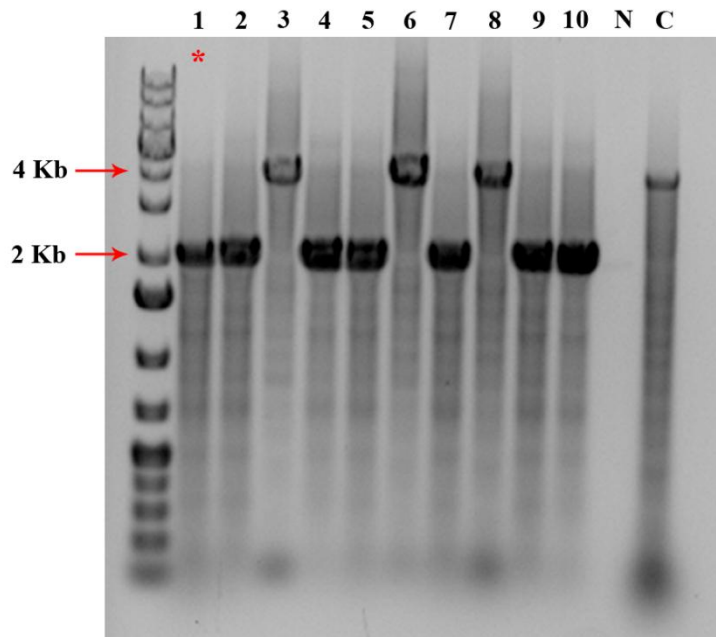


Figure 4. Confirmation of deletion of *dynA* in strain 25152. Colony PCRs were performed with primers FBE33 and FBE36 on tet-resistant colonies, 1-10, and wild-type 25152 strain. A PCR product around 2 Kb confirms deletion of *dynA* whereas 4 Kb refers to wild-type background. N, negative control, C, wild-type control. Glycerol stock was prepared from colony 1 (marked with a red asterisk).

Table 1. Values for calibration curve for standard protein samples on Superose 6 10/300 GL column. Kav, phase distribution co-efficient, MW, molecular weight.

Retention mL	Kav	MW	Log ₁₀ MW	Standards
13.01	0.32	670000	5.826074803	Thyroglobulin (bovine)
16.12	0.52	158000	5.198657087	γ-globulin (bovine)
17.73	0.63	44000	4.643452676	Ovalbumin (chicken)
18.97	0.70	17000	4.230448921	Myoglobin (horse)
21.65	0.88	1315	3.118925753	Vitamin B ₁₂

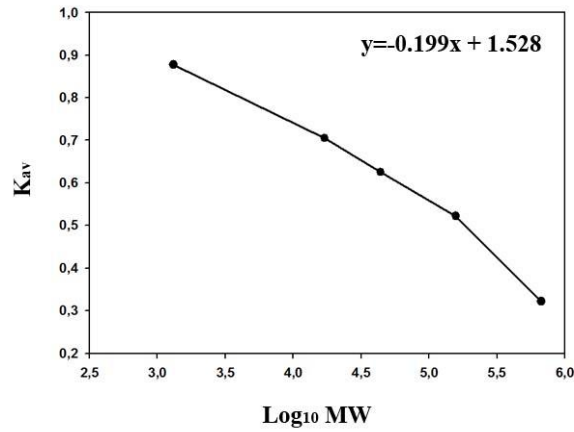


Figure 5. Calibration curve for standard protein samples on Superose 6 10/300 GL column

Table 2. Estimation of molecular weight (MW) of eluted protein. Using the above standard curve and K_{av} values obtained from elution profiles, the approximate molecular weights of peaks observed from wild-type and $\Delta 591-620$ DynA-His protein purification. $\Delta 591-620$ DynA-His purification clearly lacks dimer peak eluted at around 14-15 mL retention volume.

Retention (mL)	K _{av}	Log ₁₀ MW	MW (138alton)	MW (Kilo 138alton)
Wild-type DynA-His				
9.33	0.09	7.24745	17678678.46	17678.67846
10.81	0.18	6.770842	5899864.021	5899.864021
14.98	0.45	5.424103	265523.4912	265.5234912
17.95	0.64	4.464447	29137.12615	29.13712615
20.94	0.83	3.499638	3159.642611	3.159642611
$\Delta 591-620$ DynA-His				
8.13	0.01	7.636359	43287159.59	43287.15959
10.85	0.18	6.75782	5725581.672	5725.581672
17.61	0.62	4.574997	37583.46582	37.58346582
21.09	0.84	3.451059	2825.262868	2.825262868

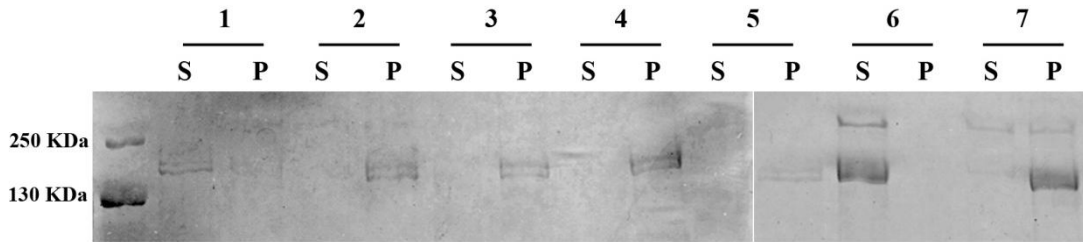


Figure 6. $\Delta 591-620$ lipid binding *in vitro*. Liposome sedimentation assay was performed with 2 μ M protein and 0.2 mg/mL PG liposomes in a total volume of 100 μ l, at 25°C for 1 hour, with necessary controls. S, supernatant, P, pellet. **1**, $\Delta 591-620$ DynA-His, **2**, $\Delta 591-620$ DynA-His + Liposomes, **3**, $\Delta 591-620$ DynA-His + Liposomes + 0.5 mM MgCl₂, **4**, $\Delta 591-620$ DynA-His + Liposomes + 1 mM GTP, **5**, $\Delta 591-620$ DynA-His + Liposomes + 0.5 mM MgCl₂ + GTP, **6**, wild-type DynA-His, **7**, wild-type DynA-His + Liposomes.

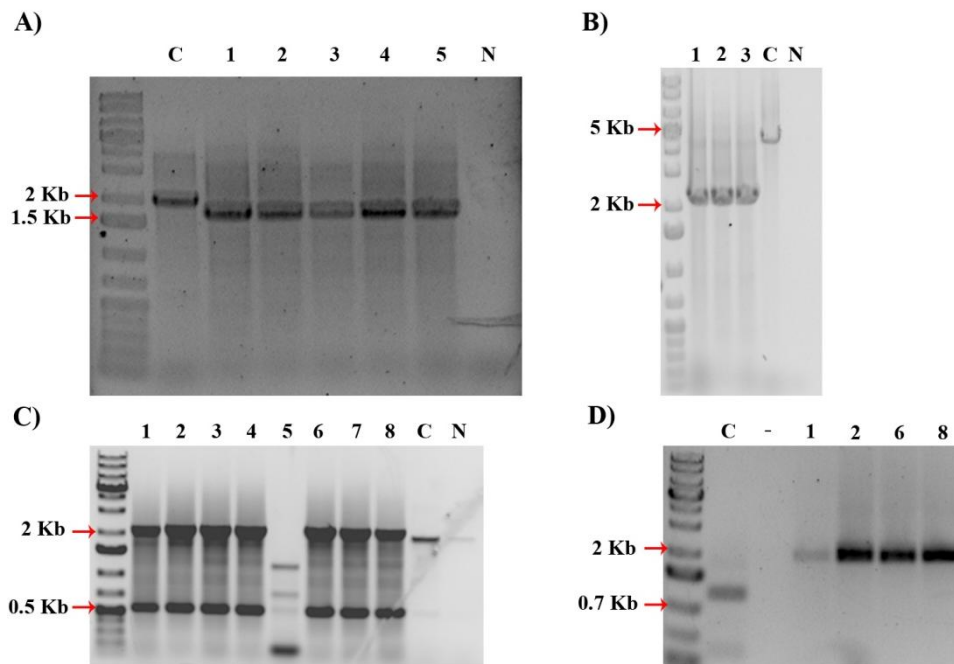


Figure 7. Deletion of *yukF*, *mfd* and *yflN*. Colony PCRs were performed on Kanamycin-resistant colonies obtained from respective transformations. (A) Primers PSP 177 (200 bps upstream) and PSP 178 (200 bps downstream) were used to verify deletion of *yukF*. PCR product corresponding of 1.5 Kb confirms deletion of the gene whereas 2 Kb refers to wild-type background. Colonies 1 and 2 confirm *yukF* deletion in WT, 3 and 4 in $\Delta dynA$ and colony 5 in PSB032 strain. (B) Primers PSP 118 and PSP 121 were used to verify *mfd* deletion in wild-type (colony 1), $\Delta dynA$ (colony 2) and PSB032 (colony 3) strains. *mfd* deletion is confirmed with a PCR product of 2.3 Kb. Deletion of *yflN* was confirmed in two steps, colony PCR (C) and digestion of the colony PCR-product with *AatII* (D). *AatII* cuts within *yflN* gene at 600 bps. Colonies 1-2, 6 and 8 refer to deletion of *yflN* in WT, $\Delta dynA$ and PSB032 strains, respectively. kanamycin resistant cassette ~800 bps. C, wild-type control, N, negative control.

Acknowledgements

I am grateful to Prof. Dr. Marc Bramkamp for his constant support and guidance throughout my PhD phase. I would like to express my heartfelt thanks to Prof. Dr. Reinhard Krämer and all my former colleagues from AG Krämer (Cologne). A major part of this thesis was funded by the International Graduate School in Development Health and Disease (IGSDHD), Cologne. I would like to express my gratitude to all IGSDHD members, especially Dr. Isabell Witt, and Kathy Joergens, for their generous support. I also wish to express a sincere thanks to Kristina Eissenberger, Nadine Germ and Laurence Karier for their genuine contribution towards this project. I would like to thank Dr. Karin Schubert for all the HPLC experiments and Mauricio Toro Nahuelpan for help with electron microscopy.

A friend in need is a friend indeed and I am lucky to have such a friend, Dr. Catriona Donovan. Cat has been an amazingly supportive friend and colleague. Thank you for being there. I would then whole-heartedly thank all the members of AG Bramkamp (Giacomo, Fabian, Juri, Boris, Karin, Nadine, Derk, Kathy, Gustavo and Lily) for all the fun times together, whether it was hiking, trips to Christmas markets or just plain drinking in the kitchen. I am grateful to be a part of this group. Words cannot express how grateful I am to my family for all the love and support they have given me. Their support has truly been over-whelming. This journey would have been less fun without all my friends from Cologne, Munich, Leicester and Mumbai. A heartfelt thanks to everyone. Finally, my deepest gratitude to my caring, loving, and supportive Oliver. You have been patient and encouraging during stressful times and I really appreciate it. Thanks a lot.

Curriculum Vitae
Prachi Sawant

Hosigastrasse 10, 81375 Munich, Germany
Phone: (0049) 01778435896 • E-Mail: Prachi.Sawant@campus.lmu.de

Education

Educational institute	Degree	Year	Subjects studied
Ludwig-Maximilians-University Munich, Germany	Doktor der Naturwissenschaften (PhD)	Since June 2011	Microbiology
University of Leicester, United Kingdom	Master of Science (MSc)	2009-2010	Molecular Genetics
Jaihind college, University of Mumbai, India	Bachelor of Science (BSc)	2006-2009	Microbiology, Chemistry, Physics
Vartak College, India	Higher secondary certificate (HSC)	2004-2006	Biology, Chemistry, Physics, Mathematics, English
J.B.Ludhani high school, India	Secondary school certificate (SSC)	2004	English, Mathematics, Science, Social sciences

Publication

F. Bürmann, **P. Sawant**, M. Bramkamp 2012. Identification of interaction partners of the dynamin-like protein DynA from *Bacillus subtilis*. *Communicative & Integrative Biology* (CIB), 5.

Other Research Experience

1) October 2010- April 2011 Laboratory rotations, Cologne, Germany

Description - 6-month training period, comprising of seven-week research projects in three different laboratories;

- Analysis of Irga6 phosphorylation by avirulent *Toxoplasma gondii* ROP18 kinase
- Genetic analysis of UV response in *Caenorhabditis elegans* by RNAi
- Investigating the role of *Cip4* and *Diaphanous* in fly tumor mode

2) 2006-2009 Microbiology Credit Course, Jaihind College, Mumbai, India

Successfully earned 8 credits in microbiology research project;

“Analysis of water samples obtained from seven lakes of the Thane city”

Description - Water samples were collected before and after the installation of aerating devices. This project required that I work methodically with regards to health and safety regulations and pay close attention to detail in order to achieve accurate results. Cultivation and detection of different microbial species from the samples was the main aim of this project.

Other qualifications

Master course in Computers (2004-2005), Bassein Computer Academy, Yashwantrao Chavan Maharashtra Open University (YCMOU), India.

Description - This course involved a thorough introduction and practical knowledge of computer basics, Microsoft disk operating system and graphical user interface.

- 1) Certificate in Office computing
- 2) Certificate in Desktop Publishing (DTP)
- 3) Maharashtra state certificate in information technology (MS-CIT)

Seminar, Workshop and Conference participation

- 05.10.14 – 08.10.14 Talk at the Annual Conference of the Association for General and Applied Microbiology (VAAM), Dresden, Germany
- 14.03.14 – 15.03.14 Conference BACELL, European *Bacillus* Community
- 10.03.13 – 13.03.13 Poster presentation at the Annual Conference of the Association for General and Applied Microbiology (VAAM), Bremen, Germany
- 23.07.12 – 25.07.12 Conference on Synthetic Biology, Centre for advanced studies (CAS), LMU, Munich, Germany.
- 10.03.12 – 21.03.12 Poster presentation at the Annual Conference of the Association for General and Applied Microbiology (VAAM), Tübingen, Germany
- 04.10.12 – 06.10.12 Poster presentation at the Annual Symposium of SFB 635, Wermelskirchen, Germany
- 18.04.12 – 20.04.12 Scientific writing course by Dr. Ruth Willmott, MPI for Plant Breeding Research, Cologne, Germany
- 09.02.12 – 10.02.12 Poster presentation at Crossroads in Biology (CIB), Graduate School for Biological Sciences, Cologne, Germany.
- 08.12.11 – 09.12.11 Scientific presentation course by Andrea Roos, Cologne, Germany
- 03.11.11 – 04.11.11 Poster presentation at the Annual Symposium of SFB 635, Erfstadt, Germany
- 15.03.2007- 16.03.2007 Workshop on “Recent Trends in Diagnostic Techniques”, Jaihind College, Mumbai, India.